ACTA PROTOZOOLOGICA

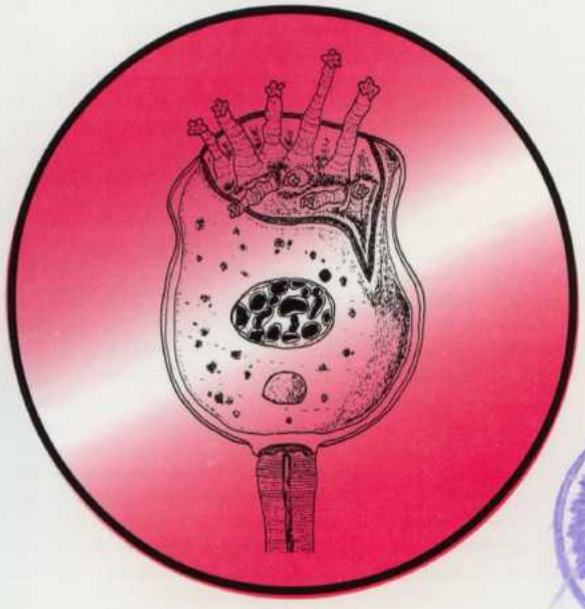

NENCKI INSTITUTE OF EXPERIMENTAL BIOLOGY
WARSAW, POLAND
2003
VOLUME 42 NUMBER 2
ISSN 0065-1583

Polish Academy of Sciences
Nencki Institute of Experimental Biology
and
Polish Society of Cell Biology

ACTA PROTOZOOLOGICA
International Journal on Protistology

ACTA PROTOZOOLOGICA appears quarterly.

The price (including Air Mail postage) of subscription to *Acta Protozoologica* at 2003 is: US $ 200.- by institutions and US $ 120.- by individual subscribers. Limited numbers of back volumes at reduced rate are available. Terms of payment: check, money order or payment to be made to the Nencki Institute of Experimental Biology account: 11101053-401050001074 at BPH PBK S. A. III O/Warszawa, Poland. For matters regarding *Acta Protozoologica*, contact Editor, Nencki Institute of Experimental Biology, ul. Pasteura 3, 02-093 Warszawa, Poland; Fax: (4822) 822 53 42; E-mail: jurek@ameba.nencki.gov.pl For more information see Web page **http://www.nencki.gov.pl/public.htm**
Circulation: 300

Front cover: Fernandez-Leborans G., Hanamura Y. and Nagasaki K. (2002) A new suctorian, *Flectacineta isopodensis* (Protozoa: Ciliophora) epibiont on marine isopods from Hokkaido (Northern Japan). *Acta Protozool.* **41:** 79-84

This publication is supported by the State Committee for Scientific Research

Desktop processing: Justyna Osmulska, Information Technology Unit of the Nencki Institute
Printed at the MARBIS, ul. Poniatowskiego 1
05-070 Sulejówek, Poland

Acta Protozool. (2003) 42: 83 - 90

ACTA
PROTOZOOLOGICA

Species Separation and Identification of *Uronychia* spp. (Hypotrichia: Ciliophora) using RAPD Fingerprinting and ARDRA Riboprinting

Zigui CHEN[1], Weibo SONG[1] and Alan WARREN[2]

[1] Laboratory of Protozoology, College of Fisheries, Ocean University of China, Qingdao, P. R. China; [2] Department of Zoology, Natural History Museum, London, UK

Summary. The 3 most common morphospecies of *Uronychia*, i.e. *U. setigera*, *U. transfuga* and *U. binucleata*, were examined *in vivo* and following protargol impregnation. Among these, *U. transfuga* is morphologically different to the others (large cell size, more macronuclear segments etc.). By contrast, *U. setigera* and *U. binucleata* are very similar and difficult to separate based only on their morphologies. Random amplified polymorphic DNA (RAPD) fingerprinting and amplified ribosomal DNA restriction analyses (ARDRA riboprinting) were therefore performed in order to confirm the division between them and to aid species identification. Using 4 different random primers the RAPD fingerprinting revealed 3 distinct patterns. Thus, 7 strains could be separated into 3 species with a similarity index of over 82% between different strains of the same species and only 30% to 40% between strains of different species. The unique restriction pattern of highly-conserved rDNA fragments (ARDRA) of different strains of *U. setigera* and *U. binucleata* using the enzyme *Msp* I was found to be species-specific and could be applicable for both species identification and species separation. According to our molecular analyses, the *Uronychia*-populations comprised at least 3 taxa (morphospecies). Moreover, the morphologically similar *U. setigera* and *U. binucleata* could be reliably separated and identified at the molecular level.

Key words: ARDRA riboprinting, identification, RAPD fingerprinting, species separation, *Uronychia.*

INTRODUCTION

The genus *Uronychia* is one of the most commonly-reported hypotrichous ciliates and is found worldwide in a range of marine and other saline biotopes (Müller 1786; Stein 1859; Quennerstedt 1867; Wallengren 1900; Buddenbrock 1920; Young 1922; Mansfeld 1923; Wang and Nie 1932; Kirby 1934; Wang 1934; Ozaki and Yagiu 1941; Fenchel 1965; Reiff 1968; Kattar 1970; Agamaliev 1971; Borror 1972a, b; Wilbert and Kahan 1981; Song 1997; Shi and Song 1999). In terms of species separation and taxonomy, however, *Uronychia* is possibly one of the most confused of all ciliate genera despite the fact that several studies concerning its taxonomy, morphology and morphogenesis have been carried out in recent years (Curds and Wu 1983, Dragesco and Dragesco-Kernéis 1986, Hill 1990,Valbonesi and Luporini 1990, Petz *et al*. 1995, Wilbert 1995, Song 1996).

Up to 1983,10 species of *Uronychia* had been described in the literature (Müller 1786, Dujardin 1841,

Address for correspondence: Weibo Song, Laboratory of Protozoology, College of Fisheries, Ocean University of China, Qingdao, 266003, P. R. China; Fax: +86 532 203 2283; E-mail: wsong@ouc.edu.cn

Claparède and Lachmann 1858, Wallengren 1900, Calkins 1902, Pierantoni 1909, Buddenbrock 1920, Young 1922, Taylor 1928, Kahl 1932, Bullington 1940, Fenchel 1965). In their taxonomic revision of the Euplotidae, Curds and Wu (1983) recognised only 4 species of *Uronychia*: *U. transfuga* (Müller, 1786) Stein, 1859, *U. setigera* Calkins, 1902, *U. binucleata* Young, 1922 and *U. magna* Pierantoni, 1909. Since then two additional species, *U. antarctica* Valbonesi and Luporini, 1990 and *U. multicirrus* Song, 1997, have been described.

Following their detailed investigation of over twenty *Uronychia*-populations collected over a 6-year period, Song and Wilbert (1997) concluded that *U. magna* and *U. antarctica* are conspecific with *U. transfuga* and *U. binucleata* respectively. Consequently, all known putative *Uronychia* spp. were allocated to one of 4 revised morphospecies: *U. transfuga*, *U. setigera*, *U. binucleata* (all of which are common) and *U. multicirrus* (which is rare).

Although Song and Wilbert (1997) significantly enhanced our knowledge and understanding of *Uronychia*-populations based on morphometric analyses, some morphological features at the species level are weak and easily overlooked. For example, the separation of *U. setigera* and *U. binucleata* is based almost exclusively on cell size and on the difference in the number of basal body pairs in the leftmost dorsal kinety, the latter character only being discernible with careful observation of high quality protargol preparations.

It has previously been reported that PCR-based methods such as RAPD (random amplified polymorphic DNA) fingerprinting and ARDRA (amplified ribosomal DNA restriction analyses, also called 'riboprinting') are suitable for the study of microbial diversity (Persing *et al*. 1993). In the field of protozoology, RAPD fingerprinting has been used to identify different parasite species (Neto *et al*. 1993), to separate different scuticociliate species (Song *et al*. 2002), to study genetic diversity within *Trypanosoma* spp. (Dirie *et al*. 1993, Mathieu-Daudé *et al*. 1995, Stothard *et al*. 2000) and in the genus *Tetrahymena* (Lynch *et al*. 1995), and to investigate the population structure of *Euplotes* spp. (Kusch and Heckmann 1996). Jerome and Lynn (1996) even suggested that PCR-based RFLP riboprinting (i.e. ARDRA) provides an alternative to traditional techniques for identifying and distinguishing *Tetrahymena* spp., while Stoeck *et al*. (2000) successfully combined two molecular techniques (RAPD and ARDRA) to reject the hypothesis of sibling species in *Paramecium caudatum*. By contrast, Foissner *et al*. (2001) failed to separate two morphospecies of the hypotrich ciliate *Gonostomum* using RAPD-fingerprinting.

During the present study, RAPD and ARDRA were used in order to investigate the relatedness between 3 species of *Uronychia*: *U. setigera* (three strains), *U. binucleata* (three strains) and *U. transfuga* (one strain). The main objective was to determine whether the separation of these 3 morphospecies is supported at the molecular level.

MATERIALS AND METHODS

Origin of isolates

Seven strains of *Uronychia* were isolated from diverse marine biotopes between 1998 and 2002. Three strains of *U. setigera* were from: (i) a crab-farming pond at Xunshan (strain 99062701); (ii) off the coast of Qingdao (strain 99102305); (iii) a shrimp-farming pond at Laizhou (strain 01041607). Three strains of *U. binucleata* were from: (i) a shellfish-farming pond at Hongdao (strain 01042001); (ii) a shrimp-farming pond at Huangdao (strain 01042106); (iii) a shrimp-farming pond at Weihai (strain 01051801). One strain of *U. transfuga* (strain 00042803) was from the shellfish-farming pond at Hongdao. Clonal cultures of each strain were established and maintained in sterile seawater at room temperature with rice grains to enrich natural bacteria as food for the ciliates. The protargol method according to Wilbert (1995) was used to reveal the infraciliature. The infraciliature and other morphological features of each strain were compared to those reported in previous papers (Song 1996, Song and Wilbert 1997).

DNA extraction and RAPD reaction

The nucleotide extraction protocols used in this study have been described in detail elsewhere (Chen and Song 2001) and involved the following steps: cells were rinsed 3 times with sterile artificial marine water after being starved overnight and were then pelleted by centrifugation (about 1000 g). 0.5 ml lysis buffer (10 mM Tris-HCl pH 8.3, 50 mM KCl, 2.5 mM $MgCl_2$, 0.6 % Tween 20, 0.6 % Nonidet P40, 60 µg/ml Proteinase K) was added and the mixture was incubated at 56°C for 1-2 h. After incubation, the DNA was extracted using an equal volume of a mixture of phenol:chloroform:isoamyl alcohol (25:24:1) and precipitated with 70% ethanol. DNA samples were stored at -20°C.

Amplifications by PCR were carried out in a total volume of 25 µl containing 10 mM Tris-HCl pH 8.3, 50 mM KCl, 0.1% Triton X-100, 3 mM $MgCl_2$, 0.2 mM dNTP, 0.5 µM of one oligonucleotide primer, 15 ng of genomic DNA and 1.5 units of Taq DNA polymerase (TaKaRa, Japan). For amplification the reaction mixtures were denatured at 94°C for 5 min, followed by the first 5 cycles consisting of denaturation for 30 s at 94°C, primer annealing for 30 s at 35°C, and extension for 1 min at 72°C. The subsequent 35 cycles comprised denaturation for 30 s at 94°C, primer annealing for 30 s at 40°C, and extension for 1 min at 72°C. Cycling was followed by a final extension step for 5 min at 72°C. Two or 3 repetitions of the PCR reaction were performed in order to assess the reproducibility of the data

(Chen *et al*. 2000). Four random primers were used, the sequences of which were as follows: S040 - 5' GTT GCG ATC C - 3'; S103 - 5' AGA CGT CCA C - 3'; S104 - 5' GGA AGT CGC C - 3'; S113 - 5' GAC GCC ACA C - 3' (Sangon Bio Co., Canada).

Ribosomal DNA amplification and digestion (ARDRA)

PCR amplifications were performed in a PCR thermal cycler. Genome DNA (50 ng) was mixed with 10 mM Tris-HCl pH 8.3, 50 mM KCl, 0.1% Triton X-100, 3 mM $MgCl_2$, 0.2 mM dNTP, and 0.5 mM of each oligonucleotide primer (16S-like F: 5' - AAC CTG GTT GAT CCT GCC AGT - 3'; 23S-like R: 5' - TTG GTC CGT GTT TCA AGA CG - 3') and 5 units of Taq Ex polymerase (TaKaRa, Japan). Distilled water was added to the mixture to a total volume of 100 µl. The reaction mixtures were denatured at 94°C for 5 min before the polymerase was added, followed by the first 5 cycles consisting of denaturation for 1 min at 94°C, primer annealing for 2 min at 56°C and extension for 2 min at 72°C. In the subsequent 35 cycles, the annealing temperature was raised to 62°C. The circulation was followed by a final extension step for 5 min at 72°C (Elwood *et al*. 1985, Medlin *et al*. 1988, Jerome and Lynn 1996).

The amplified ribosomal DNA products were purified using the UNIQ-5 DNA Gel Extraction Kit (Sangon Bio. Co., Canada) and dissolved in 50 µl Tris-EDTA solution (pH 8.0). Restriction of amplified ribosomal DNA was carried out by separate incubations at 37°C for 1.5 h with each of 10 restriction enzymes: *Kpn* I, *Taq* I (65°C), *Xba* I, *Bam*H I (30°C), *Eco*R I, *Hin*d III, *Eco*R V, *Hae* III, *Msp* I, *Pst* I (TaKaRa Bio. Co., Japan). The total volume of restriction mixtures was 10 µl containing 0.5 µl of each restriction enzyme solution, 1 µl 10x buffer for each enzyme, 1 µl BSA (0.1% w/v) and 7.5 µl PCR product (Shang *et al*. 2002).

Data analysis

The band-sharing index of RAPD fingerprinting for two individuals is based on that used by Wetton *et al*. (1987) for comparing DNA fingerprints and is given by the formula: $S = 2\ N_{AB} / (N_A + N_B)$, where N_A and N_B are the number of bands scored in ciliates A and B respectively and N_{AB} is the number shared by both.

RESULTS AND DISCUSSION

Morphological comparison

The strain of *U. transfuga* could be clearly separated from the 6 strains belonging to the other two species by the following characters: more elongated, rectangular body shape; body size *in vivo* 110-250 x 80-180 µm; macronucleus moniliform comprising several to many (6-13) segments which form a horseshoe shape; base of buccal cirrus conspicuously long and narrow (Fig. 2, Table 1). The number of macronuclear segments is considered a particularly reliable character for *U. transfuga* thereby confirming its identity unequivocally (Song and Wilbert 1997).

Uronychia setigera and *U. binucleata* are morphologically similar and are characterized as follows: two macronuclear segments often connected by short funiculus, but sometimes only one segment in globular forms of *U. setigera* (Song and Wilbert 1997); invariably with one small micronucleus between the macronuclear segments; rapidly crawling or very fast swimming movement; 4 frontal and 2 ventral cirri; 4 large and one small transverse cirri; 3 strong left marginal cirri; constantly 6 dorsal kineties. *Uronychia setigera* differs from *U. binucleata* by having fewer basal body pairs in the leftmost dorsal kinety (Fig. 1, arrowed), smaller body size, a conspicuous (*vs* inconspicuous) spur on the left cell margin and its characteristic buccal apparatus (Figs 1, 2; Table 1).

Thus, our findings confirm those of Song and Wilbert (1997) who also reported that *U. transfuga* is morphologically distinct from *U. binucleata* and *U. setigera*, and that the latter two are so morphologically similar that they can only be separated following meticulous observations of cells *in vivo* and of the infraciliature following protargol impregnation. It has been suggested that in cases such as this, molecular methods, which have the potential to provide informative data independent of the morphological organisation, might be usefully employed (Clark 1997).

RAPD fingerprinting

The RAPD fingerprinting patterns obtained with the 4 random primers revealed different polymorphic band patterns (Fig. 3). The control with no DNA template amplified no bands. Lane 7 (*U. transfuga*) was distinctly different from the other 6 samples for each of the

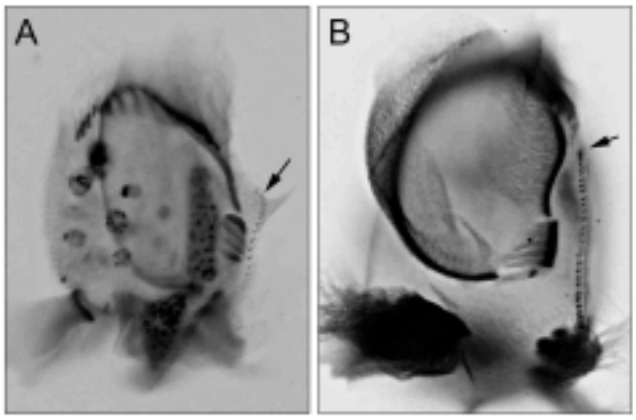

Fig. 1. Photomicrographs of *Uronychia setigera* (A) and *U. binucleata* (B) (protargol impregnations). Arrows mark leftmost dorsal kinety; note the different number of basal body pairs.

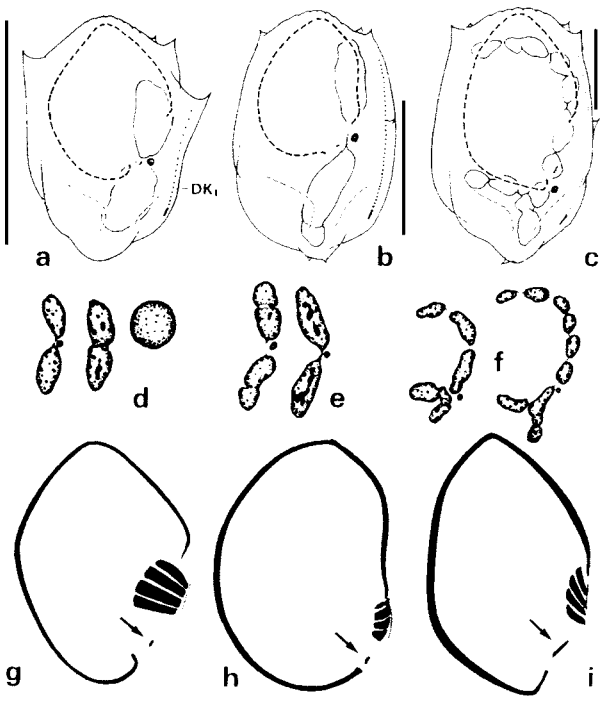

Fig. 2. Comparative diagrams of 3 *Uronychia* species: *U. setigera* (a, d, g); *U. binucleata* (b, e, h) and *U. transfuga* (c, f, i). **a-c** - showing the cell size and general body shape; **d-f** - different forms of macronuclear segments; **g-i** - showing the buccal apparatus, arrows indicate the buccal cirrus. Scale bars 50 μm (a-c) (from Song and Wilbert 1997).

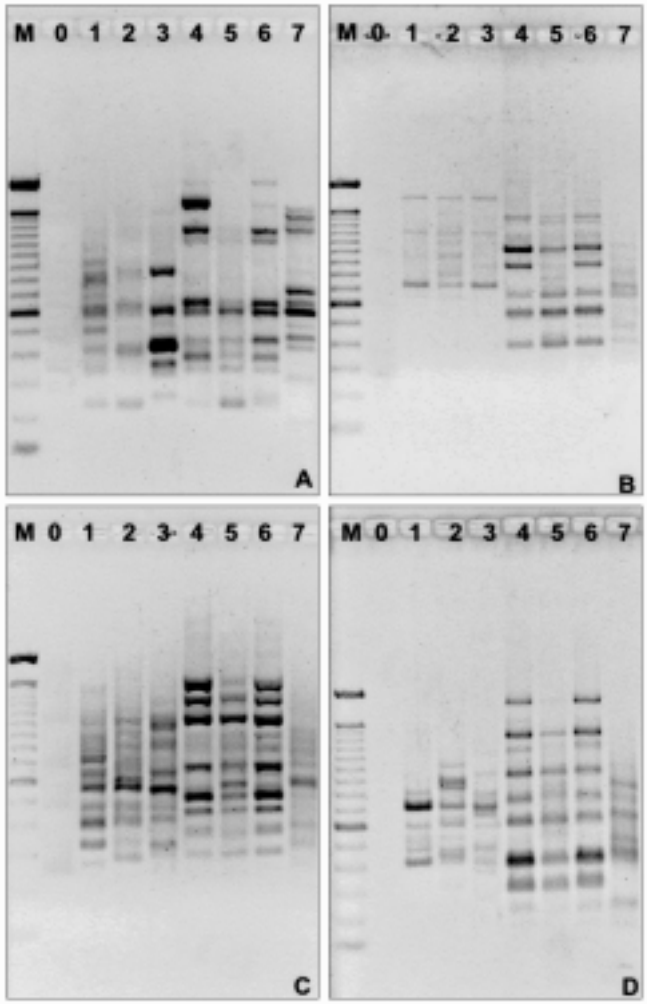

Fig. 3. RAPD banding patterns of 7 *Uronychia* strains using oligonucleotide random primers S040 (A), S103 (B), S104 (C) and S113 (D). Lane M - 100 bp molecular markers. Lane 0 - control without DNA. Lanes 1-3 - three strains of *U. setigera* (strains 99062701, 99102305, 01041607). Lanes 4-6 - three strains of *U. binucleata* (strains 01042001, 01042106, 01051801). Lane 7 - one strain of *U. transfuga* (strain 00042803).

4 primers. Lanes 4 to 6 (*U. binucleata*) shared similar band patterns though the intensity of some amplified bands varied due to the different concentration of template DNA. The same is true for lanes 1 to 3 (*U. setigera*).

Calculating the mean similarity index of the DNA banding patterns for each pair of strains, we found a genetical relatedness of 82-100% between different strains of the same species (Table 2, in bold) and only 30-40% between strains of different species (Table 2, in italics). Specifically, there was an 82-89% similarity among the 3 strains of *U. setigera*, and over 92% among the 3 strains of *U. binucleata*. The 11-18% dissimilarity among *U. setigera* strains and <8% dissimilarity among *U. binucleata* strains in the RAPD patterns can be explained by genotypical variance and genetic diversity within these species (Mathieu-Daudé *et al.* 1995, Kusch and Heckmann 1996, Kusch 1998, Stoeck and Schmidt 1998, Stoeck *et al.* 2000). On other hand, there was a mean similarity of only 35% between *U. setigera* and *U. transfuga*, 39% between *U. binucleata* and *U. transfuga* and 34% between *U. setigera* and *U. binucleata* (Table 2).

Kusch and Heckmann (1996) revealed that the similarity index was 0.38-0.46 (i.e. a 38-46% similarity) when different species of *Euplotes* were compared, and 0.60-0.78 (60-78% similarity) among strains of the same species. Our findings are consistent with these results. Thus, based on the polymorphic RAPD patterns we can confidently separate the 3 *Uronychia* species. Notably, our results confirm the separation of uronychias with two macronuclear segments into two distinct species, *U. setigera* and *U. binucleata*. This is in contrast to the findings of Foissner *et al.* (2001) who were unable to

Table 1. Morphological comparison of three *Uronychia* species. Data based on Song and Wilbert (1997).

Species	Cell length *in vivo* (µm)	Number and appearance of macronuclear segments	Base of buccal cirrus	Body shape	Number of basal body pairs in leftmost dorsal kinety
Uronychia setigera	40-70 (mostly 45-55)	1 or 2 (usually 2) sausage-like (occasionally as a single spherical mass)	short, *ca* 2-3 µm long	oval, lateral spur conspicuous	*ca* 15 (12-19)
Uronychia binucleata	70-120 (mostly 90-110)	constantly 2, sausage-like sometimes in two-doublets form	short, *ca* 3 µm long	long oval, lateral spur inconspicuous	*ca* 30 (23-40)
Uronychia transfuga	110-250 (mostly 150-210)	6-13, moniliform, forming a C-shape	conspicuously long, 10-14 µm in length	elongated rectangular, lateral spur inconspicuous	*ca* 50 (46-56)

Table 2. Similarity indices (S) of pairwise comparisons of RAPD patterns of 7 *Uronychia* strains. S was calculated according to Nei and Li (1979) from RAPD fingerprinting with 4 different primers with a total 56 polymorphic bands (*U. setigera* - strains 99062701, 99102305, 01041607; *U. binucleata* - strains 01042001, 01042106, 01051801; *U. transfuga* - strain 00042803).

	99062701	99102305	01041607	01042001	01042106	01051801	00042803
99062701	1.00						
99102305	**0.82**	1.00					
01041607	**0.89**	**0.86**	1.00				
01042001	*0.30*	*0.31*	*0.35*	1.00			
01042106	*0.36*	*0.37*	*0.42*	**0.92**	1.00		
01051801	*0.30*	*0.31*	*0.35*	**1.00**	**0.92**	1.00	
00042803	*0.36*	*0.37*	*0.33*	*0.39*	*0.40*	*0.39*	1.00

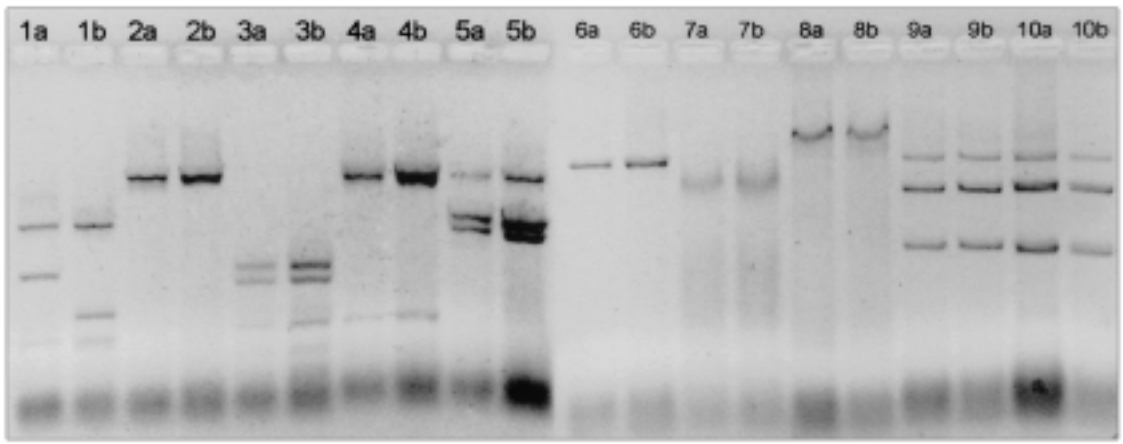

Fig. 4. ARDRA riboprints of; *U. setigera* (strain 99102305) (a**)** and *U. binucleata* (strain 01042106) (b)**,** with *Msp* I, *Xba* I, *Hae* III, *Pst* I, *Eco*R I, *Bam*H I, *Taq* I, *Kpn* I, *Hin*d III and *Eco*R V (lanes 1-10 respectively).

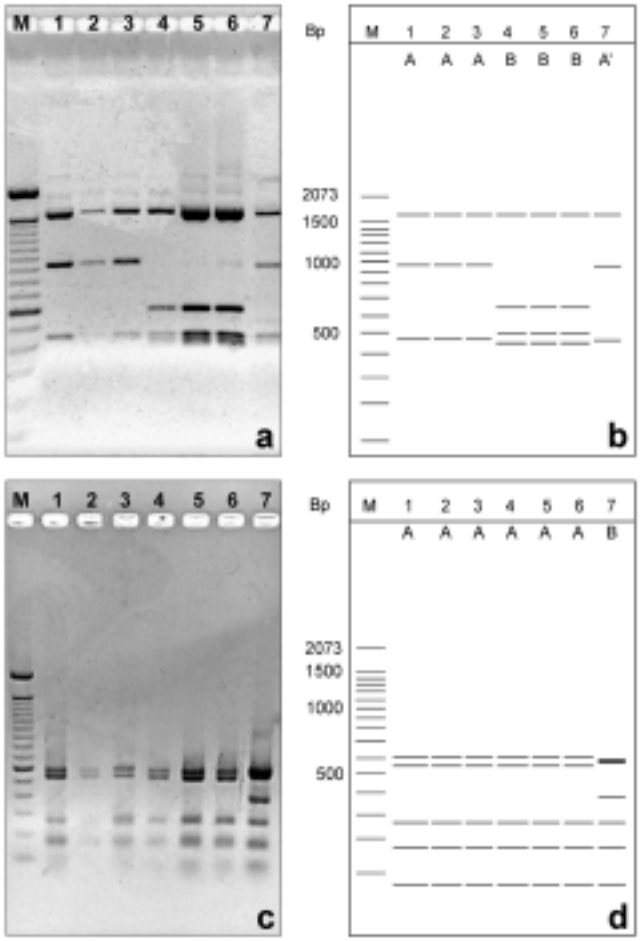

Fig. 5. ARDRA riboprint patterns and schematic representation of 7 *Uronychia* strains by *Msp* I enzymes (a, b) and by *Alu* I enzyme (c, d). Lane M - 100 bp molecular markers. Lanes 1-3 - three strains of *U. setigera* (strains 99062701, 99102305, 01041607). Lanes 4-6 - three strains of *U. binucleata* (strains 01042001, 01042106, 01051801). Lane 7 - *U. transfuga* (strain 00042803).

separate two morphospecies of the hypotrich ciliate *Gonostomum* using RAPD. Nothing is known about the DNA sequences amplified in RAPD fingerprinting, however, and specific bands cannot be associated with particular loci in the genome (Lynch 1991). Consequently RAPD data on their own are not sufficiently reliable to unambiguously identify *Uronychia setigera* or *U. binucleata*.

ARDRA

Two primers were used in order to amplify the complete small subunit (16S), and part of the large subunit (23S), ribosomal RNA gene (including internal transcribed spacers). The lengths of these amplified products were similar (*ca* 3000 bp) for each of the 7 strains. Ten restriction enzymes were used to select informative bands between two species (strain 99102305 *vs* strain 01042106) beforehand (Fig. 4). All enzymes with the exception of *Kpn* I could digest the DNA product while only *Msp* I revealed different restriction patterns between the two strains. Subsequently the amplified products were restricted with *Msp* I enzyme which revealed two kinds of patterns among the 7 strains; the 3 strains of *U. setigera* and the *U. transfuga* strain had one pattern, whereas the 3 strains of *U. binucleata* had another (Figs 5a,b). By using a second restriction enzyme (*Alu* I) it was possible to separate *U. transfuga* from *U. setigera* and *U. binucleata* since the former had a species-specific restriction band of about 400 bp which was absent in the other two (Figs 5c,d). None of the other restriction enzymes tested produced riboprints with identifiable patterns.

ARDRA riboprinting, has previously been successfully applied for the separation and identification of various protozoan taxa including species of *Entamoeba* (Clark and Diamond 1997), trypanosomes (Clark *et al*. 1995) and sibling species belonging to the *Tetrahymena pyriformis* species complex (Jerome and Lynn 1996). The results of the present study suggest that the morphologically similar *U. setigera* and *U. binucleata* can be identified among *Uronychia*-populations by their species-specific ARDRA patterns using restriction enzyme *Msp* I. Interestingly, the riboprint pattern for *U. transfuga* is similar to that of *U. setigera* (compare lanes 1-3 and lane 7, Figs 5a,b), although the two are morphologically distinct.

In conclusion, although we have shown that different strains of *Uronychia* can be characterized by the unique digestion patterns of their rDNA fragments, it cannot be stated unequivocally that these riboprints are absolutely species-specific since currently no published riboprint data are available for *Uronychia multicirrus*. Furthermore, although we were unable to separate the 3 *Uronychia* spp. using a single enzyme, *U. transfuga* could be separated from *U. setigera* and *U. binucleata* using *Alu* I, while the restriction patterns produced with *Msp* I enzyme provide a reliable basis for the identification of these latter two.

Acknowledgements. This work was supported by the "Key Program of the Education Ministry of China", the "Nature Science Foundation of China" (Project Number 30170114) and a Royal Society/NNSFC Joint Project Grant (Project Number Q822). We are grateful to Miss Huimin Shang, a graduate student of the Laboratory of Protozoology, OUC, for her assistance with the PCR procedure

and data treatment. Thanks are also due to Dr Russell Stothard (NHM) for kindly reviewing the manuscript.

REFERENCES

Agamaliev F. G. (1971) Complements to the fauna of psammophilic ciliates of the western coast of the Caspian Sea. *Acta Protozool.* **8:** 379-406

Borror A. C. (1972a) Tidal marsh ciliates (Protozoa): morphology, ecology, systematics. *Acta Protozool.* **10:** 29-71

Borror A. C. (1972b) Revision of the order Hypotrichida (Ciliophora, Protozoa). *J. Protozool.* **19:** 1-23

Buddenbrock W. (1920) Beobachtungen über einige neue oder wenig bekannte marine Infusorien. *Arch. Protistenkd.* **41:** 341-364

Bullington W. E. (1940) Some ciliates from Tortugas. *Pap. Tortugas Lab.* **32:** 179-221

Calkins C. N. (1902) Marine protozoa from Woods Hole. *Bull. U. S. Fish Comm.* **21:** 413-468

Chen Z., Song W. (2001) Phylogenetic positions of *Uronychia transfuga* and *Diophrys appendiculata* (Euplotida, Hypotrichia, Ciliophora) within hypotrichous ciliates inferred from the small subunit ribosomal RNA gene sequences. *Europ. J. Protistol.* **37:** 291-301

Chen Z., Song W., Warren A. (2000) Studies on six *Euplotes* spp. (Ciliophora: Hypotrichida) using RAPD fingerprinting, including a comparison with morphometric analyses. *Acta. Protozool*. **39:** 209-216

Claparède E., Lachmann J. (1858) Études sur les infusoires et les rhizopodes. *Mém. Ins. Nat. gen.* **5:** 1-260

Clark C. G. (1997) Riboprinting: a tool for the study of genetic diversity in microorganisms. *J. Euk. Microbiol.* **44:** 277-283

Clark C. G., Diamond L. S. (1997) Intraspecific variation and phylogenetic relationships in the genus *Entamoeba* as revealed by riboprinting. *J. Euk. Microbiol.* **44:** 142-154

Clark C. G., Martin D. S., Diamond L. S. (1995) Phylogenetic relationships among anuran trypanosomes as revealed by riboprinting. *J. Euk. Microbiol.* **42:** 92-96

Curds C. R., Wu I. C. H. (1983) A review of the Euplotidae (Hypotrichida, Ciliophora). *Bull. Br. Mus nat. Hist.* (*Zool.*) **28:** 1-63

Dirie M. F., Murphy N. B., Gardiner P. R. (1993) DNA fingerprinting of *Trypanosoma vivax* isolates rapidly identifies intraspecific relationships. *J Euk. Microbiol* **40:** 132-134

Dragesco J., Dragesco-Kernéis A. (1986) Ciliés libres de l'Afrique intertropicale. *Faune Tropicale* **26:** 1-559

Dujardin F. (1841) Histoire Naturelle des Zoophytes. Infusoires. Librairie Encylopédique de Roret, Paris

Elwood H. J., Olsen G. J., Sogin M. L. (1985) The small-subunit ribosomal RNA gene sequences from the hypotrichous ciliates *Oxytricha nova* and *Stylonychia pustulata*. *Mol. Biol. Evol.* **2:** 399-410

Fenchel T. (1965) Ciliates from Scandinavian molluscs. *Ophelia* **2:** 71-174

Foissner W., Stoeck T., Schmidt H. and Berger H. (2001) Biogeographical differences in a common soil ciliate, *Gonostomum affine* (Stein), as revealed by morphological and RAPD-fingerprint analysis. *Acta Protozool.* **40:** 83-97

Hill B. F. (1990) *Uronychia transfuga* (O. F. Müller, 1786) Stein, 1859 (Ciliophora, Hypotrichia, Uronychiidae): cortical structure and morphogenesis during division. *J. Protozool.* **37:** 99-107

Jerome C. A., Lynn D. H. (1996) Identifying and distinguishing sibling species in the *Tetrahymena pyriformis* complex (Ciliophora, Oligohymenophorea) using PCR/RFLP analysis of nuclear ribosomal DNA. *J. Euk. Microbiol.* **43:** 492-497

Kahl A. (1932) Urtiere oder Protozoa I: Wimpertiere oder Ciliata (Infusoria) 3. Spirotricha. *Tierwelt Dtl.* **25:** 399-650

Kattar M. R. (1970) Estudo dos protozoarios ciliados psamofilos do litoral Brasileiro. *Bol. Fac. Filos Cienc. Univ. S. Paulo Zool. Biol. Mar. N.S.* **27:** 123-206

Kirby H. (1934) Some ciliates from salt marshes in California. *Arch. Protistenkd.* **82:** 114-133

Kusch J. (1998) Local and temporal distribution of different genotypes of pond-dwelling *Stentor coeruleus. Protist* **149:** 147-154

Kusch J., Heckmann K. (1996) Population structure of *Euplotes* ciliates revealed by RAPD fingerprinting. *Ecoscience* **3:** 378-384

Lynch M. (1991) Analysis of population genetic structure by DNA fingerprinting. In: DNA Fingerprinting: Approaches and Applications, (Eds. T. Burk, G. Dolf, A. J. Jeffreys, R. Wolff). Birkhäuser-Verlag, Basel, 113-126

Lynch T. J., Brickner J., Nakano K. J., Orias E. (1995) Genetic map of randomly amplified DNA polymorphisms closely linked to the mating type locus of *Tetrahymena thermophila. Genetics* **141:** 1315-1325

Mansfeld K. (1923) 16 neue oder wenig bekannte marine Infusorien. *Arch. Protistenkd.* **46:** 97-140

Mathieu-Daudé F., Stevens J., Welsh J., Tibayrenc M., McClelland M. (1995) Genetic diversity and population structure of *Trypanosoma brucei*: clonality versus sexuality. *Mol. Biochem. Parasitol.* **72:** 89-101

Medlin L., Elwood H. J., Stickel S., Sogin M. L. (1988) The characterization of enzymatically amplified eukaryotic 16S-like rRNA-coding regions. *Gene* **71:** 491-499

Müller O. F. (1786) Animalcula Infusoria Fluviatilia et Marina. N. Mölleri, Hauniae

Nei M., Li W. H. (1979) Mathematical model for studying genetic variation in terms of restriction endonucleases. *Proc. Natl. Acad. Sci. USA* **76:** 5269-5273

Neto E. D., Steindel M., Passos L. K. F. (1993) The use of RAPD's for the study of the genetic diversity of *Schistosoma mansoni* and *Trypanosoma cruzi*. In: DNA Fingerprinting: State of Science (Eds. S. D. J. Pena, R. Chakraborty, J. T. Epplen, A. J. Jeffreys). Birkhäuser-Verlag, Basel, 339-345

Ozaki Y., Yagiu R. (1941) Studies on the marine ciliates of Japan, mainly from the Setonaikai (the inland sea of Japan) - I. *J. Sci. Hirosima Univ.* **10:** 21-52 (in Japanese)

Persing D. H., Smith T. F., Tenover F. C., White T. J. (1993) Diagnostic Molecular Microbiology Principles and Applications. ASM Press, Washington D. C.

Petz W., Song W., Wilbert N. (1995) Taxonomy and ecology of the ciliate fauna (Protozoa, Ciliophora) in the endopagial and pelagial of the Weddell Sea, Antarctica. *Stapfia* **40:** 1-223

Pierantoni N. (1909) Su alcuni Euplotidae del Golfo di Napoli. *Boll. Soc. Nat. Napoli* **1909:** 53-64

Quennerstedt A. (1867) Bidrag till Sveriges Infusorie-fauna. II. *Acta Univ. Lund* **4:** 1-48

Reiff I. (1968) Die genetische Determination multipler Paarungstypen bei dem Ciliaten *Uronychia transfuga* (Hypotricha, Euplotidae). *Arch. Protistenkd.* **110:** 372-397

Shang H., Chen Z., Song W. (2002) Species separation among seven *Euplotes* spp. (Protozoa: Ciliophora: Hypotrichida) using PCR/RFLP analysis of nuclear ribosomal DNA. *J. Zool. London* **258:** 375-379

Shi X., Song W. (1999) Morphogenetic studies on *Uronychia uncinata* (Ciliophora, Hypotrichida). *Acta Hydrobiol. Sin.* **23:** 146-150 (In Chinese with English summary)

Song W. (1996) Morphogenetic studies on *Uronychia uncinata* (Protozoa, Ciliophora). *Acta Oceanol. Sin.* **15:** 93-99

Song W. (1997) On the morphology and infraciliature of a new marine hypotrichous ciliate, *Uronychia multicirrus* sp. n. (Ciliophora: Hypotrichida). *Acta Protozool.* **36:** 279-285

Song W., Wilbert N. (1997) Morphological investigation on some free living ciliates (Protozoa, Ciliophora) from China sea with description of a new hypotrichous genus, *Hemigastrostyla* nov. gen. *Arch. Protistenkd.* **148:** 413-444

Song W., Shang H., Chen Z., Ma H. (2002) Comparison of some closely-related *Metanophrys*-taxa with description of a new species *Metanophrys similis* nov. spec. (Ciliophora, Scuticociliatida). *Europ. J. Protistol.* **38:** 45-53

Stein F. (1859) Der Organismus der Infusionsthiere nach eigenen Forschungen in systematischer Reihenfolge bearbeitet I. W. Engelmann, Leipzig

Stoeck T., Schmidt H. J. (1998) Fast and accurate identification of European species of the *Paramecium aurelia* complex by RAPD-fingerprinting. *Micro. Ecol.* **35:** 311-317

Stoeck T., Welter H., Seitz-Bender D., Kusch J., Schmidt H.-J. (2000) ARDRA and RAPD-fingerprinting reject the sibling species concept for the ciliate *Paramecium caudatum* (Ciliophora, Protoctista). *Zool. Script.* **29:** 75-82

Stothard J. R., Frame I. A., Carrasco H. J., Miles M. A. (2000) Analysis of genetic diversity of *Trypanosoma cruzi*: an application of riboprinting and gradient gel electrophoresis methods. *Mem. Inst. Oswaldo Cruz* **95:** 545-551

Taylor C. V. (1928) Protoplasmic reorganization of *Uronychia uncinata* sp. nov. during binary fission and regeneration. *Physiol. Zool.* **1:** 1-25

Valbonesi A., Luporini P. (1990) A new species of *Uronychia* (Ciliophora, Hypotrichida) from Antarctica: *Uronychia antarctica. Boll. Zool.* **57:** 365-367

Wallengren J. (1900) Zur Kenntnis der vergleichenden Morphologie der hypotrichen Infusorien. *Bih. K. svenska Vetensk. Akad. Handl.* **26:** 1-31

Wang C. C. (1934) Notes on the marine infusoria of Amoy. *Rep. Mar. Biol. Assoc. China* **3:** 50-70

Wang C. C., Nie D. (1932) A survey of the marine protozoa of Amoy. *Contr. Biol. Lab. Sci. Soc. China* **8:** 285-385

Wetton J., Carter R., Parkin D., Walters D. (1987) Demographic study of a wild house sparrow population by DNA fingerprinting. *Nature* **327:** 147-149

Wilbert N. (1995) Benthic ciliates of salt lakes. *Acta Protozool.* **34:** 271-288

Wilbert N., Kahan D. (1981) Ciliates of solar lake on the Red Sea shore. *Arch. Protistenkd.* **124:** 70-95

Young D. B. (1922) A contribution to the morphology and physiology of the genus *Uronychia*. *J. Exp. Zool.* **36:** 353-395

Received on 24th September, 2002; revised version on 31st January, 2003; accepted on 2nd March, 2003

Acta Protozool. (2003) 42: 91 - 97

ACTA
PROTOZOOLOGICA

Comparison of Lectin Induced Chemotactic Selection and Chemical Imprinting in *Tetrahymena pyriformis*

László KŐHIDAI, Csaba BÁNKY and György CSABA

Department of Genetics, Cell and Immunobiology, Semmelweis University Budapest, Hungary

Summary. In case of hormonal (chemical) imprinting, the first encounter of a mixed cell population with a bioactive molecule provokes changes in the receptor-signal transduction system. In case of chemotactic selection, from the mixed cell culture the chemotactically most affine cells are selected and maintained. In the present experiments chemotactic effects elicited by three lectins (Concanavalin-A = Con A, lens, Helix) were studied in *Tetrahymena pyriformis* GL unicellular model, for comparing the effect of imprinting and selection. *Tetrahymena* (without selection or imprinting) showed a molecule-dependent (positive) chemotactic reaction to lectins. Subpopulations gained by chemotactic selection were inducible in a ligand-specific scale with preference of [α-Man-α-Glu] or N-Ac-Gal specificity lectins, producing a significant affinity to Helix and non-significant affinity to Con A, and negative chemotaxis to lens. Similar results were shown in case of selection and imprinting with Con-A (except the significant affinity of mixed population), nevertheless in case of Helix and lens lectins (having similar, however not identical sugar specificity) differences had been observed between selection and imprinting. These accordances and deviations of results in imprinting and selection studies suggest that chemotaxis receptors share functional moieties with lectin receptors of unicellular organisms. The experiments call attention to the possible role of selection in the development of imprinting however, this is dependent on the nature of the imprinter molecule.

Key words: chemotactic selection, chemotaxis, hormonal imprinting, lectin, *Tetrahymena pyriformis* GL.

INTRODUCTION

Lectins are multifunctional monovalent or complex peptide-type substrates possessing carbohydrate specificity. Wide ranges of biological entities (plants, animals, bacteria or viruses) have the ability to synthesize these molecules. Their roles are very diverse as some of these ligands are essential intracellular regulatory components of the protein traffic and sorting in the rER (L-type lectins, calnexin) or in the Golgi/post-Golgi system (P type lectins), while others have role in the ER associated degradation of glycoproteins (M-type lectins). Some lectins have the ability to influence the turnover of glycoproteins; others are effector molecules of enzyme targeting (R-type lectins). Other distinct group of lectins have cell surface or extracellular matrix associated functions: several types of lectins contribute to the cell adhesion (e.g. C- and I-type lectins); others are members of the innate immunity (cell lectins) or promote

Address for correspondence: György Csaba, Department of Genetics, Cell and Immunobiology, Semmelweis University, POB 370, Nagyvárad tér 4, 1445 Budapest, Hungary; Fax: (36-1) 303-6968; E-mail: csagyor@dgci.sote.hu

cross-linking between glycan components (galectins) of the extracellular matrix (Drickamer and Taylor 1998).

Extracellular activities of lectins with their specific recognition of saccharide components provides a primordial, "immune system"-like significance of these molecules in organisms possessing no genuine humoral and cellular immune network (e.g. sponges, tunicates). Other basic cell-physiological functions like phagocytotic behaviour, the target reaction of chemotaxis, and growing of cells are also influenced by lectins at higher and lower levels of phylogeny (Agrell 1966). Chemoattractant or chemorepellent moieties of lectins are essential even on these levels; distinct subpopulations of cells are mobilized or localized by them. This activity of lectins is also detectable at unicellular level; animal and plant type lectins - Helix, Con A etc., can induce or suppress chemotactic responses of the eukaryotic ciliate *Tetrahymena pyriformis* (Kőhidai and Csaba 1996*)*. Ciliary membrane of these cells possess numerous binding sites for lectins (Pagliaro and Wolfe 1987, Csaba and Kovács 1991, Kovács *et al*. 1995, Driscoll and Hufnagel 1999), in one of the experiments sixteen Con-A binding polypeptides were demonstrated (Dentler 1992), in an other experiment the Con-A binding protein seemed to be a 66 kDa glycoprotein (Leick *et al.* 2001). Lectins are also applied to follow changes of carbohydrate composition or membrane fluidity in the ciliate surface membrane as a result of treatments with bioactive substances (Kőhidai *et al*. 1986).

Tetrahymena is a frequently used model cell in the study of cellular signaling (Csaba 1985, 1994). Its homologies to the higher vertebrates is present at membrane receptor level (i.e. insulin receptor) (Kovács and Csaba 1990a, b; Christopher and Sundermann 1995; Leick *et al*. 2001; Christensen *et al*. 2001) in intracellular second messenger systems as cAMP (Csaba and Lantos 1976), cGMP (Kőhidai *et al.* 1992), Ca-calmodulin system (Schultz *et al*. 1983; Kovács and Csaba 1987a, b), inositol lipids (Kovács and Csaba 1990a, b) and in homologies of hormonally influenced metabolic responsiveness (Kőhidai and Csaba 1985). On the basis of the mentioned characteristics was observed the hormonal imprinting, which develops at the cell's first encounter with a biologically active molecule and persists also after hundreds of generations. As a result of imprinting the binding capacity of receptors is influenced permanently as well, as signal transduction and responsiveness (Csaba 1994, 2000).

Chemotactic activity of these unicellular ciliates is one of the most essential cell-physiological properties. They can distinguish slight diversities of small and relatively big ligands i.e. amino acids (Levandowsky *et al.* 1984) and insulins (Csaba *et al.* 1994). Chemotactic selection, a recently developed technique provides the possibility to select these cells upon their chemotactic responsiveness towards bioactive molecules (e.g. hormones or chemokines) (Kőhidai and Csaba 1998, Kőhidai *et al.* 2000). Selected subpopulations are dedicated groups of cells for studying backgrounds of chemotaxis, short- and long-term signalling in eukaryotic models (Kőhidai 1999).

On the basis of the above described phylogenetical and cell-physiological characteristics of lectins in the present study our objectives were: (i) to study ability of lectins to select subpopulations *via* their chemotactic potency; (ii) to study the effect of pretreatments (imprinting) with lectins on the chemotactic responsiveness of subpopulations; (iii) to compare the results of imprinting and chemotactic selection.

MATERIALS AND METHODS

Cells and culturing

Cells of *Tetrahymena pyriformis* GL strain were maintained in axenic cultures containing 1% tryptone (Difco, Michigan, USA) and 0.1% yeast extract, without addition of antibiotics, at 28 °C. According to the certificate analysis, the two basic components of media were free of lectins. However, the potential of interference of the used lectins with the media composing peptides is given, the non-synthetic type of media was used as our earlier experiments (Kőhidai and Csaba 1998, Kőhidai 1999) and reference works of the chemotaxis-literature of *Tetrahymena* were done in such systems (Almagor *et al.* 1981, Francis and Hennessey 1995, Kuruvilla and Hennessey 2001). Cultures were in logarithmic phase of growth; density of samples was 10^4 cells/ml.

Chemicals and buffers

The studied lectins were purified from plants *Canavalia ensiformis* (Con A), *Lens culinaris* (lens) and snail *Helix pomatia* (Helix). All the three lectins were obtained from Sigma Chemical Co., St. Louis, MO, USA. In the experiments (PBS), 0.05 M phosphate buffer containing 0.9% NaCl at pH 7.2 was also used.

Chemotaxis assay

The chemotactic ability of cells was determined in a two-chamber capillary assay system modified by us (Kőhidai *et al.* 1995). According to this setup tips of a multi-8-channel automatic pipette served as an inner chamber to minimize the standard error of sampling, while microtitration plates were used as outer chambers. The outer chamber was filled with the cells to be tested; the inner one contained the test substance of the lectins. In control experiments culture medium was

used as attractant (absolute control). For validation of the assay two chemoattractants 10^{-9} M f-Met-Leu-Phe (f-MLF; Sigma, St. Louis, USA) and 10^{-11} M interleukin-8 (IL-8; Promega, Madison, USA) were also tested as positive controls. After 15 min incubation the samples of inner chambers, containing the chemotactically positive responder cells, were fixed in 4% formaldehyde containing PBS. The samples were evaluated in a Neubauer hemocytometer.

Chemotactic selection

This technique deals with the chemotactic capacity of different signal molecules to form sub-populations from mixed cultures of cells. First we applied the chemotaxis assay (see above). The inner chamber of the system contained the test substance of the lectins (10^{-9} M in case of Con-A and 10^{-6} M in case of lens and Helix). In control experiments culture medium was used as attractant (absolute control). At the end of incubation, the positive responder cells were transferred to fresh culture medium for cultivation. Both cultures selected with a lectin (in general L) and controls (C) were consecutively transferred in every 48 h. The chemotactic response of cultures was studied again after one week in the following combinations: L/L - cells selected with the lectin in the first run and assayed to the signal substance in the second run; L/C - cells selected with the lectin in the first run and assayed to the control substance in the second run; C/L - cells selected with the control substance in the first run and assayed to the signal substance in the second run; C/C - cells selected with the control substance in the first run and assayed to the control substance in the second run.

Pretreatment (imprinting) with lectins

Tetrahymena cells were pretreated with 10^{-6} M lectins (Con A, lens and Helix) for 1 h at room temperature. Controls were treated with fresh culture medium. After treatments the samples were washed trice with PBS and then aliquots of cell-suspensions were transferred into fresh culture medium. Pretreated and control cultures were transferred consecutively in every 48 h. After one week chemotactic responsiveness of cultures was tested by the chemotaxis assay described above. Similar combinations were applied as in the chemotactic selection study: C/C, C/L, L/C, L/L (abbreviations are given above).

Statistical evaluation

Each lectin was tested in ten replica assays, the figures demonstrate the averages of these results. The statistical analysis was done by ANOVA of Origin 4.0.

RESULTS AND DISCUSSION

In an earlier experiment (Kőhidai and Csaba 1996) all the three investigated lectins proved to have chemoattractant ability, however the concentration optimum was characteristic to each chemoattractant ligand (Table 1). The effective chemoattractant concentration was wide in the case of both plant lectins. In the case of the Con A - possessing α-mannose and α-glucose specificity - a two-peak (10^{-9} and 10^{-6} M) dose-dependency was detected with the peak at 10^{-9} M. In contrast, the α-mannose specific lens lectin had a wide range chemoattractant character, its maximal chemoattractant effect was elicited only in the higher concentration range at 10^{-6} M. Profile of concentration dependency of chemotaxis elicited by the N-acetyl-galactose-amine specific Helix lectin was similar to lens, its maximal chemoattractant effect was observed also at the highest tested concentration (10^{-6} M). In this study Helix proved to be the only chemorepellent lectin, this negative responsiveness of the model cells was elicited at 10^{-11} M. The most positively effective concentration was chosen for the chemotactic selection assay in each case.

Table 1. Concentration course study on chemotactic activity of three lectins in *Tetrahymena pyriformis* GL cells. (x- $p<0.05$; y- $p<0.01$; z- $p<0.001$).

Conc. log molar [M]	Con A [%]	Lens [%]	Helix [%]
-12	120^{x}	127^{y}	106
-11	109	109	79
-10	128^{x}	154^{y}	98
-9	159^{y}	172^{y}	131^{x}
-8	144^{y}	209^{z}	137^{x}
-7	131^{y}	190^{y}	167^{y}
-6	150^{y}	227^{z}	181^{y}

Chemotactic selection provides the possibility to distinguish signaling mechanisms used by different ligands. In classical way chemotaxis is a result of a specific interaction of ligands and their receptors in the plasma membrane. As a consequence of the downstream signaling in the cytoplasm reorganisation of cytoskeletal network is triggered and migratory behaviour of cells is changed. Dynamic presence of chemotaxis-receptor components can determine consistence of chemotactic responsiveness in progeny generations, unstable structure or fast turn-over of some binding sites make them responsible for "short-term" chemotactic responsiveness, while other fixed, constant and genetically well preserved units of the plasma membrane might work as receptors of "long-term" acting chemoattractant ligands. During chemotactic selection the most responsive cells are selected and maintained, forming a special group of the original cell population.

In the present study the three lectins could select subpopulations chemotactically in different ways (Fig. 1). Chemotactic responses were detected in sub-

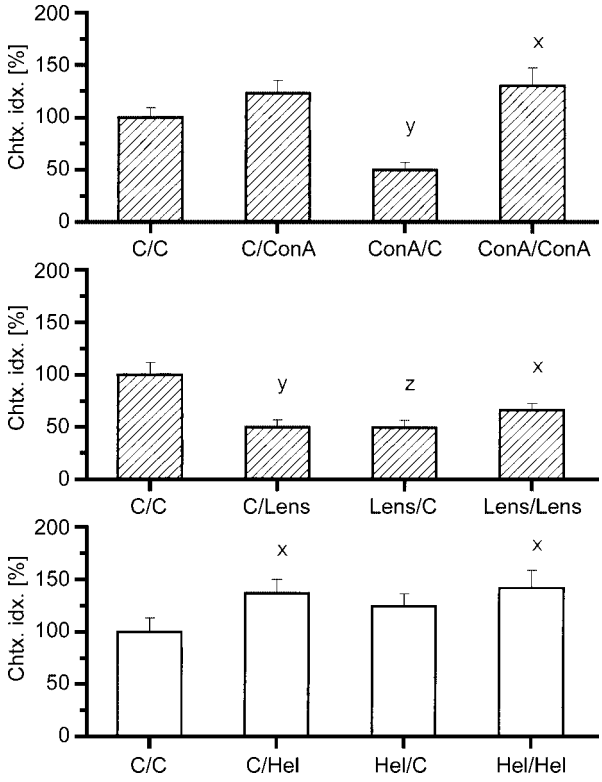

Fig. 1. Chemotactic selection of *Tetrahymena* cells with lectins (Con A, lens, Helix). Chemotactic responsiveness of cells selected with the identical lectin (L) or the control substance (C) was assayed in four combinations: the first letter refers to the type of ligand applied at selection; the second letter refers to the ligand used at the second chemotaxis assay 1 week after selection. (x- $p<0.05$; y- $p<0.01$; z- $p<0.001$).

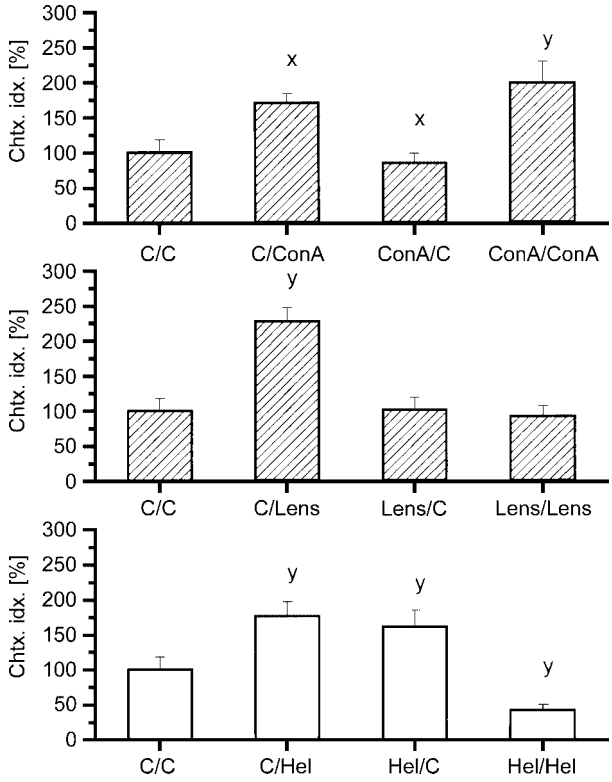

Fig. 2. Effect of imprinting with 10^{-6} M lectins (Con A, lens, Helix) on *Tetrahymena*. Chemotactic responsiveness of pretreated cells with the identical lectin (L) or the control substance (C) was assayed in four combinations: the first letter refers to the type of ligand applied at pretreatments; the second letter refers to the ligand used at the second chemotaxis assay 1 week after pretreatments. (x- $p<0.05$; y- $p<0.01$; z- $p<0.001$).

populations selected with the plain culture medium. We considered these results as relative controls of the successful chemotaxis assay with the identical lectin. However, it was found that the chemotactic potency and activity of the subpopulations selected with chemotaxis was characteristically different. In control-medium-selected cells, the control medium itself (composed of tryptone and yeast extract) was observed to have a potent selector effect on *Tetrahymena*. Comparing the results of our selection a study determining different chemotactic responses of *Tetrahymena* with varying concentration courses of the same lectins shows that the response of cells selected with this control substance was ligand-dependent. In the present experiment the responsiveness was decreased with Con A (159% *vs.* 122.9%; not significant) and lens (227 *vs.* 49.8; $p<0.01$) and increased with Helix (136.9%; *vs.* 181.2% $p<0.05$).

Subpopulations selected with lectins expressed also ligand-dependent responsiveness. Chemotactic responsiveness of subpopulations selected with Con A or lens sharing in ligand-specificity to a-mannose was significantly decreased (Con A/C and lens/C), while a moderate, increased chemotactic ability (124.7%) was detected in subpopulations selected with the oligosaccharide specific Helix lectin (Hel/C).

Results of the repeated encounter with the selector lectin showed that the diverse membrane level changes responsible for different forms of chemotactic responsiveness in selection studies are detectable even for lectin-type ligands. In Con A selected group (Con A/Con A) the identical lectin could elicit a statistically significant and increased chemotactic response, while lens lectin (lens/lens) could not induce positive response, in contrast, the selected subpopulation showed negative chemotactic behaviour to the lens lectin. Subpopulations selected with Helix lectin expressed positive chemotaxis towards the selector ligand, however this activity of cells was not enhanced compared to their relative controls

(Hel/Hel = 142% *vs*. Hel/C = 124.7% or C/Hel = 136.9%). The considerable range in the effect of the two monosaccharide specific lectins (Con A/Con A = 129.9% *vs*. lens/lens = 66.2%) suggests that in the fine adjustment of chemotactic signaling carbohydrate moieties of the membrane play also important role. Data obtained suggest that in our ciliated model a concurrent α-mannose and α-glucose binding is required for induction responses of long-term selection, while the single α-mannose specific binding fails to do so. On the other hand, relative positive effectiveness of Helix lectin raise the possibility that plasma membrane is furnished with constant, however non-inducible constituents e.g. N-acetyl-galactose-amine residues.

While in case of chemotactic selection a rapid incubation is used to assort cells from a mixed population with high responsiveness, in case of imprinting (pretreatment) with biologically active substances are still applied to a mixed population to tune/adjust cells in a time- and concentration-dependent way, however the investigated cultures are still mixed. Series of former experiments proved that *Tetrahymena* is a sensitive model for imprinting; long-lasting or transient modifications of the plasma membrane were characterized in binding studies with hormones (Kovács *et al.*1984) or lectins (Csaba and Kovács 2000). In the present experiment our goal was to evaluate whether the lectin induced chemotactic selection and imprinting have homologies or deviations in signaling.

In this setup chemotactic responsiveness of lectin-pretreated cells was tested to the identical lectin used for imprinting or to the fresh culture medium as control. To validate the experiments an absolute control (C/C) and a second control (C/L) were applied, in which the chemoattractant ability of the used lectin was tested. Proper sensitivity of our system was confirmed by the significant positive chemotactic indices of all the three second controls (C/Con A, C/lens and C/Hel) (Fig. 2).

In case of Con A, imprinting had dual effect: the pretreated cells expressed an increased chemotactic responsiveness to Con A at the second encounter (Con A/Con A=198.4%), while the plain culture medium was recognized as chemorepellent (Con A/C = 84.6%).

Lens lectin could not induce long-lasting positive effects like Con A. Pretreatment with lens abolished the positive chemotactic responsiveness of *Tetrahymena* cells to the lectin (lens/lens = 92.3%), nevertheless a decrease in the native chemotactic ability of the lens pretreated cells (lens/lens = 92.3% or lens/C = 101.2% *vs*. C/lens = 227.2%) was also detected.

Pretreatments with *Helix* lectin presented also a unique and characteristic outcome. In contrast Con A and lens lectins the native chemotactic activity of the Helix pretreated cultures (Hel/C = 160.7%) was enhanced, whereas we failed to apply the identical lectin as a chemoattractant ligand, it worked as a very strong chemorepellent substance (Hel/Hel = 42%), what means that a negative imprinting developed.

As it was presented above, interaction of the three lectins with the target cells has a long lasting effect considering their chemotactic ability. Results of repeated encounters with the ligand applied at the pretreatment suggest that lectins possessing slight diversities in carbohydrate specificity (see variance of α-glucose specificity of Con A to lens) can result an increase or decrease of chemotaxis receptors however, the diversity in the protein configurations of lectins also have to be considered, as this can also influence the affinity or repellence. This means that only the comparison of the results gained by imprinting or selection leads to clear and exact conclusions, the results of inter-lectin comparison suggest only possible explanations. One of this explanations is that while selection of sensitive cells might have a role in the development of imprinting (e.g in case of Con-A), this is not regular, as other factors also could play a role, which turned to negative imprinting of the positive selection (e.g. in case of Helix lectin).

Cultures of the present study were maintained for one week after pretreatments, the reexposed cells, due to the short cell cycle of *Tetrahymena*, were ~70th generation of the culture, this made possible to study long-term persisting receptors and the associated activities. Potential significance of lectin receptors in chemotaxis- working as a probable subclass of chemotaxis receptors - is underlined in two reasons (i) the investigated group of lectins could characteristically induce the expression of saccharide components of the plasma membrane capable as components of the responsible binding sites (e.g. coexistence of α-mannose and α-glucose is required for the positive outcome) and (ii) can elicit chemotactic responses in a high carbohydrate-specific manner (e.g. the amino-sugar N-acetyl-galactose-amine linked signaling could "freeze" the required chemotactic pathways).

Comparison of results gained by chemotactic selection and pretreatment show that ligands e.g. lectins, possessing deep phylogenetical backgrounds have molecule-specific potency to act as chemotactic agents. Chemotactic responsiveness induced by imprinting has similarities and diversities to chemotactic selection: con-

gruence of positive Con A/Con A results of the two different experiments raises the possibility that imprinting might have a selector capacity, too; however other ligand (Helix lectin) could work also as a good selector but a reversed, negative effect was registered after imprinting. It is not unusual that different lectins having similar sugar affinity disparately influence cell functions: this was observed in case of cell aggregation (Csaba and Kovács 1991), and conjugation (Ofer *et al.* 1976).

In conclusion, present data point out that three lectins, that are phylogenetically ancient signal molecules, can elicit molecule-specific chemoattractant responses in unicellular model. Investigations of chemotactic selection and imprinting with the lectins call attention that chemotaxis is based upon fine receptor-ligand interactions and that carbohydrate moieties are potent functional components of chemotaxis receptors. In earlier experiments similar phenomenon was demonstrated in case of insulin receptors (Kovács *et al.* 1987, 1996). The experiments demonstrate that in contrast to the similarities in the provocation of reaction (treatment with a bioactive molecule and study of later response), the selected population can show similar or disparate reaction in chemotactic assay, depending on the sugar affinity (and maybe on the protein structure) of the provoking molecule.

Molecular-genetic backgrounds of the described phenomena is still obscure. As both selection and pretreatments have the potency to interfere with the genetic mechanisms of this protozoon, causing changes in long-term cell-physiological responsiveness, we intend to broaden our analysis into genetic aspects.

Acknowledgements. This work was supported by grant from the Hungarian Research Fund (OTKA, T032533 and T037303).

REFERENCES

Agrell I. P. (1966) Phytohaemagglutinin as a mitotic stimulator on free-living amoebae. *Exp. Cell Res*. **42:** 403-406

Almagor M., Ron A., Bar-Tana J. (1981) Chemotaxis in *Tetrahymena thermophila. Cell Motil.* **1:** 261-268

Christensen S.T, Guerra C. F., Awan A. (2001) Insulin-like receptors in *Tetrahymena thermophila. Mol. Biol. Cell.* **12:** Suppl. 2446

Christopher G. K., Sundermann C. A. (1995) Isolation and partial characterization of the insulin binding sites of *Tetrahymena pyriformis. Biochem. Biophys. Res. Commun*. **212:** 515-523

Csaba G. (1985) The unicellular *Tetrahymena* as a model cell for receptor research. *Int. Rev. Cytol.* **95:** 327-377

Csaba G. (1994) Phylogeny and ontogeny of chemical signaling: origin and development of hormone receptors. *Int. Rev. Cytol.* **155:** 1-48

Csaba G. (2000) Hormonal imprinting: its role during the evolution and development of hormones and receptors. *Cell Biol. Int.* **24:** 407-414

Csaba G., Kovács P. (1991) Binding of lectins (Con-A, lens, helix, PHA) to binding sites induced in *Tetrahymena* by insulin and lectins. *Acta Microbiol. Hung.* **38:** 29-32

Csaba G., Kovács P. (2000) Insulin uptake, localization and production in previously insulin treated and untreated *Tetrahymena*. Data on the mechanism of hormonal imprinting. *Cell Biochem. Funct.* **18:** 161-167

Csaba G., Lantos T. (1976) Effect of cAMP and theophylline on phagocytotic activity of *Tetrahymena pyriformis. Experientia* **32:** 321

Csaba G., Kovács, P., Kőhidai L. (1994) *Tetrahymena* cells distinguish insulins according to their amorphous and crystalline condition or their bovine and porcine origin. Study of imprinting in aspects of hormone binding and chemotaxis. *Microbios* **80:** 215-221

Dentler W. L. (1992) Identification of *Tetrahymena* surface proteins labeled with sulfosuccinimidyl 6-(biotinamido) hexanoate and Concanavalin A and fractionated with Triton X-114. *J. Protozool.* **39:** 368-378

Drickamer K., Taylor M. E. (1998) Evolving views of protein glycosilation. *Trends Biochem. Sci.* **23:** 321-324

Driscoll C., Hufnagel L. A. (1999) Affinity purification of Concanavalin A-binding ciliary glycoconjugates of starved and feeding *Tetrahymena thermophila. J. Euk. Microbiol*. **46:** 142-146

Francis J. T., Hennessey T. M. (1995) Chemorepellents in *Paramecium* and *Tetrahymena. J. Euk. Microbiol*. **42:** 78-83

Kovács P., Csaba G. (1987a) Cytochemical investigation into the Ca-dependence of positive and negative hormonal imprinting in *Tetrahymena. Histochemistry* **87:** 619-622

Kovács P., Csaba G. (1987b) The role of Ca^{2+} in hormonal imprinting of the *Tetrahymena. Acta Physiol. Hung.* **69:** 167-179

Kovács P., Csaba G. (1990a) Evidence of the receptor nature of the binding sites induced in *Tetrahymena* by insulin treatment. A quantitative cytofluorimetric technique for the study of binding kinetics. *Cell Biochem. Funct*. **8:** 49-56

Kovács P., Csaba G. (1990b) Involvement of the phosphoinositol (PI) system in the mechanism of hormonal imprinting. *Biochem. Biophys. Res. Comm.* **170:** 119-126

Kovács P., Csaba G., Lászlo V. (1984) Study of the imprinting and overlap of insulin and concanavalin-A at the receptor level in a protozoan (*Tetrahymena*) model system. *Acta Physiol. Hung*. **64:** 19-23

Kovács P., Csaba G., Darvas Z., Liszkay G. (1987) Effect of modification of membrane saccharides on hormonal imprinting in *Tetrahymena. Acta Physiol. Hung.* **69:** 189-195

Kovács P., Sundermann C., Estridge B. H. Csaba G. (1995) A confocal microscopic evaluation of the effects of insulin imprinting on the binding of Concanavalin A. *Cell Biol. Int.* **19:** 973-978

Kovács P., Sundermann C. A., Csaba G. (1996) Investigations of receptor-mediated phagocytosis by hormone-induced (imprinted) *Tetrahymena pyriformis. Experientia* **52:** 769-773

Kőhidai L. (1999) Chemotaxis: The proper physiological response to evaluate phylogeny of signal molecules. *Acta Biol. Hung.* **50:** 375-394

Kőhidai L., Csaba G. (1985) Effects of insulin and histamine in themselves and in combination on the glucose metabolism of *Tetrahymena. Acta Biol. Hung*. **36:** 281-285

Kőhidai L., Csaba G. (1996) Different and selective chemotactic responses of *Tetrahymena pyriformis* to two families of signal molecules: lectins and peptide hormones. *Acta Microbiol. Immunol. Hung.* **43:** 83-91

Kőhidai L. Csaba G. (1998) Chemotaxis and chemotactic selection induced with cytokines (IL-8, RANTES and TNFa) in the unicellular *Tetrahymena pyriformis. Cytokine* **10:** 481-486

Kőhidai L., Kovács P., Nozawa Y., Csaba G. (1986) Effects of membrane fluidity changes on lectin binding of *Tetrahymena pyriformis*. *Cell. Mol. Biol.* **32:** 303-308

Kőhidai L., Barsony J., Roth J., Marx S. J. (1992) Rapid effects of insulin on cyclic GMP location in an intact protozoan. *Experientia* **48:** 476-481

Kőhidai L., Lemberkovits É., Csaba G. (1995) Molecule dependent chemotactic responses of *Tetrahymena pyriformis* elicited by volatile oils. *Acta Protozool*. **34:** 181-185

Kőhidai L., Schiess N., Csaba G. (2000) Chemotactic selection of *Tetrahymena pyriformis* GL induced with histamine, diiodotyrosine or insulin. *Comp. Biochem. Physiol*. **126C:** 1-9

Kuruvilla H. G. and Hennessey T. M. (2001) Purification and characterization of a novel chemorepellent receptor from *Tetrahymena thermophila. J. Membr. Biol*. **162:** 51-57

Leick V., Bog-Hansen T. C., Juhl H. A. (2001) Insulin/FGF-binding ciliary membrane glycoprotein from *Tetrahymena. J. Membr. Biol*. **181:** 47-53

Levandowsky M., Cheng T., Kehr A., Kim J., Gardner L., Silvern L., Tsang L., Lai G., Chung C., Prakash E. (1984) Chemosensory responses to amino acids and certain amines by the ciliate *Tetrahymena*: a flat capillary assay. *Biol. Bull*. **167:** 322-330

Ofer L., Levkovitz H., Loyter A. (1976) Conjugation in *Tetrahymena pyriformis*. The effect of polylysine, Concanavalin A, and bivalent metals on the conjugation process. *J. Cell Biol*. **70:** 287-293

Pagliaro L., Wolfe J. (1987) Concanavalin A binding induces association of possible mating-type receptors with the cytoskeleton in Tetrahymena. *Exp. Cell Res*. **168:** 138-152

Schultz J. E., Schönfeld W., Klumpp S. (1983) Calcium/calmodulin-regulated guanylate cyclase and calcium-permeability in the ciliary membrane from *Tetrahymena. Eur. J. Biochem*. **137:** 89-94

Received on 4th October, 2002; revised version on 24th January, 2003; accepted 4th February, 2003

Acta Protozool. (2003) 42: 99 - 104

ACTA
PROTOZOOLOGICA

Population Dynamics and Food Preferences of the Testate Amoeba *Nebela tincta major-bohemica-collaris* Complex (Protozoa) in a *Sphagnum* Peatland

Daniel Gilbert[1], Edward A. D. Mitchell[2], Christian Amblard[3], Gilles Bourdier[3] and André-Jean Francez[4]

[1]Laboratoire de Biologie et Écophysiologie, USC INRA, Université de Franche-Comté, Besançon, France; [2]Department of Biological Sciences, University of Alaska Anchorage, Anchorage, U.S.A.; [3]Laboratoire de Biologie Comparée des Protistes, UMR CNRS, Université de Clermont-Ferrand, Aubière Cedex, France; [4]Equipe Interactions Biologiques et Transferts de Matière, UMR CNRS Ecobio, Université de Rennes I, Rennes Cedex, France

Summary. Population dynamics and food preferences of the testate amoeba species complex *Nebela tincta major-bohemica-collaris ("Nebela collaris sensu lato")* were described from a *Sphagnum* peatland over one growing season. The average abundance of *Nebela collaris sensu lato* was 29582 ind. l^{-1} active, and 2263 ind. l^{-1} encysted forms. On average, 17.4% of *Nebela collaris sensu lato* specimens were observed associated with prey, 71% of which could not be identified because of their poor preservation state. Among the identified prey, those most frequently ingested were micro-algae (45% of the total predator-prey associations, especially diatoms: 33%), and spores and mycelia of fungi (36%). Large ciliates, rotifers and small testate amoebae were also ingested, but mainly in summer. The seasonal variations in the proportions of prey categories in the ecosystem and the percentage of identifiable prey lead us to hypothesise that (1) *Nebela collaris sensu lato* ingest mainly immobile, senescent or dead organisms, and (2) that the more mobile micro-organisms such as ciliates and micro-Metazoa become more accessible, in relatively dry conditions, when the water film is thin.

Key words: microbial food web, Nebelidae, population dynamics, Rhizopoda, soil micro-organisms, Wetland.

INTRODUCTION

In aquatic environments, knowledge on the trophic interactions within microbial food webs has benefited from the use of artificial or fluorescent-labelled prey. This approach is used to study the bacterivorous activity of micro-organisms in marine and lacustrine pelagic ecosystems (Borsheim 1984, Pace and Bailiff 1987, Sanders *et al.* 1989, Simek *et al.* 1990, Carrias *et al.* 1996). More recently the same principle has been applied using labelled eukaryotes (Premke and Arndt 2000). By contrast in environments where an interface between the solid and liquid exists (including the benthic zone of fresh- and salt-water bodies in aquatic ecosystems, the upper horizons of soils in terrestrial ecosystems, bryophytes, and lichens) these techniques are difficult to use mainly because many predators feed on

Address for correspondence: Daniel Gilbert, Laboratoire de Biologie et Écophysiologie, EA 3184, USC INRA, Université de Franche-Comté, F-25030 Besançon, France; Fax: (33) (0) 381665797; E-mail: daniel.gilbert@univ-fcomte.fr

fixed and/or mobile prey and that the potential range of these prey is impossible to reconstruct artificially.

As a result, although the functional importance of the microbial loop has been established in several interface environments such as soils (Clarholm 1994, Coleman 1994, Bonkowski and Brandt 2002), and peatlands (Gilbert *et al*. 1998a, b), little data is available on the feeding habits of protozoa in these environments. Information on the feeding habit of testate amoebae especially is very scarce (Coûteaux and Pussard 1983, Coûteaux 1984, Chardez 1985, Yeates and Foissner 1995, Gilbert *et al*. 2000), although this group represents an important part of the protozoan biomass in these interfaces (Gilbert *et al*. 1998a, b; Mitchell *et al.* 2003). This study therefore aimed at establishing the feeding habits of one of the most abundant testate amoeba group in *Sphagnum* peatland, the *Nebela tincta major-bohemica-collaris* complex (hereafter "*Nebela collaris sensu lato*") (Deflandre 1936, Heal 1964, Warner 1987), in natural conditions, in relation to the seasonal dynamics of their potential prey.

MATERIALS AND METHODS

The study was carried out in the Pradeaux peatland (Puy de Dôme, France, 3°55 E, 45°32 N, altitude 1350 m. a. s. l.), a drained *Carex rostrata/Sphagnum fallax* fen covering a surface of 10 ha (Francez 1992).

Three PVC tubes 25 cm in diameter and 30 cm in length were permanently inserted vertically in the peat in macroscopically identical locations in order to get triplicate measurements. Once a month, from April to November 1995, 50 ml water samples were collected in each tube by pressing the moss surface with a sieve (mesh size 1.5 mm) and sucking the water up with a syringe. During each site visit pH and conductivity were measured *in situ* with a Chekmate M90 multiparametric probe (pH: ± 0.01 unit; conductivity: ± 0.01 μScm^{-2}). Water levels were measured with 30 cm piezometers inserted in the peat. Because of the high water holding capacity of *Sphagnum* and the relatively high water table levels it was possible to sample water every month except in August. This method, which was already used by Grolière (1977) for ciliates and by Francez (1988) for rotifera, allows the recovery of most microorganisms. However, this method probably underestimates the densities of at least some microbial groups because they may be attached to the *Sphagnum* mosses, or because they may be living inside the large, empty cells of *Sphagnum* called hyalocysts. Conversely, an advantage of this method is that as the *Sphagnum* carpet is very little affected by the sampling, repeated sampling at the exact same place is possible. This is important because fine-scale heterogeneity in testate amoeba distributions may occur even in a macroscopically homogeneous *Sphagnum* moss carpet (Mitchell *et al.* 2000). The water samples were fixed with glutaraldehyde (2% final concentration) and stored at 4°C in the dark. Cyanobacteria, fungi, micro-algae, protozoa, rotifers, and nematodes were identified using a sedimentation (plankton) chamber and an inverted microscope (Utermöhl 1958). Biovolumes of morphotypes within each community were estimated by assuming geometric shapes and converted to biomass using conversion factor according to Gilbert *et al.* (1998a).

For each sample, we observed a minimum of 20 specimens of *Nebela collaris sensu lato* (total for this study: 684 active or encysted specimens). Among the active specimens, we distinguished those with an attached prey. We defined as "prey" any organic matter particle, even if precise identification was not possible because of poor preservation (e.g. decomposed organic matter or partly decomposed micro-organisms). The glutaraldehyde solution fixes efficiently all micro-organisms and we were able to verify that this method does not separate the prey from the predator, even after homogenizing the sample through the vortex.

RESULTS AND DISCUSSION

Physico-chemical environment

The water table level fluctuates during the year according to the relative importance of precipitations and evapotranspiration and the drainage of the site. These fluctuations are especially important in the case of drained peatlands such as the site we studied. At our site, the water table level remained high in spring (11 cm below the surface of the moss carpet). It then became gradually lower, until the beginning of summer when it reached 19.3 cm. During August, the water table fell below 30 cm, and it was impossible to sample surface water. The autumn rainfall did not fully compensate for this water deficit and the water level had only risen to 14 cm by November (Table 1). The water temperature at the surface of the peatland fluctuated between 0.7 and 24.4°C during the course of the study. The mean values for water pH and conductivity were 4.7 and 43.1 μScm^{-2} respectively. The concentration of dissolved oxygen fluctuated between 2.0 mg l^{-1} in June and 9.8 mg l^{-1} in November (Table 1). The dissolved oxygen concentration was logically negatively correlated to water temperature ($n = 12$, $r = -0.99$, $P < 0.001$). The conductivity was also negatively correlated to water temperature ($n = 18$, $r = -0.457$, $P = 0.05$), probably because the activity of *Sphagnum*, and therefore the nutrient uptake, increases with the temperature.

Population dynamics

Nebela collaris sensu lato was regularly present in *Sphagnum* mosses (averages: 29582 ± 9650 ind l^{-1}, for the active forms, and 2263 ± 1620 ind l^{-1}, for the encysted forms) (Fig. 1). The highest abundance of active

Table 1. Temporal variations in physico-chemical variables (mean ± SE, ND not determined).

Months	Water table depth (cm)	Temperature (°C)	pH	Dissolved oxygen (mg l^{-1})	Conductivity (µS cm^{-2})
April	11.0 ± 2.6	5.4 ± 0.6	4.5 ± 0.2	ND	56.4 ± 4.7
May	14.0 ± 2.0	13.2 ± 0.5	4.7 ± 0.1	5.8 ± 0.6	33.7 ± 8.6
June	16.3 ± 4.7	20.7 ± 0.1	4.5 ± 0.0	2.1 ± 0.2	26.7 ± 3.9
July	19.3 ± 2.1	19.8 ± 0.6	4.4 ± 0.2	ND	48.5 ± 7.0
August	> 30.0 ± 0.0	ND	ND	ND	ND
September	22.3 ± 2.5	ND	ND	ND	ND
October	22.3 ± 3.5	11.9 ± 0.4	4.3 ± 0.1	6.3 ± 0.2	47.2 ± 11.5
November	14.3 ± 2.1	6.7 ± 0.6	5.4 ± 0.2	9.5 ± 0.1	43.6 ± 10.7

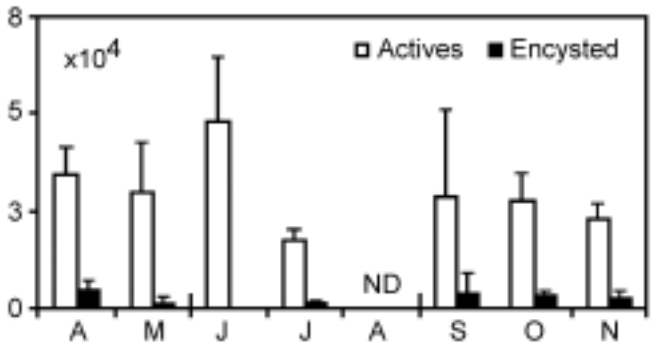

Fig. 1. Temporal variations of the abundance (ind. l^{-1}) of active and encysted *Nebela tincta major-bohemica-collaris* complex (ND - not determined).

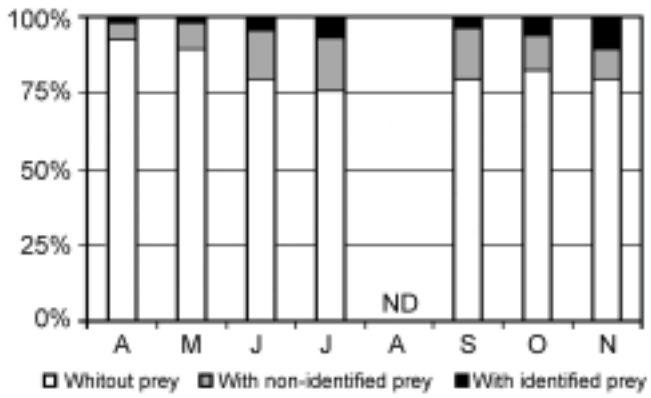

Fig. 2. Temporal variations of the relative proportion (%) of *Nebela tincta major-bohemica-collaris* complex individuals associated with a prey (ND - not determined).

forms was observed at the end of June (up to 37947 ± 9843 ind. l^{-1}) and the lowest in July (13172 ± 3137 ind. l^{-1}) (Fig. 1). This pattern seems to be characteristic for drained peatland, with winters being too cold and summers being too dry for microbial development Similar temporal patterns were described before in *Sphagnum* for microalgae (Schoenberg and Oliver 1988) and ciliates (Grolière 1977). In the same way, the encysted forms were most abundant at the beginning of spring (4634 ± 2347 ind. l^{-1} in April) when the water temperatures were still low, and after the dry period (mean for September, October and November: 2934 ± 2845 ind. l^{-1}) (Fig. 1). Cyst abundance was negatively correlated with temperature (r = -0.86, P = 0.03) and positively correlated with conductivity (r = 0.86, P = 0.03).

Seasonal feeding activity and general feeding habits

The frequencies of *Nebela collaris sensu lato* specimens observed associated with a prey (M=17.4 ± 6.0%) were low in spring (8.0% in April), rising until July (24.1%), and then decreasing in autumn (Fig. 2). However, these variations were not significant, and the number of specimens observed in association with a prey was positively correlated with the number of active individuals (n = 21, r = 0.53, P = 0.01). Thus our data suggest that the fraction of *Nebela collaris sensu lato* actively feeding is relatively constant throughout the year.

Among the identified prey, those most frequently ingested were micro-algae (45% of the total identified predator-prey associations, especially diatoms 33%), and spores and mycelia of fungi (36%). Predation on large ciliates (12%), rotifers (3%) and small testate amoebae (4%, among which *Trinema* spp. and *Euglypha* spp.) appeared to be more marginal (Figs 3, 4). However, on average, 71 ± 27% of the prey could not be identified because of their poor preservation state. These unidentified prey were most likely *Sphagnum* leaf fragments, other plant cells, or prey without rigid skeleton, such as green algae, ciliates, and most bdelloïd

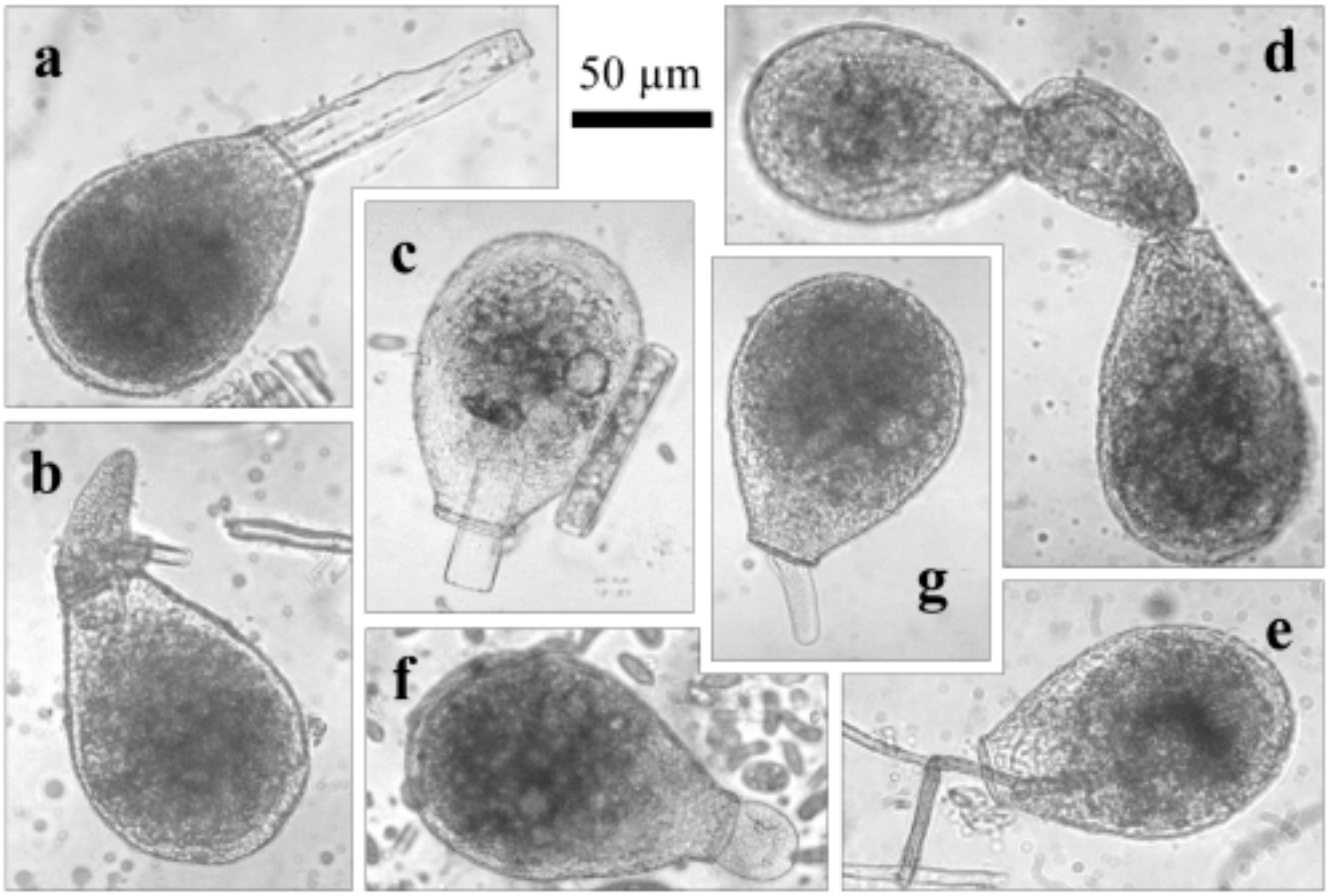

Figs 3 a-g. *Nebela tincta major-bohemica-collaris* complex associated with; **a** - plant cell; **b** - ciliate; **c** - diatom; **d** - rotifer; **e** -fungi mycelium; **f** - testate amoeba; **g** - individual without prey.

rotifers. Fungi spores and mycelia as well as diatoms and testate amoebae were easily identifiable, even dead, because of their internal or external skeleton, or rigid cell walls. Thus the ingestion frequencies obtained for fungi, diatoms, and testate amoebae are probably quite accurate, whereas those obtained for rotifers and ciliates are most likely underestimated. However, glutaraldehyde being a very efficient fixative, we do not believe that the poor preservation stage of the majority of the prey is due to their degradation between the time of sampling and the time of analysis. We rather infer that the unrecognisable prey might have been dead before the amoeba started to feed on them. If true this would suggest that *Nebela collaris sensu lato* is mainly detritivorous. Nevertheless, *in vivo* observations of carnivorous Nebelidae populations (*Nebela* spp., *Hyalosphenia papilio*) showed that they are also capable of attacking living or senescent ciliates (Gilbert *et al*. 2000).

Seasonal feeding habits

The dominant kind of ingested prey varied with time. Because of the relatively low numbers of predators-prey associations observed in each sample, we grouped the sampling periods into three categories: spring (April and May), summer (June and July), and autumn (September, October and November). In spring and autumn, identified prey were dominated by fungi and autotrophic microorganisms, while during the summer period the main prey were autotrophic microorganisms, protozoa, and micro-metazoa (Fig. 5a). The biomass of different categories of selected prey was estimated in order to compare the nature and variations of their feeding habits to the seasonal dynamics of their prey. Figure 5b shows the biomass variations of the same microbial groups: fungi (mycelia and spores), micro-algae, protozoa and micro-metazoa. A significant relationship was found between the biomass of fungi in the environment and the

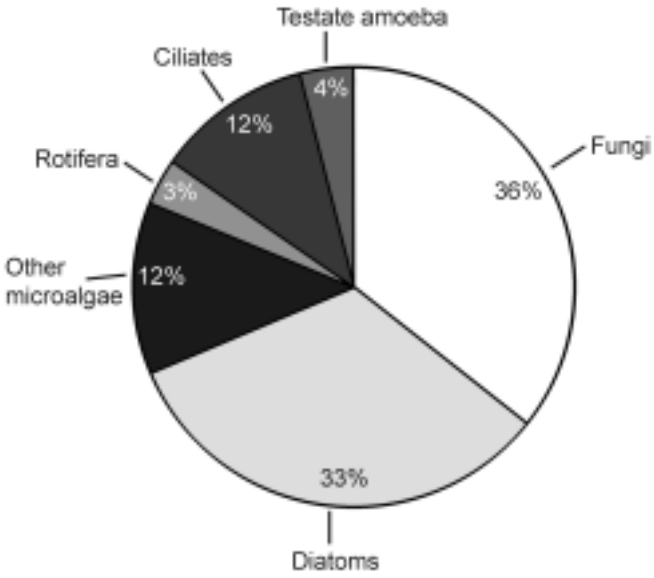

Fig. 4. Relative proportions (%) for the different identified prey categories (ND - not determined).

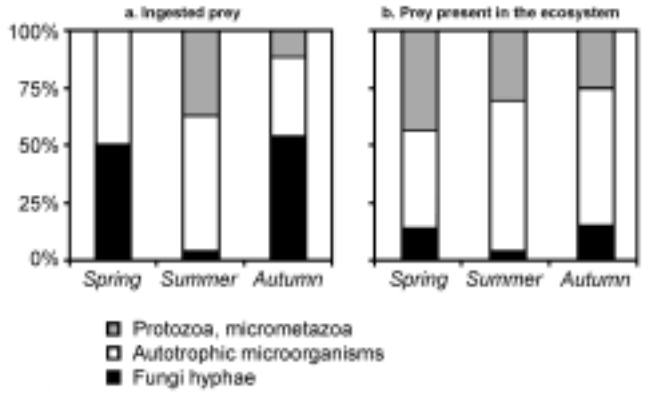

Figs 5 a, b. Temporal relative proportion of variations (**a**) of identified ingested prey and (**b**) of the relative proportion of the biomass of the same categories of prey in *Sphagnum* (ND - not determined).

frequency of their ingestion by *Nebela collaris sensu lato* ($r = 0.99$, $P = 0.04$), but no such relationship was found for the other groups. Because the size of our data set is limited, it is difficult to draw strong conclusions regarding the ability of *Nebela collaris sensu lato* to select their prey. Direct observations of microcosms with a range of prey types could clarify this question. Furthermore we described the predator-prey relationships with a low taxonomic resolution for the prey, but *Nebela collaris sensu lato* may select their prey at the species level. Thus, it remains possible that *Nebela collaris sensu lato* selects specific species of ciliates and rotifers that are more abundant or more accessible in summer when the lower water content of mosses makes these prey types more accessible. Indeed, the water content of *Sphagnum* mosses may play an important role in determining the ability of predators to catch their prey. *In vivo* observations showed that micro-organisms were located primarily between the leaves and on the stems of *Sphagnum*. In dry periods the water film in which micro-organisms live becomes thinner and their concentration therefore increases. In such conditions slow moving organisms like testate amoebae may be able to catch mobile predatory micro-organisms, such as ciliates or rotifers, otherwise too fast for them, whereas immobile, senescent or dead organisms, are accessible all year round.

The methodology we used neither allowed us to quantify the consumption of bacteria, because they are invisible, nor of naked amoebae, because they are difficult to observe, even alive. Furthermore, although glutaraldehyde is a fixing agent widely used in predation experiments of micro-organisms (Borsheim 1984, Pace and Bailiff 1987), the interpretations of results is difficult because many prey were not identifiable when they were fixed. Nevertheless, our study establishes that (1) *Nebela collaris sensu lato* feed on a wide range of living, senescent, or dead micro-organisms (fungi, microalgae, ciliates, other testate amoebae, rotifers) and organic remains, and (2) the proportion of predators among the identified prey is higher during the summer. Some prey seems to be selected, but further studies are needed to determine the importance of this phenomenon.

Acknowledgements. This study was conducted as part of a European Community environmental programme (3rd Framework, Contract No. EV5V-CT92-0099) and was financed by the CEREMCA Association. We also thank two anonymous reviewers for valuable comments on an earlier version of this paper.

REFERENCES

Bonkowski M., Brandt F. (2002) Do soil protozoa enhance plants growth by hormonal effects*? Soil Biol. Biochem.* **34:** 1709-1715

Borsheim K. (1984) Clearance rates of bacteria-sized particles by freshwater ciliates, measured with monodisperse fluorescent latex beads. *Oecologia* **63:** 286-288

Carrias J. F., Amblard C., Bourdier G. (1996) Protistan bacterivory in a oligomesotrophic lake: Importance of attached ciliates and flagellates. *Microb. Ecol.* **31:** 249-268

Chardez D. (1985) Protozoaires prédateurs de Thécamoebiens. *Protistologica* **21:** 187-194

Clarholm M. (1994) The microbial loop in soil. In: Beyond the Biomass (Eds. K. Ritz, J. Dighton, K. Giller). British Society of Soil Science. John Wiley & Sons, Chichester, 221-230

Coleman D. C. (1994) The microbial loop as used in terrestrial soil ecology studies. *Microb. Ecol.* **28:** 245-250

Coûteaux M.-M. (1984) Relationships between testate amoeba and fungi in humus microcosms. *Soil. Biol. Biochem*. **17:** 339-345

Coûteaux M.-M., Pussard M. (1983) Nature du régime alimentaire des protozoaires du sol. In: New Trends in Soil Biology (Ed. P. Lebrun *et al*.). Proceedings of the VIII. International Colloquium of Soil Biology, Louvain-la-Neuve (Belgium), 179-195

Deflandre G. (1936) Étude monographique sur le genre *Nebela* Leidy. *Annls Protist.* **5:** 210-286

Francez A.-J. (1988) Le peuplement de rotifères libres de deux lacs-tourbičres du Puy-de-Dôme (France). *Vie Milieu* **38:** 281-292

Francez A.-J. (1992) Croissance et production primaire des sphaignes dans une tourbičre des monts du Forez (Puy-de-Dôme, France). *Vie Milieu* **42:** 21-34

Gilbert D., Amblard C., Bourdier G., Francez A.-J. (1998a) The microbial loop at the surface of a peatland: structure, functioning and impact of nutrients inputs. *Microb. Ecol.* **35:** 83-93

Gilbert D., Amblard C., Bourdier G., Francez A.-J. (1998b) Short effect of nitrogen enrichment on the microbial communities of a peatland. *Hydrobiologia* **373/374:** 111-119

Gilbert D., Amblard C., Bourdier G., Francez A.-J., Mitchell E. A. D. (2000) Le regime alimentaire des Thécamoebiens (Protista, Sarcodina). *Année Biol.* **39:** 57-68

Grolière C.-A. (1977) Contribution à l'étude des ciliés des sphaignes: II- Dynamique des populations. *Protistologica* **13:** 335-352

Heal O. W. (1964) Observations on the seasonal and spatial distribution of Testacea (Protozoa: Rhizopoda) in *Sphagnum*. *J. Anim. Ecology* **33:** 395-412

Mitchell E. A. D., Borcard D., Buttler A., Grosvernier P., Gilbert D., Gobat J.-M. (2000) Horizontal distribution patterns of testate amoebae (Protozoa) in a *Sphagnum magellanicum* carpet. *Microb. Ecol.* **39:** 290-300

Mitchell E. A. D., Gilbert D., Buttler A., Grosvernier P., Amblard C., Gobat J.-M. (2003) Structure of microbial communities in *Sphagnum* peatlands and effect of atmospheric carbon dioxide enrichment. *Microb. Ecol.* (in press)

Pace M., Bailiff M. (1987) Evaluation of a fluorescent microsphere technique for measuring grazing rates of phagotrophic microorganisms. *Mar. Ecol. Prog. Ser.* **40:** 185-193

Premke K., Arndt H. (2000) Predation on heterotrophic flagellates by protists: Food selectivity determined using a live-staining technique. *Archiv Hydrobiol.* **150:** 17-28

Sanders R. W., Porter K. G., Bennett S. J., DeBiase A. E. (1989) Seasonal patterns of bacterivory by flagellates, ciliates, rotifers and cladocerans in a freshwater planktonic communities. *Limnol. Oceanogr*. **34:** 673-687

Schoenberg S. A., Oliver J. D. (1988) Temporal dynamics and spatial variation of algae in relation to hydrology and sediment characteristics in the Okefenokee Swamp, Georgia. *Hydrobiologia* **162:** 123-133

Simek K., Macek M., Vyhnalek V. (1990) Uptake of bacteria-sized fluorescent particles by natural protozoan assemblage in a reservoir. *Arch. Hydrobiol. Beih.* **34:** 275-281

Utermölh H. (1958) Zur vervollkommnung der quantative phytoplankton-methodik. *Mitt. Int. Verein. Theor. Angew. Limnol*. **9:** 1-38

Warner B. (1987) Abundance and diversity of testate amoeba (Rhizopoda, Testacea) in *Sphagnum* peatlands in Southwestern Ontario, Canada. *Arch. Protistenkd*. **133:** 173-180

Yeates G. W., Foissner W. (1995) Testate amoebae as predators of nematodes. *Biol. Fertil. Soils* **20:** 1-7

Received on 18th November 2002; revised version on 11th February, 2003; accepted on 25th February 2003

Acta Protozool. (2003) 42: 105 - 111

ACTA
PROTOZOOLOGICA

Morphology, Biometry and Ecology of *Arcella excavata* Cunningham, 1919 (Rhizopoda: Arcellinida)

Milcho TODOROV and Vassil GOLEMANSKY

Institute of Zoology, Bulgarian Academy of Sciences, Sofia, Bulgaria

Summary. Testate amoeba *Arcella excavata* Cunningham, 1919, isolated from the aeration tanks of the Sofia's Wastewater Treatment Plant and its morphology, biometry and ecology have been investigated. Based on the rich live material (120 specimens), a detailed morphological description of *A. excavata* and new data about the cytoplasm and the nuclei of the species are supplied. It was found out that *A. excavata* is a multinuclear species and the nuclei are usually 3 or 4, rarely 5-6 (1-2% only). These new data, as well as the characteristic shape of the shell and its bigger depth, show clearly that *A. excavata* is a separate, well distinguishing species. The size frequency distribution analysis indicates that *A. excavata* is a size-monomorphic species, characterized by a main-size class and a small-size range (all measured individuals have a shell length of 60-70 μm and 98% have a shell breadth of 55-66 μm). The present study shows that *A. excavata* inhabits polluted waters also and this fact does not confirm the conclusion of Snegovaya that it can be used as a bioindicator of the waters with the saprobity β-α. Probably, it is also a freshwater eurybiont as well as the majority of the known species of family *Arcellidae*.

Key words: *Arcella excavata*, biometry, ecology, morphology, Rhizopoda, Testacea.

INTRODUCTION

The genus *Arcella* is one of the most numerous testacean genera. More than 130 taxa of the genus have been described till now. The majorities of them are cosmopolite and inhabit mainly the freshwater pools, moist mosses and rarely soil litter (Deflandre 1928, Chardez 1989).

Besides, some rare species, with a restricted distribution, have been described. The scanty data about their morphology, biometry, distribution and ecological preferences for many of them exist in the literature. Furthermore, the cytoplasm, the types of pseudopodia and nuclei for the majority of these species have not been observed and this causes difficulties in their systematical identification. *Arcella excavata* Cunningham, 1919, is one of these rare and poorly studied species of the genus *Arcella*.

Arcella excavata was observed and described in a small swamp near Durham, N. Carolina (USA) (Cunningham, 1919). The empty shells were observed only. According to the original description the shape of the shell is "somewhat like a quarter-section of cantaloupe, the mouth being situated in the cup. The color is brown to almost black. The sizes of the shell are: length

Address for correspondence: Milcho Todorov, Vassil Golemansky, Institute of Zoology, Tsar Osvoboditel Blvd. 1, 1000 Sofia, Bulgaria; Fax: (3592) 988-28-97; E-mail: zoology@bulinfo.net

55 μm, width 50 μm, total depth 45 μm, depth of depression 25 μm, mouth 15 x 20 μm".

According to Cunningham *A. excavata* is close to *A. curvata* Wailes, 1913, but differs from it by the considerably smaller sizes and by the height of the shell. Later Deflandre (1928) described *A. curvata* as a variety of *A. polypora,* Penard and reported that the sizes of this species range from 125 to 130 μm in diameter.

Deflandre (1928) included *A. excavata* in his monograph of the genus *Arcella* after the description and the figures of Cunningham (1919). Deflandre had a doubt about his independence and noted that: "il serait intéressant de voir si elle est réellement fixée dans la station d'où elle provient et si des exemplaires cultivés ne rétrograderaient pas vers une *Arcella discoides* type or plutôt var. *scutelliformis*, dont les dimensions sont approchantes".

More than forty years after the original description *A. excavata* was not observed in USA and Europe. Štěpánek (1953, 1954) reported the finding of empty shells of *A. excavata* in Moravice River and in aquatic mosses near the Janské Lazni, Krkonoše (Czech Republik). According to Štěpánek the sizes of the observed specimens range as follows: diameter 63-67 μm, depth 35-42 μm, diameter of aperture 16-24 μm, depth of the aperture collar 3 μm. Living specimens have not been observed.

In his monograph Bartoš (1954) also reported *A. excavata* in the Czech Republik (on the data of Štěpánek). He added that it inhabited the sapropele among the aquatic plants. The sizes pointed by Bartoš were borrowed from Štěpánek (1954). Later Geltzer and Korganova (1976), and Geltzer *et al*. (1985) reported the presence of *A. excavata* in Russia also.

Recently Alekperov and Snegovaya (1999, 2000) observed *A. excavata* in four of the studied 5 freshwater pools from Apsheron Peninsula (Azerbaijan). Snegovaya (2001) described *A. excavata* also in a dam of Djeiran-Batan (Azerbaijan). According to Snegovaya (2001) *A. excavata* occurs in comparatively pure water and can be used as a bioindicator of water with saprobity β-α. However, in the above papers no data about the cytoplasm and detailed morphometrical characterization was provided.

During our investigation on the testate amoebae from the aeration tanks of Sofia's Wastewater Treatment Plant we have observed an abundant material of living specimens of *A. excavata* with a high population density. This allows us to make more detailed studies on their morphology, on the variation of his sizes and on the cytoplasm. The results of our studies are the subject of the present paper.

MATERIALS AND METHODS

The material for the present study was collected in July and August 2001 from the aeration tank No 1 of the Sofia's Wastewater Treatment Plant. The water in this aeration tank during the period of the study is characterized by the following chemical parameters: ammonium nitrogen (NH_4-N) - between 8.7 and 13.1 mg N/l; nitrite nitrogen (NO_2-N) - between 0.07 and 0.09 mg N/l; nitrate nitrogen (NO_3-N) - between 0.5 and 0.6 mg N/l; undissolved substances - between 7.0 and 15.1 mg/l.

The fresh material was cultivated in a laboratory at room temperature. Thus we were able to observe living specimens, young forms and variability of the shells of *A. excavata*. Some of the observations, measurements and photos were made by optical microscope. For scanning electron microscopy the shells were isolated, cleaned by several transfers through distilled water, mounted directly on stubs and air-dried. The shells were coated evenly with gold in a vacuum coating unit. The microphotographs were obtained by using a Phillips SEM 515, operating at 25 kV.

The morphometric characterization of the species and the construction of an ideal individual from the median of the shell measurements were made according to Schönborn *et al*. (1983). The following parameters were calculated: $\bar{x}$ - arithmetic mean; M - median (this value is used to construct the ideal individual); SD - standard deviation; SE - standard error of the arithmetic mean; CV - coefficient of variation in %; Min, Max - minimum and maximum values; n - number of examined individuals. The shell size was measured under light microscope at 400 x magnification.

RESULTS AND DISCUSSION

Morphology of the shell

The shell is colourless or yellowish in young specimens and brown in older specimens, oval or circular in apertural view and croissant-like in lateral view (Figs 1-4, 7-10). The large axis of the shell (length) in almost all observed specimens is in perpendicular direction to the shell's protuberances, when the shape of the shell in apertural view is not circular. Rarely (about 5% of the observed individuals) the large axis of the shell is parallel to the shell's protuberances. The apertural surface is deeply invaginated forming two pronounced protuberances with circular or elliptical aperture at the bottom of invagination. The aperture is bordered by a small lip, of about 3-4 μm (Fig. 5). Štěpánek (1953) notes that small

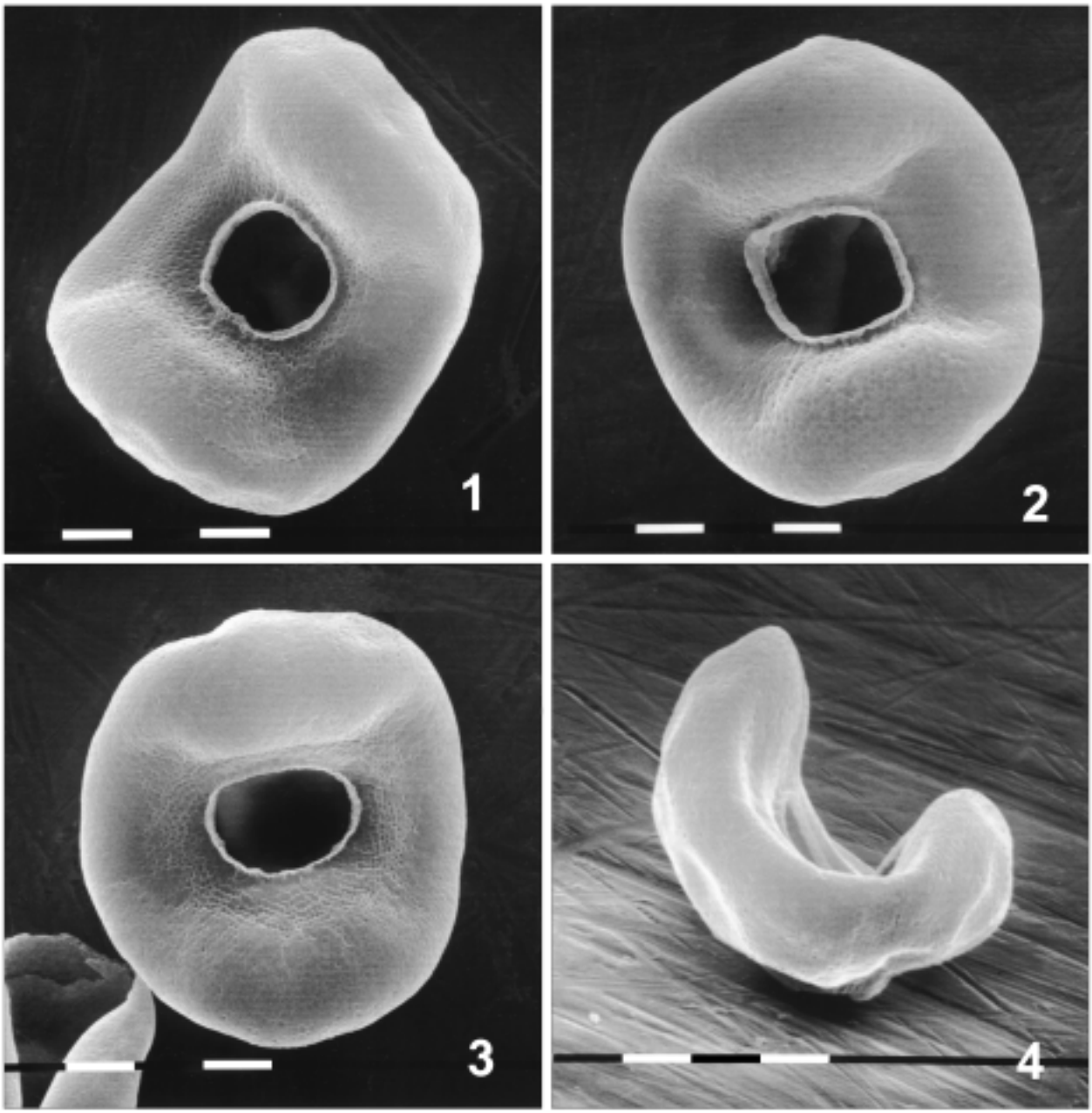

Figs 1-4. SEM photographs of *Arcella excavata*. **1-3 -** apertural views, showing different shell and apertural shape; **4 -** lateral view, showing invagination of apertural surface. Scale bars 10 µm.

pores border the aperture, however in our study we do not observe such pores. The aboral hemispherical region usually has a series of regular depressions (Fig. 7). The shell wall is composed of numerous alveoli in diameter of 1-1.5 µm, made of a proteinaceous material, and arranged in one layer. The shell surface is smooth or irregular and has numerous small pores (Figs 6, 9).

Cytoplasm

The cytoplasm does not quite fill the shell cavity and numerous thin cytoplasmic strands (epipodes) attach it to the inner shell wall (Fig. 7).

The nuclei are 3 or 4, rarely 5-6 (1-2% only) and are large, spherical, between 9.5 and 10.5 ìm in diameter.

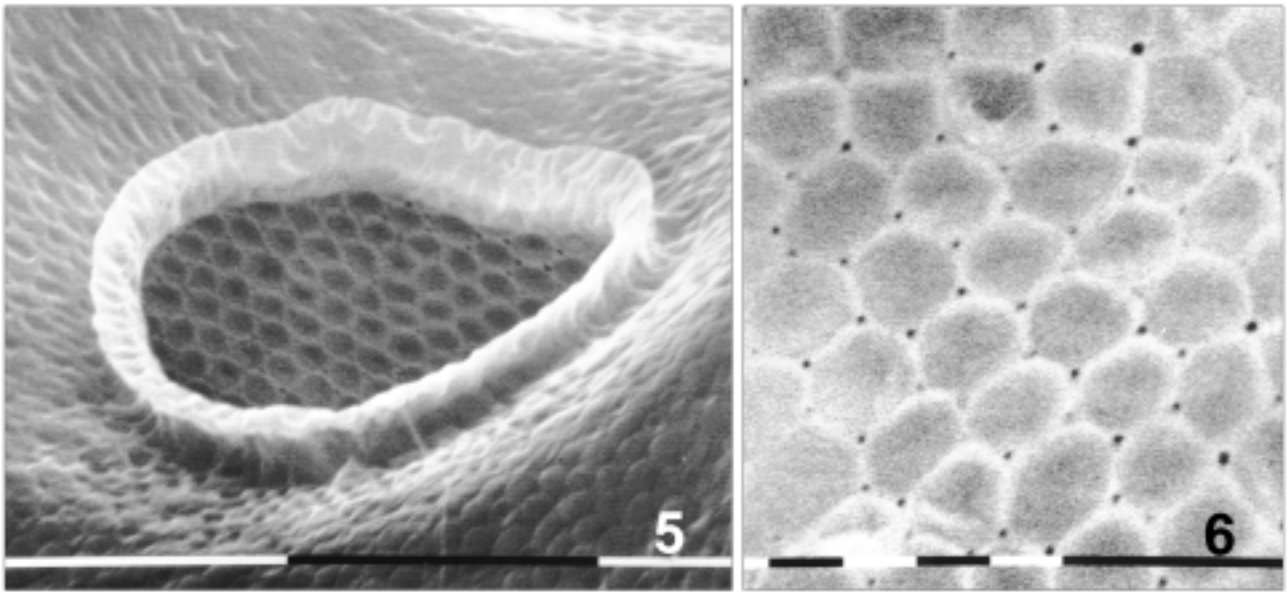

Figs 5-6. *Arcella excavata.* **5** - apertural view to illustrate the small lip, bordering the aperture; **6** -surface of shell showing proteinaceous alveoli and small pores. Scale bars 10 μm (5); 1 μm (6).

Table 1. Morphometric characterization of *Arcella excavata* (measurements in μm).

Character	x	M	SD	SE	CV	Min	Max	n
lenght	64.8	65	2.6	0.2	4.0	60	70	120
breadth	61.1	61	2.8	0.3	4.6	53	70	120
diameter of aperture	19.5	20	0.9	0.1	4.5	18	22	120
depth	40.1	40	1.8	0.2	4.5	36	45	120
apertural invagination	18.9	19	1.7	0.2	9.0	14	25	120

Table 2. Measurements (in μm) of *Arcella excavata* according to different authors.

Authors	Length of shell	Breadth of shell	Depth of shell	Diameter of aperture	Depth of depression	Number of measured specimens
Cunningham 1919	55	50	45	15x20	25	no data
Deflandre 1928	55	50	45	15x20	25	no data
Štěpánek 1953	67	67	35	16	-	1
Štěpánek 1954	63	63	42	24	-	no data
Bartoš 1954	63	63	42	24	-	no data
Present work	60-70	53-70	36-45	18-22	14-25	120

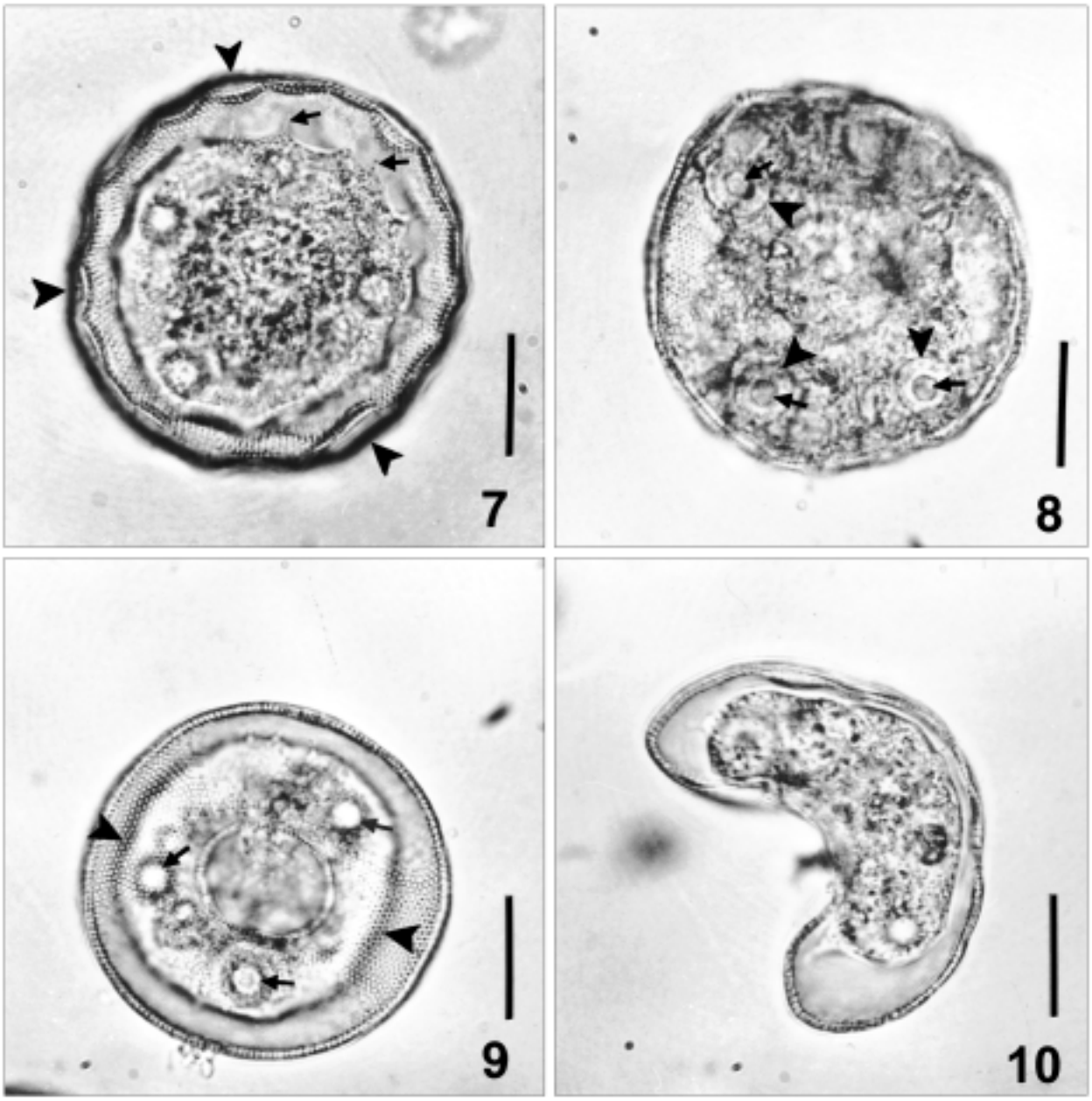

Figs 7-10. Photomicrographs of *Arcella excavata*. **7** - aboral view, showing shell depressions (arrowheads) and thin cytoplasmic strands - epipodes (arrows); **8** - apertural view, showing the nuclei (arrowheads) and the nucleoli (arrows); **9** - apertural view, showing the nuclei (arrows) and the shell structure (arrowheads); **10** - lateral view. Scale bars 20 μm.

They have one central nucleolus (about 5 μm in diameter), easily visible in each of the nuclei (Figs 8, 9). The number of the nuclei, as well as the characteristic shape of the shell and it's bigger depth, show clearly that *A. excavata* is a separate, well distinguished species and it has nothing common with *A. discoides* and *A. discoides* var. *scutelliformis* (as Deflandre, 1928 doubt) or with *A. polypora* var. *curvata* (with that it was compared by Cunningham 1919).

Normally one big contractile vacuole, between 12 and 14 μm in diameter, occurs in the cytoplasm.

The lobopodia are usually 3 or 4, but sometimes they may fuse to form a single fan-like pseudopodium with a ruffled edge.

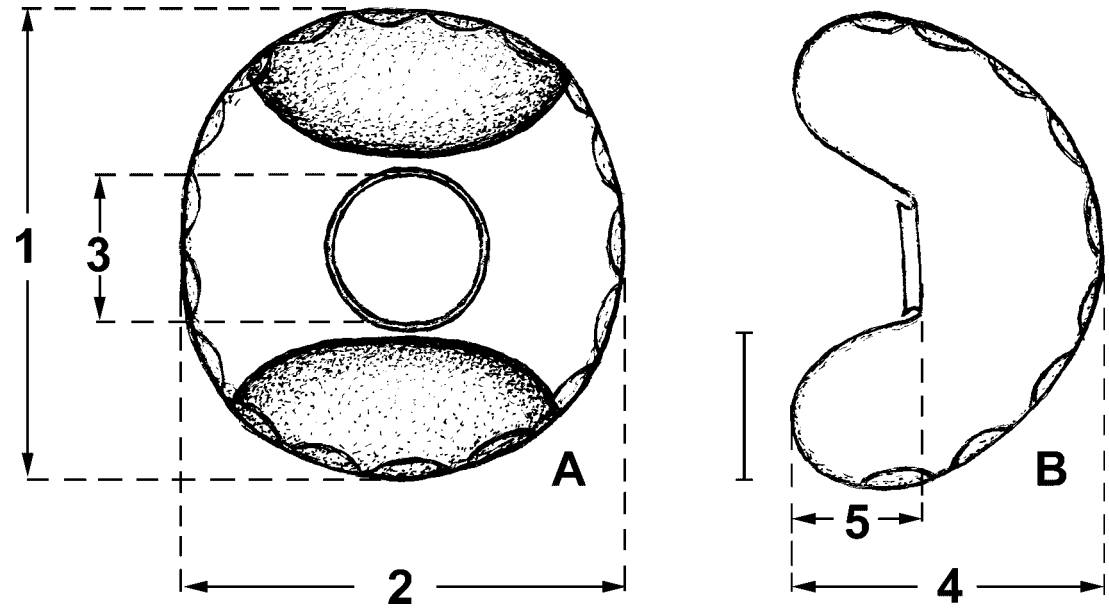

Figs 11 A, B. Ideal individual of *Arcella excavata*, constructed from median values of all measured specimens; **A** - apertural view: 1 - length, 2 - breadth, 3 - diameter of aperture; **B** - lateral view: 4 - depth, 5 - apertural invagination. Scale bar 20 μm.

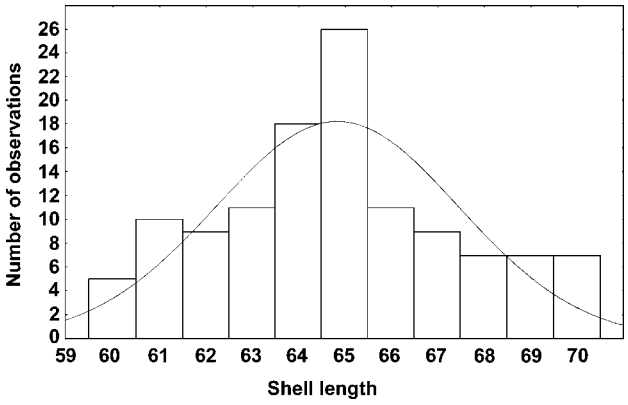

Fig. 12. Histogram showing the size frequency of shell length of *Arcella excavata.*

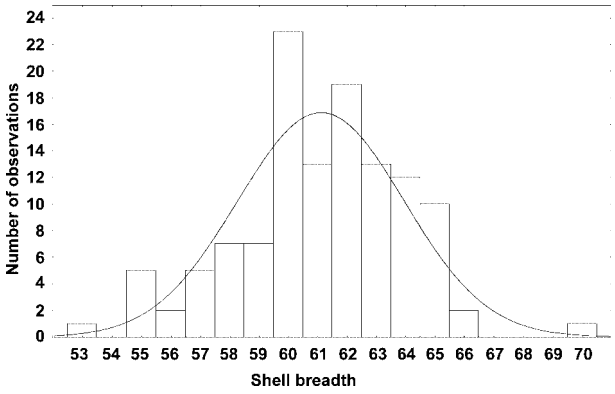

Fig. 13. Histogram showing the size frequency of shell breadth of *Arcella excavata.*

Biometry

Table 1 shows the morphometric characterization of *A. excavata* according to our studies. The ideal individual of this species is constructed from median values of all characters in Fig. 11. Shell measurements with the exception of character (5) are fairly constant and have low variability (CV between 4.0 and 4.5). Our values agree well with those of Štěpánek (1953, 1954) and Bartoš (1954), and are bigger than those of Cunningham (1919) and Deflandre (1928) (Table 2).

Size frequency distribution analysis indicates that *A. excavata* is a size-monomorphic species characterized by a main-size class and a small size range (Figs 12, 13). Figure 12 shows that all measured individuals have a shell length 60-70 μm and more than half of them (55%) are within the limits of 63-66 μm.

The frequency analysis of the shell breadth shows almost the same results (Fig. 13). Ninety-eight percent of all measured individuals have a shell breadth between 55 and 66 μm and about three-fourths of them (75%) are within the limits of 60-65 μm. Only 0.8% has a shell

breadth less than 55 μm and 0.8% has a shell breadth above 66 μm.

Ecology

Since the original descriptions of *A. excavata* there have been scanty data about the ecology of this species. Cunningham (1919) and Deflandre (1928) pointed out that this species occurred in small swamps. According to Štěpánek (1953, 1954) and Bartoš (1954) *A. excavata* inhabits the aquatic mosses and the sapropele among the aquatic plants. Štěpánek (1953) noted that this species is betamesosaprobic. Snegovaya (2001) reported that *A. excavata* occurred in comparatively pure water and could be used as a bioindicator of water with the saprobity β-α.

Our investigation shows that *A. excavata* inhabits also polluted waters of the aeration tanks of Sofia's Wastewater Treatment Plant. This fact does not confirm the conclusion of Snegovaya (2001) that *A. excavata* can be used as a bioindicator of water with the saprobity β-α. Probably *A. excavata* is also a freshwater eurybiont, as well as the majority of the known species of the family *Arcellidae*.

Geographical distribution: Azerbaijan, Bulgaria, Czech Republik, Russia and United States of America.

Acknowledgements. We thank to the student from the University of Sofia Ms I. Christova for the collection of living material from the aeration tanks of the Sofia's Wastewater Treatment Plant.

REFERENCES

Alekperov I., Snegovaya N. (1999) Specific composition and number of testaceous amoebae (Testacea Lobosia, Protozoa) of Ganli-Gol Lake. *Tr. J. of Zoology* **23:** 313-319

Alekperov I., Snegovaya N. (2000) The fauna of testate amoebae (Rhizopoda, Testacea) in freshwater basins of Apsheron peninsula. *Protistology* **1:** 135-147

Bartoš E. (1954) Koreňonožce radu Testacea. *Výd. Slov. Akad. Vied*, Bratislava

Chardez D. (1989) Les Arcelles, Thécamoebiens discrets des mares et des étangs. *Les Naturalistes belges* **70:** 17-19

Cunningham B. (1919) *Arcella excavata* nov. sp. *Trans. Amer. Micr. Soc.* **38:** 242-243

Deflandre G. (1928) Le genre *Arcella* Ehrenberg. Morphologie-Biologie. Essai phylogénétique et systématique. *Arch. Protistenkd* **64:** 152-287

Geltzer Y., Korganova G. (1976) Soil testate amoebae (Protozoa, Testacea) and theirs indicatoring importance. In: Problems and Methods of the Biological Diagnostics and Indication of the Soils. *Nauka*: 116-140 (in Russian)

Geltzer Y., Korganova G., Alekseev D. (1985) Soil testate amoebae and methods of theirs study. Publishing House of the University of Moscow (in Russian)

Schönborn W., Foissner W., Meisterfeld R. (1983) Licht- und rasterelektronenmikroskopische Untersuchungen zur Schalenmorphologie und Rassenbildung bodenbewohnender Testaceen (Protozoa: Rhizopoda) sowie Vorschläge zur biometrischen Charakterisierung von Testaceen-Schalen. *Protistologica* **19:** 553-566

Snegovaya N. (2001) The fauna of testate amoebae (Protozoa, Testacea) in freshwater basins of Apsheron peninsula. Ph.D. Thesis of Bacu (in Russian)

Štěpánek M. (1953) The Rhizopodes as biological indicators of the contamination of waters. I. *Rhizopodes* and *Heliozoa* in the River Moravice (Silesia, Czechoslovakia*). Přirodov. sbor. Ostrav. kraje* **14:** 470-505

Štěpánek M. (1954) Krytenky (Testacea) z Krkonoš. *Čas. Nár. Musea, odd. přir*., **123:** 96-110

Received on 28th October, 2002; revised version on 11 December 2002; accepted on 23rd December, 2002

Acta Protozool. (2003) 42: 113 - 143

ACTA
PROTOZOOLOGICA

The Myriokaryonidae fam. n., a New Family of Spathidiid Ciliates (Ciliophora: Gymnostomatea)

Wilhelm FOISSNER

Universität Salzburg, Institut für Zoologie, Salzburg, Austria

Summary. The new family Myriokaryonidae is based on a thorough literature review and the (re) investigation of *Myriokaryon lieberkuehnii* (Bütschli, 1889) Jankowski, 1973 and *Cephalospatula brasiliensis*, a new genus and species discovered in soils of South America. The key features of the new family, which belongs to the order Spathidiida Foissner and Foissner, 1988, are the truncated anterior body end and the spoon-shaped oral bulge, respectively, circumoral kinety. The anterior truncation causes a highly characteristic bend of the oral bulge and circumoral kinety in the transition zone of spoon-shovel and spoon-handle, that is, subapically where the oral bulge and the circumoral kinety enter the ventral side of the cell. Based on literature data, *Holophrya emmae* Bergh, 1896 and *Pseudoprorodon armatus* Kahl, 1930a are classified as representatives of two further new myriokaryonid genera, viz., *Berghophrya* gen. n. and *Kahlophrya* gen. n. Genera within the Myriokaryonidae are distinguished by details of the dorsal brush and the arrangement of the somatic ciliary rows and extrusomes. *Pseudoprorodon emmae* (Bergh, 1896), as redescribed by Song and Wilbert (1989), is recognized as a new genus and species, *Songophrya armata* gen. n., sp. n., likely belonging to the gymnostomatous family Pseudoholophryidae.

Key words: biodiversity, Haptorida, infraciliature, Litostomatea, soil protozoa, South America.

INTRODUCTION

The haptorid gymnostomes ("Litostomatea") are a highly diverse ciliate assemblage, ranging from the simple *Enchelys* to the complex *Homalozoon* and from common freshwater and marine to highly specialized enterozooic species (Corliss 1979, Grain 1994). However, many gymnostomes are rather inconspicuous and thus attracted few specialists, most notably Kahl (1926, 1930a, b), Lipscomb and Riordan (1990), and myself (Foissner 1984, 1996; Foissner and Foissner 1988). Accordingly, the group contains a huge amount of undescribed taxa, as shown by a recent study on soil ciliates from Namibia, describing 10 new genera and many new species (Foissner *et al*. 2002). Detailed observations and much experience are necessary to unravel this hidden diversity. This is evident also from the present study, where a new family and four new genera will be established.

Large ciliates, such as *Myriokaryon lieberkuehnii* and *Cephalospatula brasiliensis*, are difficult to present by ordinary figures. Thus, I fragmented them into many details, which, however, strongly increased the number of pages. But this is the sole way to document such species, which tend to be misidentified, to an extent that detailed biogeographic comparisons of species and populations will be possible in future.

Address for correspondence: Wilhelm Foissner, Universität Salzburg, Institut für Zoologie, Hellbrunnerstrasse 34, A-5020 Salzburg, Austria; Fax: 0043 (0) 662 8044 5698

MATERIALS AND METHODS

Myriokaryon lieberkuehnii was found in the microaerobic mud of a boggy drainage ditch at the margin of a small bog near the village of Franking (13°E 48°2'N), Upper Austria, in April 1990. Specimens were numerous and survived in the collecting jar for weeks, but did not reproduce.

Cephalospatula brasiliensis was discovered in soil samples from three sites of South America. The type population occurred in a sample, kindly collected by Dr. L. Felipe Machado Velho (Maringá State University) in May 2001, from the high Paraná River floodplain near the town of Maringá (53°15'W 22°40'S, altitude about 500 m), State of Mato Grosso do Sul, Brazil. The sample was taken from the Aurelio Lagoon, that is, a marginal lagoon associated with the Baia River, a tributary of the Paraná River. The dark, humic soil was mixed with much partially decomposed plant litter, had pH 5.1 (in water), was air-dried in the Salzburg laboratory for about one month, and stored in a plastic bag. In November 2001, the about 300g soil were put in a Petri dish and saturated, but not flooded with distilled water to obtain a "non-flooded Petri dish culture", as described in Foissner *et al*. (2002). About two weeks after rewetting, a small population of *C. brasiliensis* developed. The second population of *C. brasiliensis* occurred in the surroundings of Rio de Janeiro (43°W 23°S), that is, in the Restingha area about 100 m inshore the Atlantic Ocean, where the ground is partially covered by grass and an up to 1 cm high litter layer. The sample, which was taken on 16.11.1996 and treated as described above, contained sandy soil, surface litter, and plant residues sieved off the very sandy soil up to a depth of 10 cm. A weak population of *C. brasiliensis* developed 8 days after rewetting the sample, which had pH 5.2 (in water), in May 1997. The third population of *C. brasiliensis* was found near the airport of Puerto Ayacucho (68°W 5°N), Venezuela, on 28.5.1997. Here are large, granitic rocks (Lajas) with many pools. The sample comprised litter, mud and soil accumulated in a pool between the cushion-like root layer of a species of the endemic Velloziaceae family. The material, which was treated as described above and had pH 5.3 (in water), was rewetted in June 1997, when a small population of *C. brasiliensis* developed after 5 days.

Specimens were studied *in vivo* using a high-power, oil immersion objective and differential interference contrast optics. The ciliary pattern and various cytological structures were revealed by protargol impregnation, as described in Foissner (1991). Counts and measurements on prepared specimens were performed at a magnification of x1000. *In vivo* measurements were conducted at magnifications of x100-1000. Although these provide only rough estimates, it is worth giving such data as specimens may change in preparations. Illustrations of live specimens were based on free-hand sketches, while those of prepared cells were made with a camera lucida. Terminology is mainly according to Corliss (1979).

RESULTS

Genus *Myriokaryon* Jankowski, 1973

Improved diagnosis: vermiform Myriokaryonidae with long mouth on steeply slanted anterior body region and many (>3) isomorphic dorsal brush rows converging to an acute pattern anteriorly. Extrusomes scattered in oral bulge. At left side of circumoral kinety many transverse kinetofragments partially connected with left side ciliary rows (basically *Supraspathidium* pattern).

Type species (by monotypy): *Prorodon Lieberkühnii* Bütschli, 1889.

Redescription of *Myriokaryon lieberkuehnii* (Bütschli, 1889) Jankowski, 1973 (Figs 1-53; Table 1)

1859 *Enchelys gigas* Stein, Organismus der Infusionsthiere, p. 80 (a nomen nudum because too briefly described without figure).

1889 *Prorodon Lieberkühnii* Bütschli, Protozoa, explanation to figure 6 of plate LVII (single figure, here reproduced as figure 91; without description).

1914 *Spathidium gigas* (Stein 1859) - Cunha, *Mem. Inst. Osw. Cruz*, 6: 173 (synonymy doubtful; possibly a "true", large *Spathidium*/*Arcuospathidium*; Fig. 96).

1930 *Pseudoprorodon (Prorodon) lieberkühni* Bütschli, 1889 - Kahl, *Tierwelt Dtl*., 18: 71 (first reviser and important new observations; Figs 97, 99).

1972 *Pseudoprorodon lieberkühni* Bütschli - Dragesco, *Annls Fac. Sci. Univ. féd. Cameroun*, 11: 73 (redescription, mainly from life; Figs 92, 93, 95, 98).

1973 *Myriokaryon lieberkühnii* (Bütschli, 1889) Jankowski comb. n. - Jankowski, *Zool. Zh*., 52: 424 (solid redescription and transfer to the new genus *Myriokaryon*; in Russian with English summary; Fig. 101).

1986 *Myriokaryon lieberkühni* (Bütschli, 1889) Jankowski, 1973 - Dragesco and Dragesco-Kernéis, *Fauna tropicale*, 26: 169 (brief review and description of a Benin population; Fig. 94).

Material and types: Jankowski (1973) stored 29 neotype slides with 70 conventionally (various hematoxylin methods, Feulgen reaction, bromphenol) prepared specimens of *M. lieberkuehnii* at the marine biological laboratory of the Russian Academy of Sciences in St. Peterburg. Although these slides do not show all the details necessary for a reliable identification, I suggest to accept them as a neotype because the known data agree with my material. The specimens of Dragesco (1972) and Dragesco and Dragesco-Kernéis (1986) are likely still in the private collection of Prof. Jean Dragesco. Furthermore, they are poorly prepared, as obvious from the mistakes in the description (see discussion). My material is excellently prepared and fully described below. Five slides with protargol-impregnated

Table 1. Morphometric data on *Myriokaryon lieberkuehnii*.

Characteristics[a]	x	M	SD	SE	CV	Min	Max	n
Body, length	1321.0	1320.0	280.1	61.1	21.2	860.0	1800.0	21
Body, width about 100 µm posterior of anterior end	52.8	53.0	5.1	1.1	9.7	45.0	63.0	21
Body, maximum width	77.1	75.0	9.3	2.0	12.0	68.0	110.0	21
Body length:maximum width, ratio	17.3	16.9	3.9	0.8	22.5	9.1	24.3	21
Mouth, length (anterior end to proximal end of circumoral kinety, distance)	328.3	330.0	57.1	12.5	17.4	240.0	450.0	21
Body length:mouth length, ratio	4.1	3.9	0.9	0.2	21.4	3.0	6.3	21
Mouth, anterior width (distance between circumoral kinety in head area)	10.5	11.0	2.0	0.6	19.0	7.0	14.0	13
Mouth, mid-region width (distance between circumoral kinety)	6.9	7.0	1.3	0.3	18.6	5.0	10.0	18
Mouth, posterior width (distance between circumoral kinety)	11.2	10.0	2.2	0.5	19.5	8.0	15.0	17
Macronuclei, length	8.9	8.0	4.1	0.9	46.6	4.0	18.0	21
Macronuclei, width	3.6	4.0	0.6	0.1	16.7	3.0	5.0	21
Micronuclei, length	3.0	3.0	0.5	0.1	16.0	2.2	4.0	21
Micronuclei, width	3.0	3.0	0.5	0.1	16.0	2.2	4.0	21
Excretory pores, number per vacuole	2.3	2.0	0.6	0.1	28.2	1.0	3.0	21
Somatic kineties, number in mid-oral area[b]	82.8	82.0	-	-	-	73.0	100.0	21
Somatic kineties, number in mid-body[b]	94.3	95.0	-	-	-	83.0	110.0	21
Kinetids, number in 10 µm in oral area	6.1	6.0	1.0	0.2	15.7	5.0	9.0	21
Kinetids, number in 10 µm in mid-body	5.0	5.0	0.8	0.2	15.5	4.0	7.0	21
Kinetids, number in 10 µm near posterior end	3.1	3.0	0.2	0.1	7.2	3.0	4.0	21
Dorsal brush kineties, number near anterior body end	7.5	7.5	0.6	0.1	8.1	6.0	8.0	20
Anterior body end to end of dorsal brush, distance[b]	508.3	500.0	-	-	-	300.0	680.0	21

[a] Data based on protargol-impregnated (Wilbert's method; see Foissner 1991), mounted, morphostatic field specimens. Measurements in µm. CV - coefficient of variation in %, M - median, Max - maximum, Min - minimum, n - number of individuals investigated, SD - standard deviation, SE - standard error of arithmetic mean, x - arithmetic mean. [b] Approximate values.

(Wilbert's method) specimens have been deposited in the Biologiezentrum of the Oberösterreichische Landesmuseum in Linz (LI), Austria. Relevant specimens are marked with black ink on the cover glass.

Description of Austrian population: true size difficult to ascertain because contractile by about one third of body length and contraction, respectively, extension occur so slowly that is is impossible to recognize whether or not the cell is fully extended, as also mentioned by Engelmann in Bütschli (1889). Thus, size variability is high, viz., 900-2000 x 70-120 µm *in vivo*, usually near 1500 x 90 µm, with conspicuous length:width variation of 9-24:1 in protargol preparations, where cell width is rather distinctly shrunken (Table 1). Jankowski (1973), however, mentions that it does not contract when touched, but he might have overlooked the slow contraction described above. He measured 34 specimens and noted also a pronounced variability: length 625-1250 µm, usually 825-950 µm; width at anterior end 37-52 µm; width at proximal oral bulge end 47-62 µm; width in mid-body 100-175 µm, usually 100-125 µm.

Basically elongate knife-shaped with blade (=oral area) occupying 25% of body length on average, handle thus much longer than blade; anterior and posterior quarter flattened laterally up to 2:1, anterior body end acute due to steeply slanted mouth area and indistinct oral bulge gradually merging into body proper proximally (Figs 1-4, 12, 20); usually widest in or near mid-body, rarely in blade-like oral area making specimens somewhat club-shaped (Fig. 11); contracted cells widened in mid-body (Figs 2, 3). Largest specimens with about 5000 (!) macronuclear nodules scattered throughout body in an about 15 µm thick, subcortical layer; individual nodules globular to elongate ellipsoidal with several minute and small nucleoli of various shape (Figs 1, 10, 14, 18, 33, 35, 40, 45, 46; Table 1). Micronuclei less numerous than macronuclear nodules, likely between 100-200, minute, that is 3-4 µm across. A large contractile vacuole with several excretory pores in rear end and about 60 small contractile vacuoles each with one to three intrakinetal excretory pores scattered throughout cortex (Figs 1, 10, 16, 19, 22-24, 33). Extrusomes (likely toxicysts) accumu-

lated in both sides of oral bulge and scattered throughout cytoplasm in conspicuous bundles; individual extrusomes rod-shaped and very flexible, straight to slightly curved, about 80 x 0,5 µm in size; those attached to oral bulge never impregnate with the protargol method used, while cytoplasmic bundles often stain deeply with individual rods frequently somewhat disordered and irregularly curved (Figs 1, 5-7, 10, 29, 30, 33-37, 42, 43). A second type of minute (about 1-1.5 x 0.4 µm), rod-shaped structures, likely mucocysts (Fauré-Fremiet and André 1968), forms oblique rows in the oral bulge and is scattered throughout the cortex and cytoplasm, where rods are up to 2 µm long and occasionally impregnated with protargol (Figs 7, 8, 10, 33, 36, 39, 46). Cortex conspicuous because 3-4 µm thick and sharply separated from granular cytoplasm by a distinct *tela corticalis* described by Fauré-Fremiet and André (1968); in most specimens rather densely covered with 2-4 µm long bacterial rods (Figs 1, 8, 10, 29, 31, 33, 39). Cytoplasm colourless, packed with lipid droplets 1-10 µm across and surprisingly small, viz., 10 µm-sized food vacuoles containing colourless, granular remnants and golden lipid droplets, indicating heterotrophic and autotrophic protists as main food source (Figs 1, 10, 30); unfortunately, definite food inclusions were neither found *in vivo* nor prepared cells, indicating that prey is rapidly lysed either outside the cell or in the food vacuoles. Swims and crawls worm-like in and on the sediment and microscope slide, showing great flexibility, viz., may curl-up and/or spiralize along main body axis (Fig. 4).

Cilia about 12 µm long *in vivo* and narrowly spaced, especially right of oral bulge, arranged in an average of 95 rows in mid-body and of only 82 rows in mid-oral area due to gradual shortening along circumoral kinety (Figs 15, 17, 25, 37, 40, 41, 44; Table 1), while some rows are added postorally and along left margin of dorsal brush (Figs 16, 48-53). Ciliary rows equidistantly and narrowly spaced (about 2 µm), extend meridionally; right side rows loosely ciliated anteriorly and shortened successively abutting on circumoral kinety in steep angles, while densely ciliated and strongly curved anterior end of left side ciliary rows abuts on circumoral kinety at almost right angles; furthermore, many additional, small kinetofragments of unknown origin occur along left side of circumoral kinety, a special feature also found in *Cephalospatula brasiliensis* (Figs 15, 17, 19, 25-28, 37, 38, 40, 41, 44). These fragments look like dileptid "adesmokineties", a term coined by Jankowski earlier than the American "paratenes". Kinetids of posterior body region associated with long fibres forming conspicuous, subcortical bundles extending anteriorly (Fig. 22). Dorsal brush at anterior portion of six to eight slightly left laterally located, ordinary somatic ciliary rows, longest brush kineties occupy 38% of body length on average (Table 1); composed of narrowly spaced dikinetids with posterior bristles up to 5 µm long and inflated distal end curved anteriorly (Figs 1, 9, 29, 39); kineties gradually shortened from left to right, except of the three rightmost rows, bristles mixed with ordinary cilia posteriorly, that is, before brush kineties extend as ciliary rows to rear body end; middle brush rows, additionally, slightly shortened anteriorly, where the unshortened marginal rows curve right and converge subapically near the circumoral kinety, providing the brush with an acute end, another unique feature of the somatic ciliary pattern of *Myriokaryon* (Figs 16, 20, 21, 23, 24, 26, 27, 29, 38, 39, 48-53; Table 1).

Mouth occupies steeply slanted and slightly convex anterior 25% of body, *in vivo* distinct due to the numerous and long extrusomes contained, basically, however, indistinct because oral bulge hardly set off from body proper, that is, only about 5 µm high and 12 µm wide. Oral bulge elongate dumbbell-shaped in frontal view, curved anterior portion slightly thicker (higher) and wider than straight proximal part; oral slit stands out as a whitish (unimpregnated) cleft from brownish impregnated bulge wall, containing a fibrous reticulum and innumerable extrusomes, as described above. Circumoral kinety composed of very narrowly spaced, oblique dikinetids having ciliated only one basal body, likely consists of many kinetofragments of varying length, as indicated by minute breaks making kinety somewhat irregular; of same shape as oral bulge, that is, elongate dumbbell-shaped with highly characteristic, sharp bend in the transition zone of transverse-truncate anterior body end and curved ventral portion. Oral basket rods originate from circumoral dikinetids, very fine and short (about 30 µm) as compared to size of cell, basket thus inconspicuous in protargol preparations and invisible *in vivo*, where it is easily confused with the more distinct and longer, rod-shaped extrusomes (Figs 1-5, 7, 11-13, 15, 17, 25-29, 32, 37, 40, 41, 43-45, 47; Table 1).

Distribution and ecology: all reliable records of *M. lieberkuehnii* are from the Holarctic and African region (Bütschli 1889, Kahl 1930a, Dragesco 1972, Jankowski 1973, Dragesco and Dragesco-Kernéis 1986, present study). Cunha (1914) reported it from freshwater in the surroundings of Manguinhos, Brazil, where it occurred only once, but in great numbers (Fig. 96). However, I agree with Kahl (1930a) that conspecificity

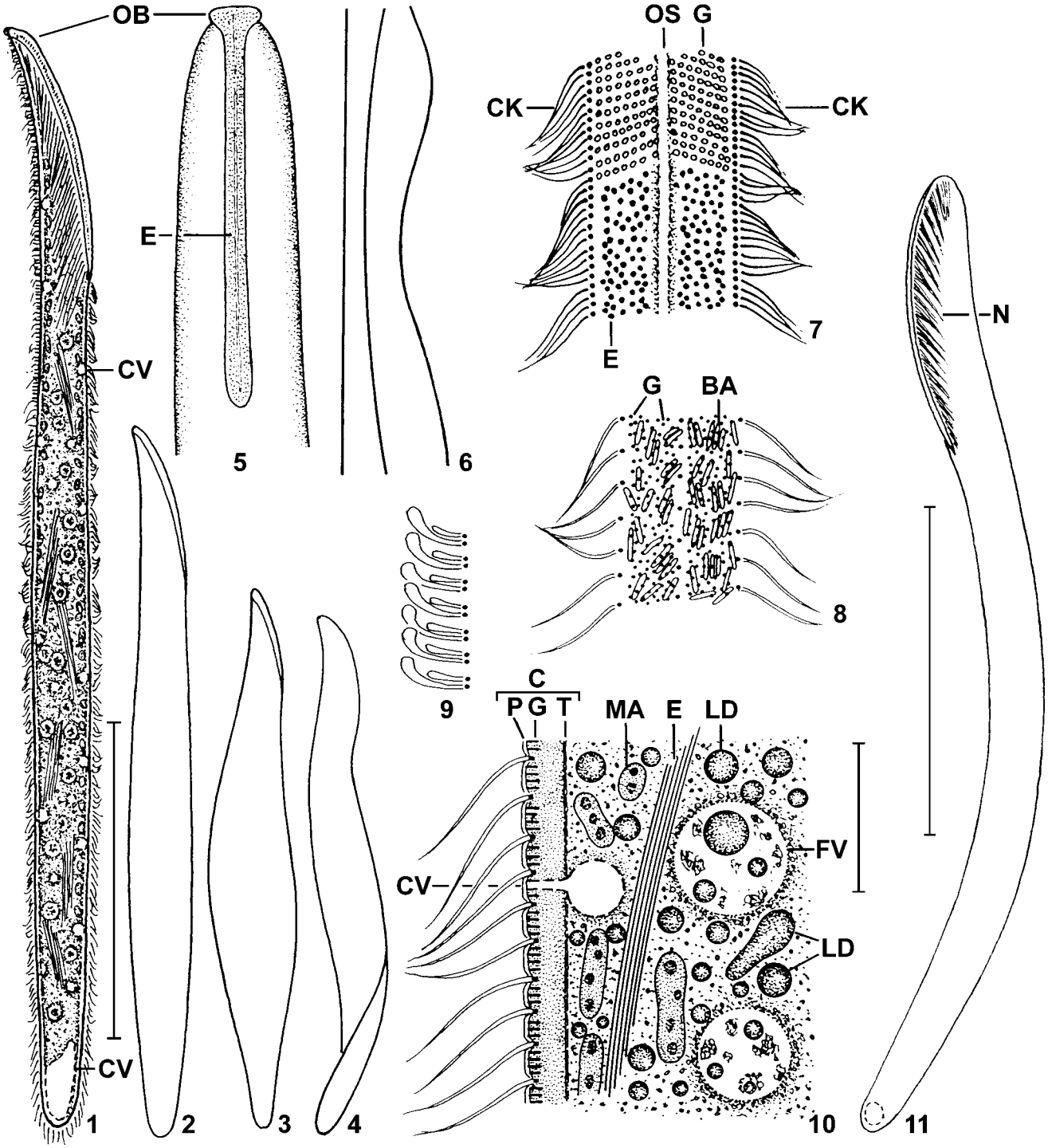

Figs 1-11. *Myriokaryon lieberkuehnii* from life (1-10) and after protargol impregnation (11). **1** - right side view of a representative specimen, length 1400 µm. For details, see figure 10; **2, 3** - a specimen extended and contracted; **4** - a slightly spiralized specimen; **5** - ventral view of oral area; **6** - oral bulge extrusomes, length 80 µm; **7** - ventral view of oral bulge showing cortical granules (upper half) and extrusomes underneath (lower half); **8** - surface view showing cortical granules and epicortical bacteria; **9** - part of a dorsal brush row with posterior bristles 5 µm long and inflated distally; **10** - optical section showing the 3-4 µm thick cortex and main cytoplasmic inclusions. Note that the extrusome bundle (80 µm) is not shown in full length; **11** - a specimen widest in oral area. B - dorsal brush; BA - epicortical bacteria; C - cortex; CK - circumoral kinety; CV - contractile vacuoles; E - extrusomes; FV - food vacuole; G - cortical granules; L - lipid droplets; MA - macronuclear nodule; N - nematodesmata; OB - oral bulge; OS - oral slit; P - pellicle; T - tela corticalis. Scale bars 10 µm (10); 400 µm (1, 11).

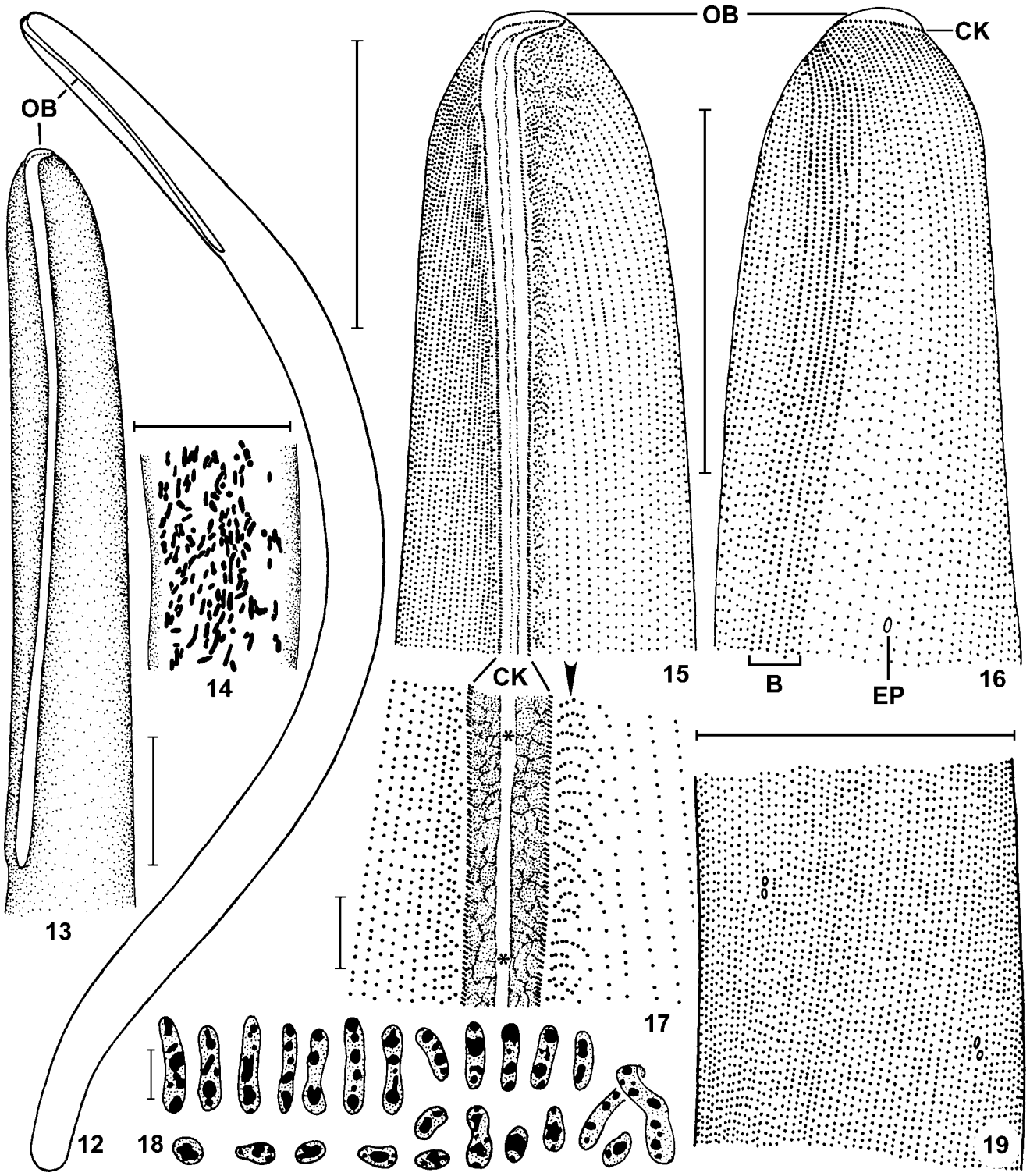

Figs 12-19. *Myriokaryon lieberkuehnii*, main voucher specimen after protargol impregnation. **12, 13** - ventrolateral overview (length 1800 µm) and oral area at higher magnification; **14** - upper layer of macronuclear nodules in mid-body; **15, 16** - oral and somatic ciliary pattern of ventral and dorsal anterior body portion; **17** - ciliary pattern of mid-oral area at high magnification. Arrowhead marks kinetofragments, some obviously connected with the ciliary rows, at left margin of circumoral kinety. Asterisks denote oral slit; **18** - variability of macronuclear nodules, drawn to scale (6 µm); **19** - ciliary pattern in mid-body. B - dorsal brush; CK - circumoral kinety; EP - excretory pore; OB - oral bulge. Scale bars 6 µm (17, 18); 70 µm (13, 14-16, 19); 400 µm (12).

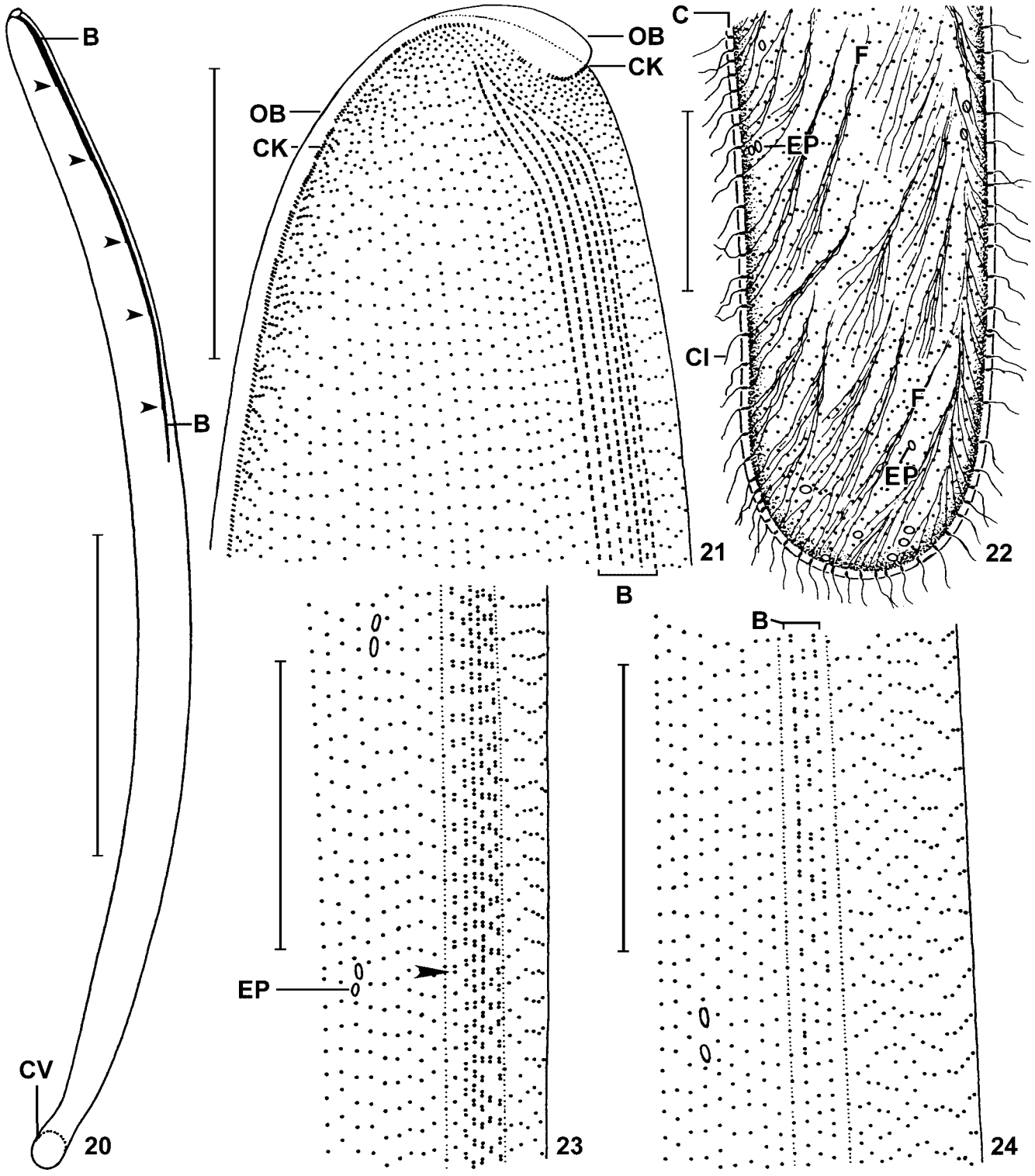

Figs 20-24. *Myriokaryon lieberkuehnii*, infraciliature after protargol impregnation. **20, 21, 23, 24** - dorsolateral overview (20) and details of dorsal brush in anterior (21), middle (23), and posterior (24) region. The brush rows gradually decrease in length from left to right (arrowheads) and continue posteriorly as ordinary somatic ciliary rows (24). Anteriorly, the middle brush rows are slightly shortened, while the marginal ones converge, forming a highly characteristic, pointed anterior brush end (21); **22** - posterior body region with subcortical fibre bundles originating from basal bodies of cilia. B - dorsal brush; C - cortex; CI - cilia; CK - circumoral kinety; CV - contractile vacuole; EP - excretory pores; F - fibre bundles; OB - oral bulge. Scale bars 30 µm (21-24); 400 µm (20).

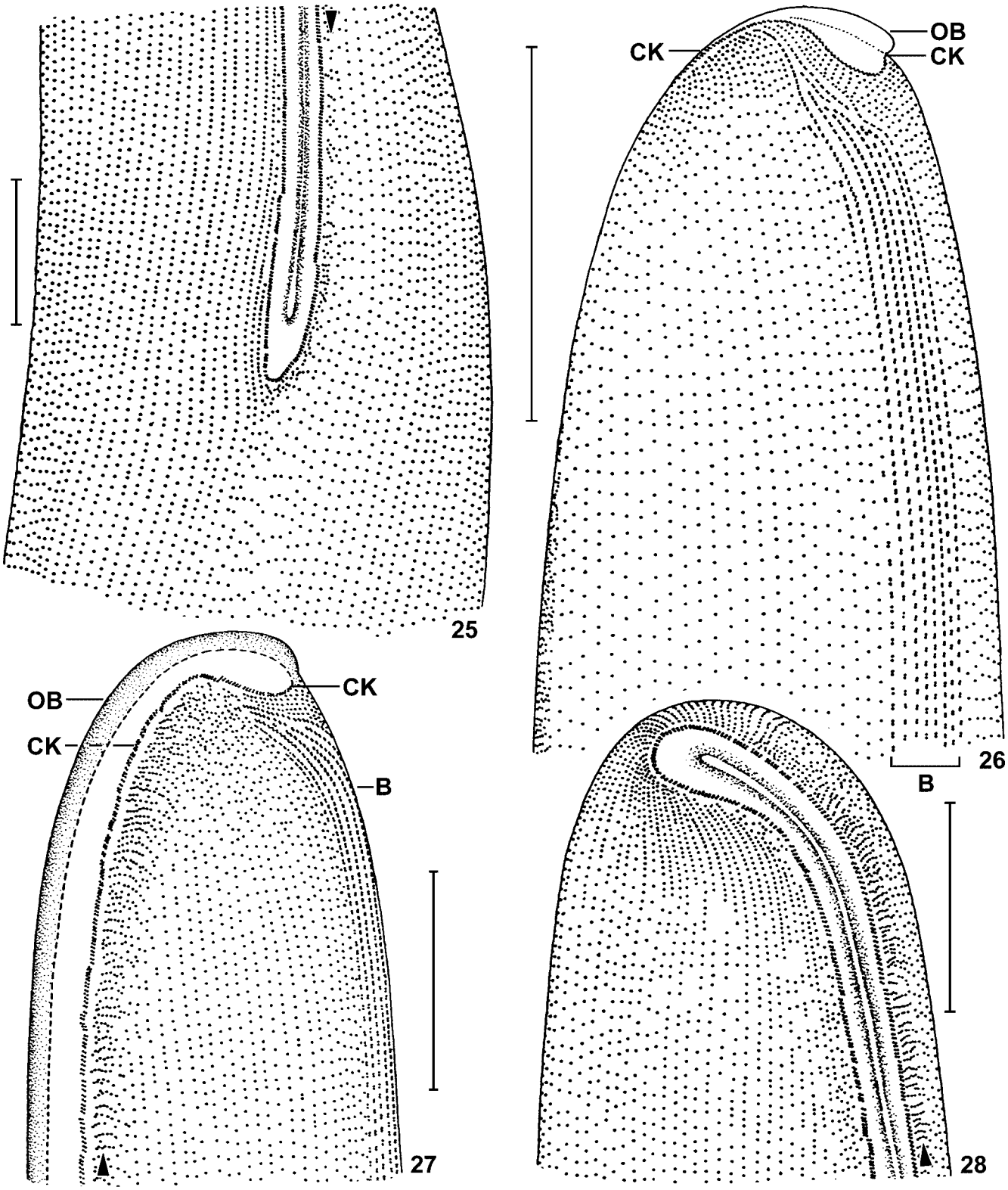

Figs 25-28. *Myriokaryon lieberkuehnii*, details of ciliary pattern after protargol impregnation. At right, the ciliary rows abut on the circumoral kinety in very steep angles, whereas at left many small kinetofragments, some obviously connected with the ciliary rows, occur and abut on the circumoral kinety at right angles (arrowheads). **25, 28** - ventral and frontal view showing the slightly widened posterior and anterior mouth end; **26, 27** - lateral views showing the main family features, viz., the strongly curved anterior portion of the oral bulge and circumoral kinety. Note the pointed anterior brush end. B - dorsal brush; CK - circumoral kinety; OB - oral bulge. Scale bars 30 µm.

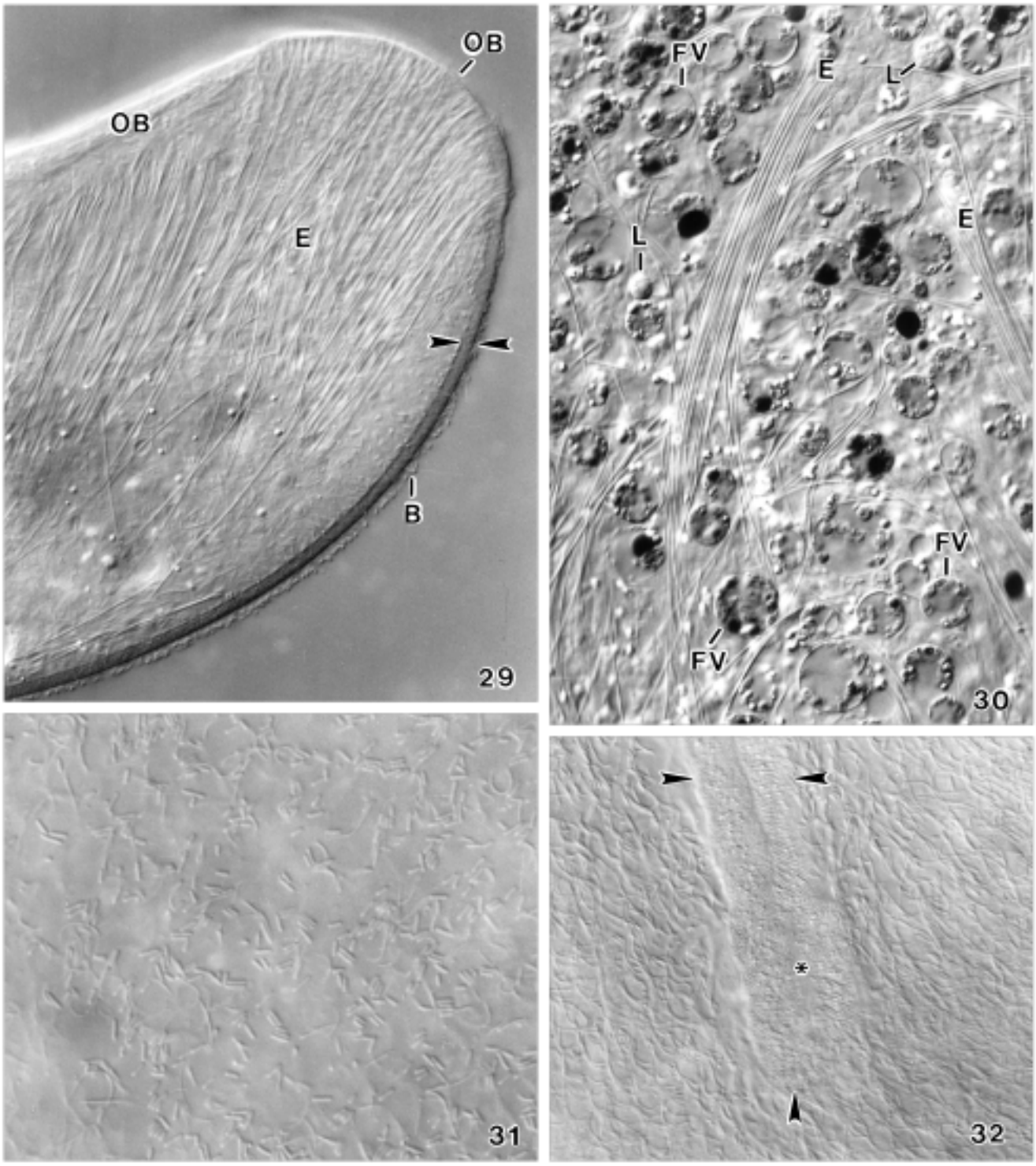

Figs 29-32. *Myriokaryon lieberkuehnii* from life (interference contrast). **29 -** anterior body portion of a slightly squashed specimen showing the 80 µm long extrusomes attached to the oral bulge. The opposed arrowheads mark the unusually thick cortex; **30 -** the cytoplasm is packed with extrusome bundles and about 10 µm-sized food vacuoles containing golden (and thus dark in the micrograph) lipid droplets, indicating that this specimen fed on autotrophic protists; **31 -** surface view showing the cortex covered with bacterial rods; **32 -** ventral view of posterior mouth end. The oral bulge, marked by arrowheads, is finely striated by rows of cortical granules, likely mucocysts; underneath are the extrusomes, whose anterior ends appear as minute granules (cp. figure 7). Asterisk denotes the mouth slit. B - dorsal brush; E - extrusomes; FV - food vacuoles; L - lipid droplets; OB - oral bulge.

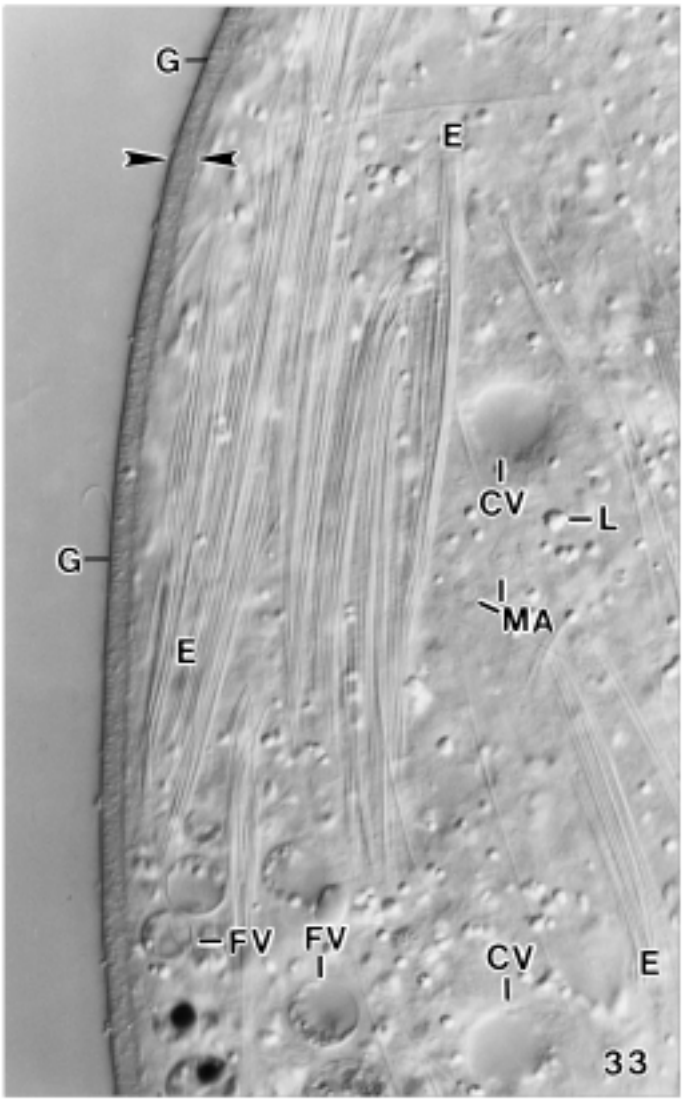

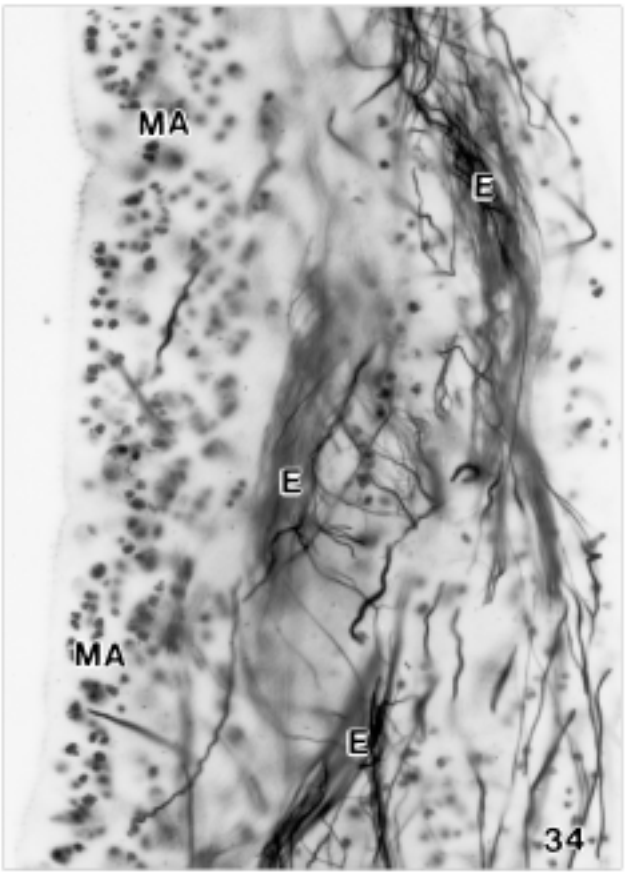

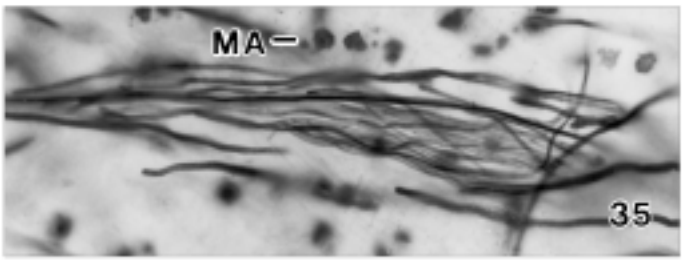

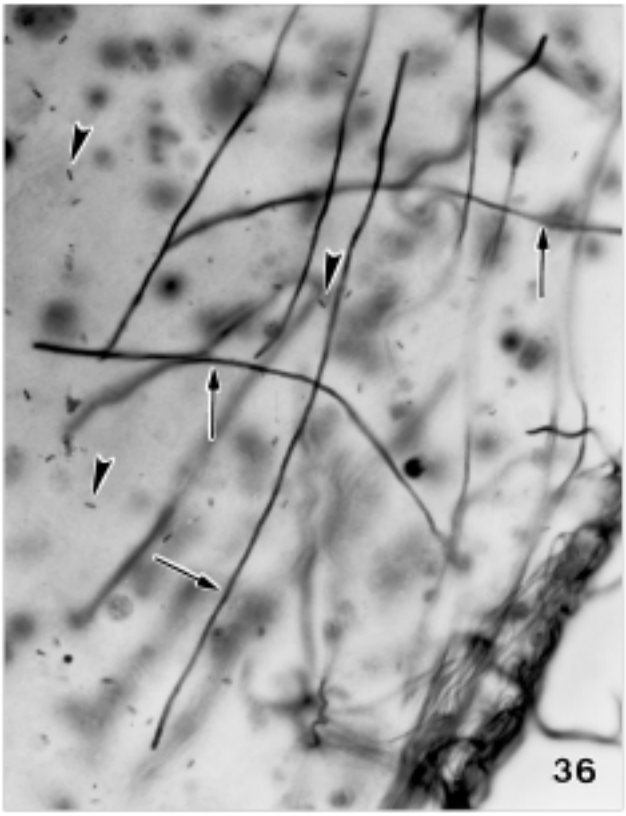

Figs 33-36. *Myriokaryon lieberkuehnii* from life (33) and after protargol impregnation (34-36). **33 -** optical section in mid-body showing the 3-4 µm thick cortex, marked by opposed arrowheads, and many about 80 µm long extrusome bundles; **34, 35** - overviews in mid-body, showing the cell packed with macronuclear nodules and extrusome bundles; **36 -** long (toxicysts, arrows) and short (likely mucocysts, arrowheads) extrusomes occur in the cytoplasm. CV - contractile vacuoles; E - extrusome bundles; FV - food vacuoles; G - cortical granules, likely mucocysts; L - lipid droplets; MA - macronuclear nodules.

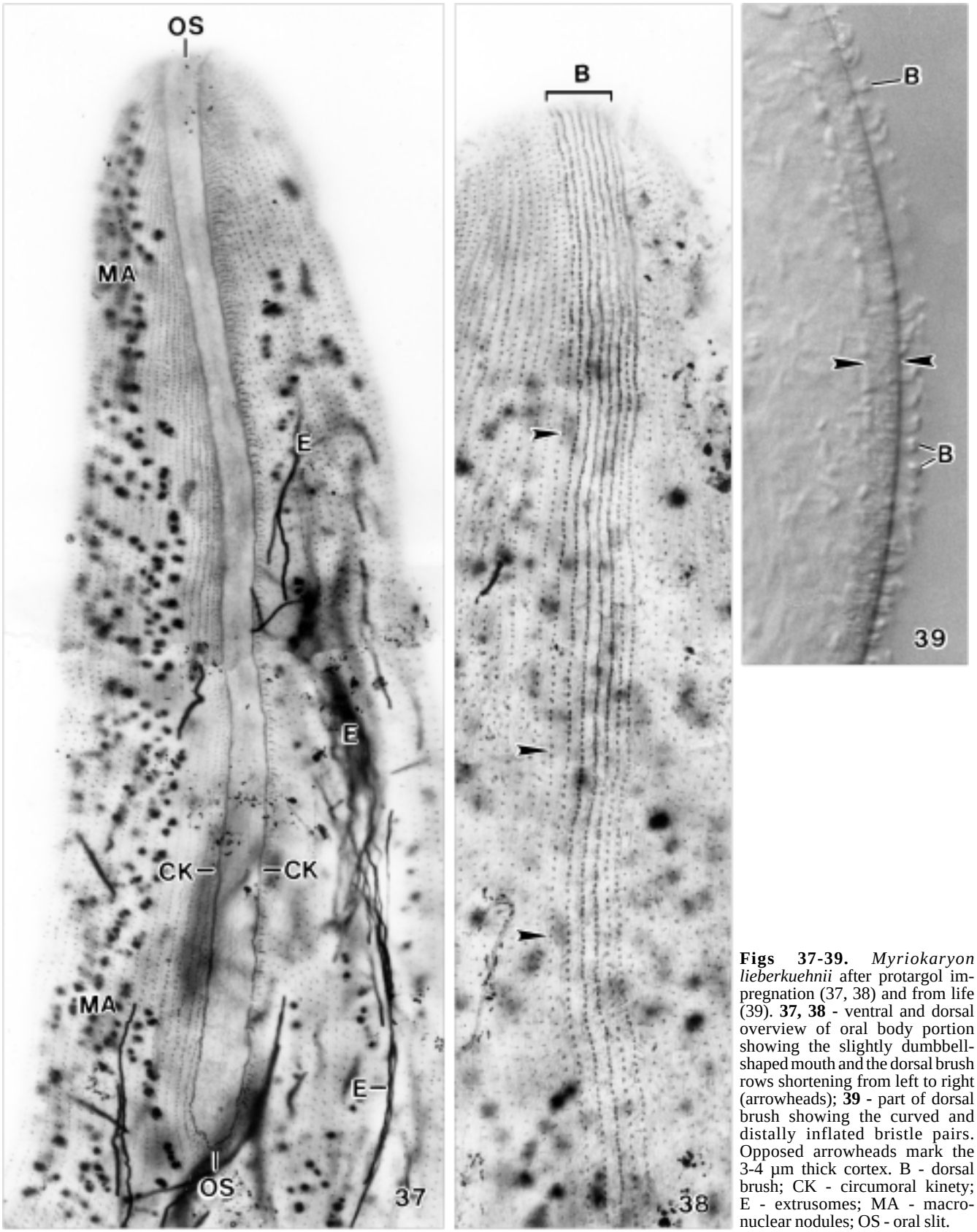

Figs 37-39. *Myriokaryon lieberkuehnii* after protargol impregnation (37, 38) and from life (39). **37, 38** - ventral and dorsal overview of oral body portion showing the slightly dumbbell-shaped mouth and the dorsal brush rows shortening from left to right (arrowheads); **39** - part of dorsal brush showing the curved and distally inflated bristle pairs. Opposed arrowheads mark the 3-4 µm thick cortex. B - dorsal brush; CK - circumoral kinety; E - extrusomes; MA - macronuclear nodules; OS - oral slit.

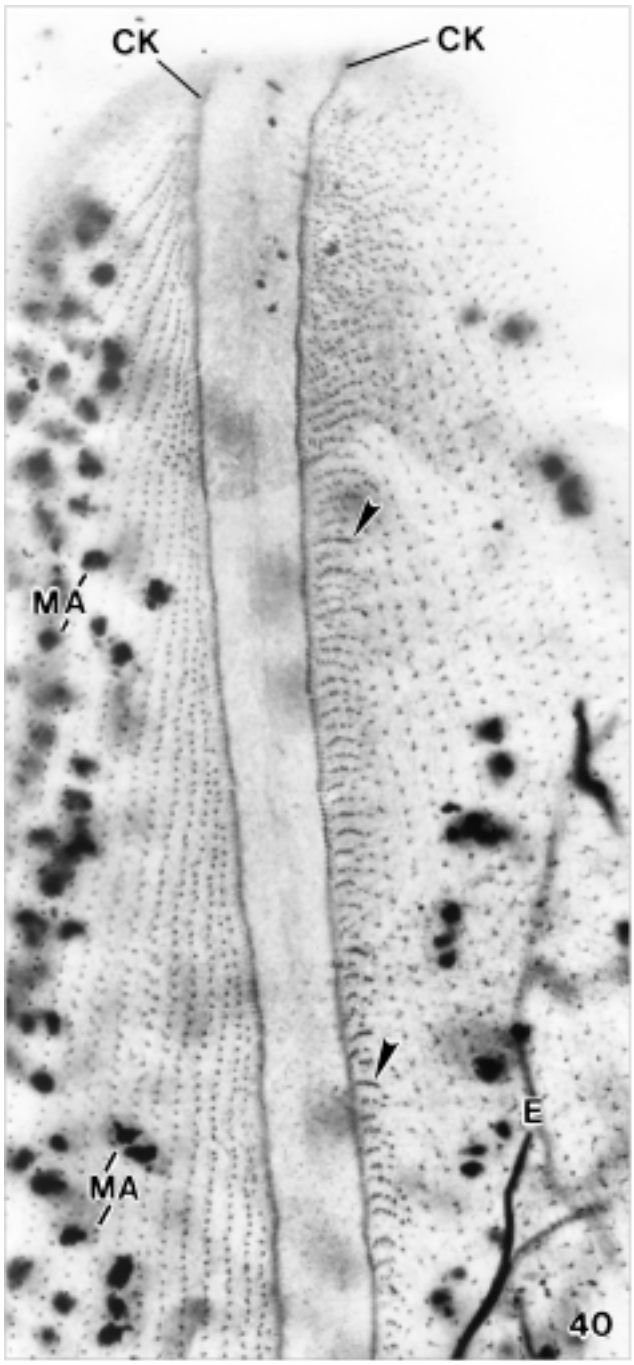

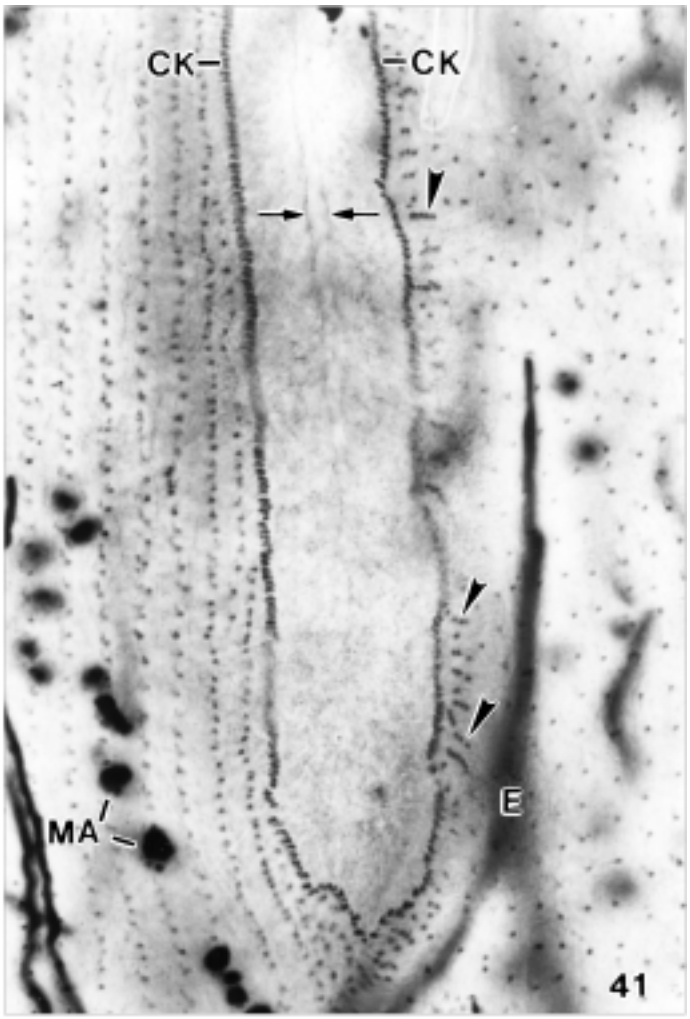

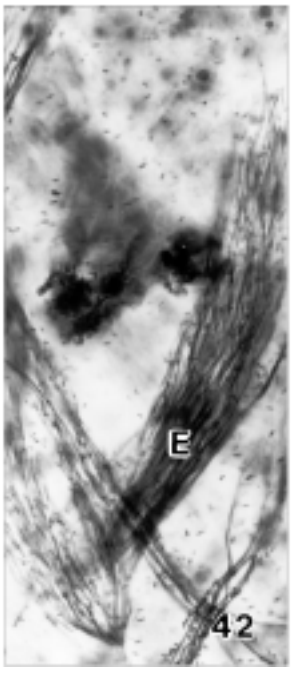

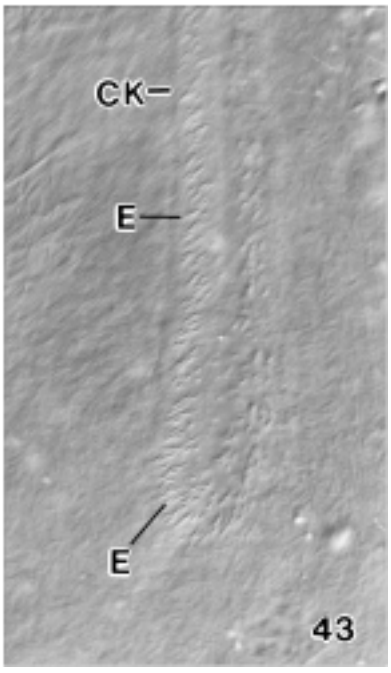

Figs 40-43. *Myriokaryon lieberkuehnii* after protargol impregnation (40-42) and from life (43). **40, 41** - anterior and posterior portion of mouth at high magnification (for an overview, see figure 37). At right, the somatic ciliary rows abut to the dikinetidal circumoral kinety in steep angles, while at left many transversely oriented, monokinetidal kinetofragments occur (some marked by arrowheads), some of which are obviously connected with the ciliary rows. Opposed arrows mark the mouth slit sensu stricto; **42** - extrusome bundles in the cytoplasm; **43** - surface view of posterior portion of oral bulge packed with extrusomes. CK - circumoral kinety; E - extrusomes; MA - macronuclear nodules.

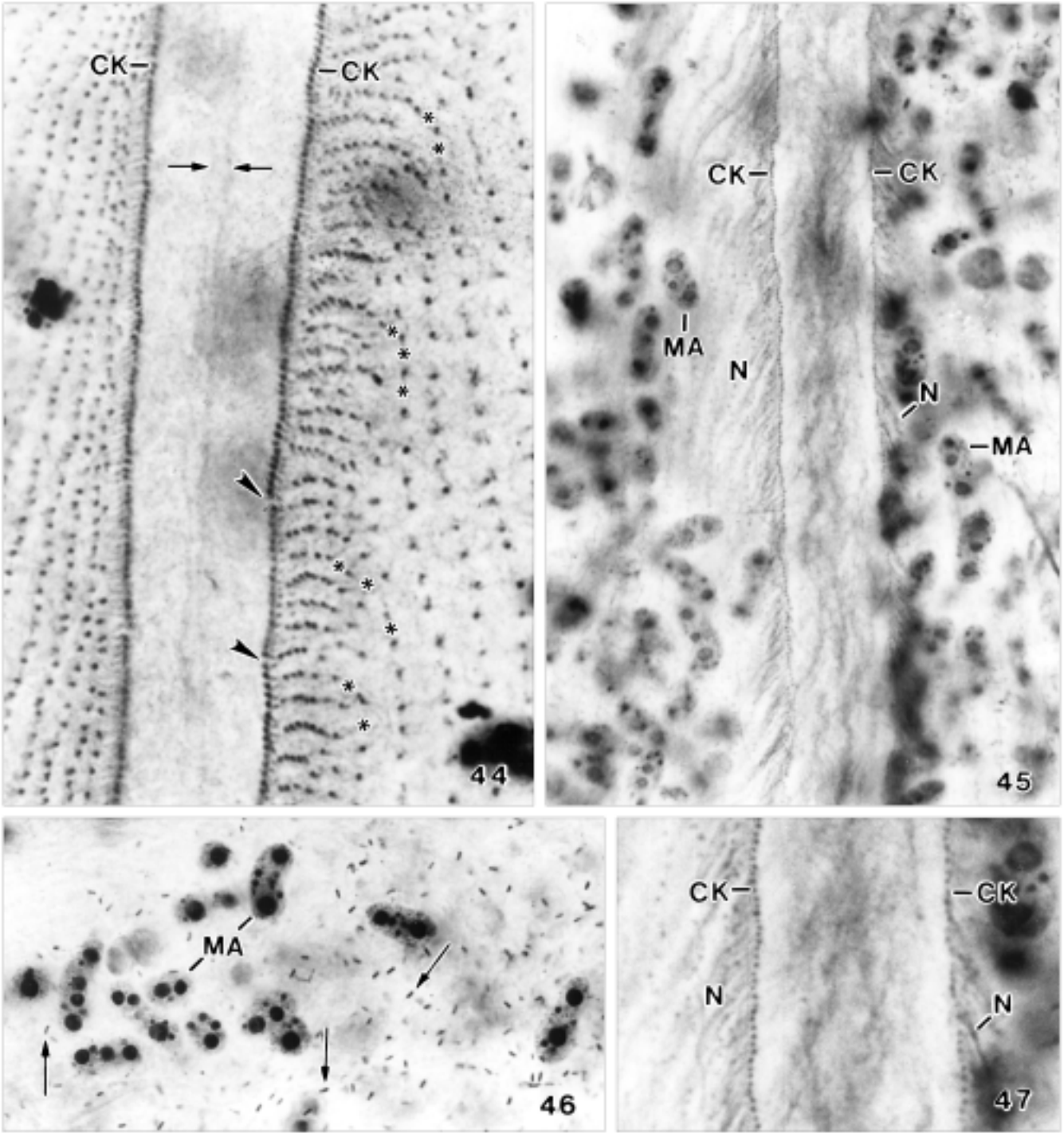

Figs 44-47. *Myriokaryon lieberkuehnii* after protargol impregnation. **44, 45, 47 -** oral infraciliature at high magnification and two focal planes, viz., at level of basal bodies (44) and tightly underneath (45, 47) to show the peripherically arranged macronuclear nodules and the very fine oral basket rods (nematodesmata) associated with the circumoral dikinetids (kinety). The circumoral kinety consists of dikinetidal kinetofragments, of which one is marked by arrowheads (44). Opposed arrows in figure 44 denote the faintly impregnated oral slit sensu stricto. At right, the somatic ciliary rows abut on the circumoral kinety at steep angles, while at left many transversely oriented, monokinetidal kinetofragments occur, some of which are obviously connected with the somatic ciliary rows (asterisks). This pattern reminds on *Spathidium* and *Supraspathidium*; **46 -** macronuclear nodules and 2 µm long rods (arrows), likely developing mucocysts, in subcortical layer. CK - circumoral kinety; MA - macronuclear nodules; N - nematodesmata.

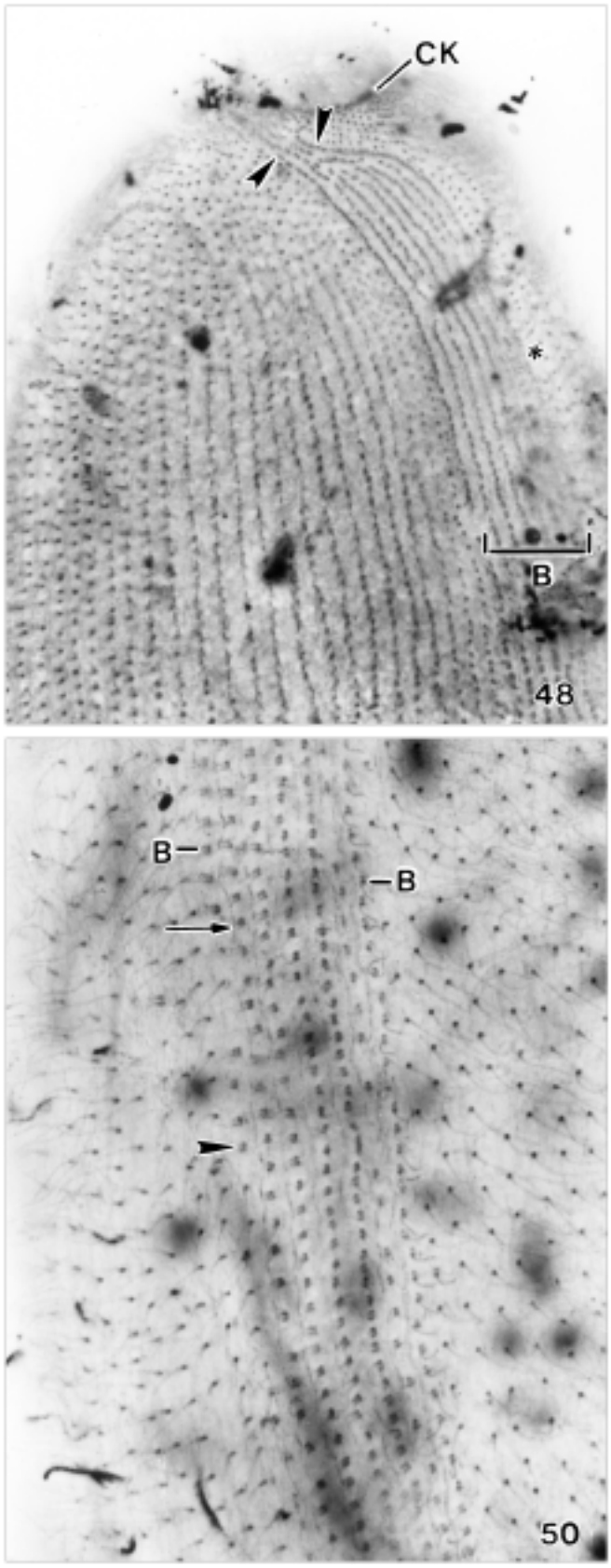

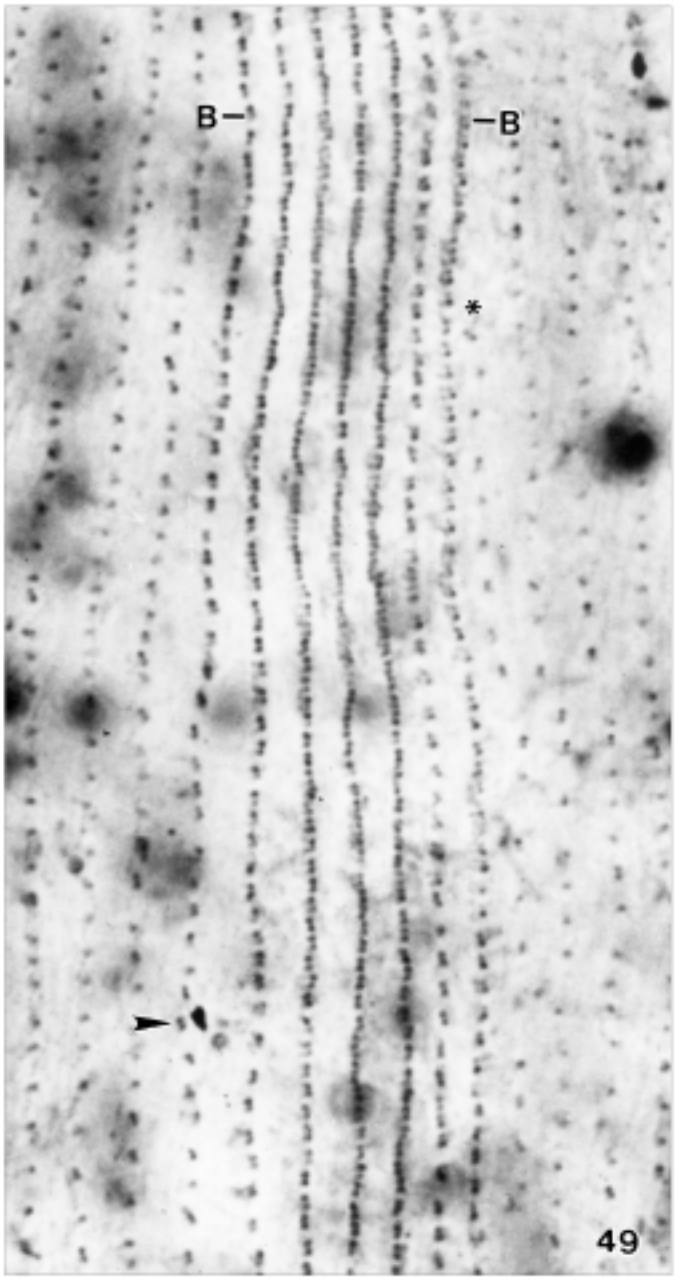

Figs 48-50. *Myriokaryon lieberkuehnii*, dorsal brush after protargol impregnation. The brush consists of narrowly spaced dikinetids in the anterior third of six to eight dorsal ciliary rows (Table 1). Kineties (asterisks) are successively inserted left of the brush. Thus and due to successive addition of kineties along the right mouth margin, kinety number is higher in mid-body than in the oral area. **48 -** anteriorly, the middle brush rows are shortened, while the unshortened marginal rows converge (arrowheads) and produce a unique, pointed brush end; **49, 50 -** subapical brush region of two other specimens, showing that the brush rows are successively shortened from left to right (arrowheads) and continue as ordinary somatic kineties posteriorly (see also following figures). Arrow in figure 50 marks a fine fibre (?) between the brush rows. B - dorsal brush; CK - circumoral kinety.

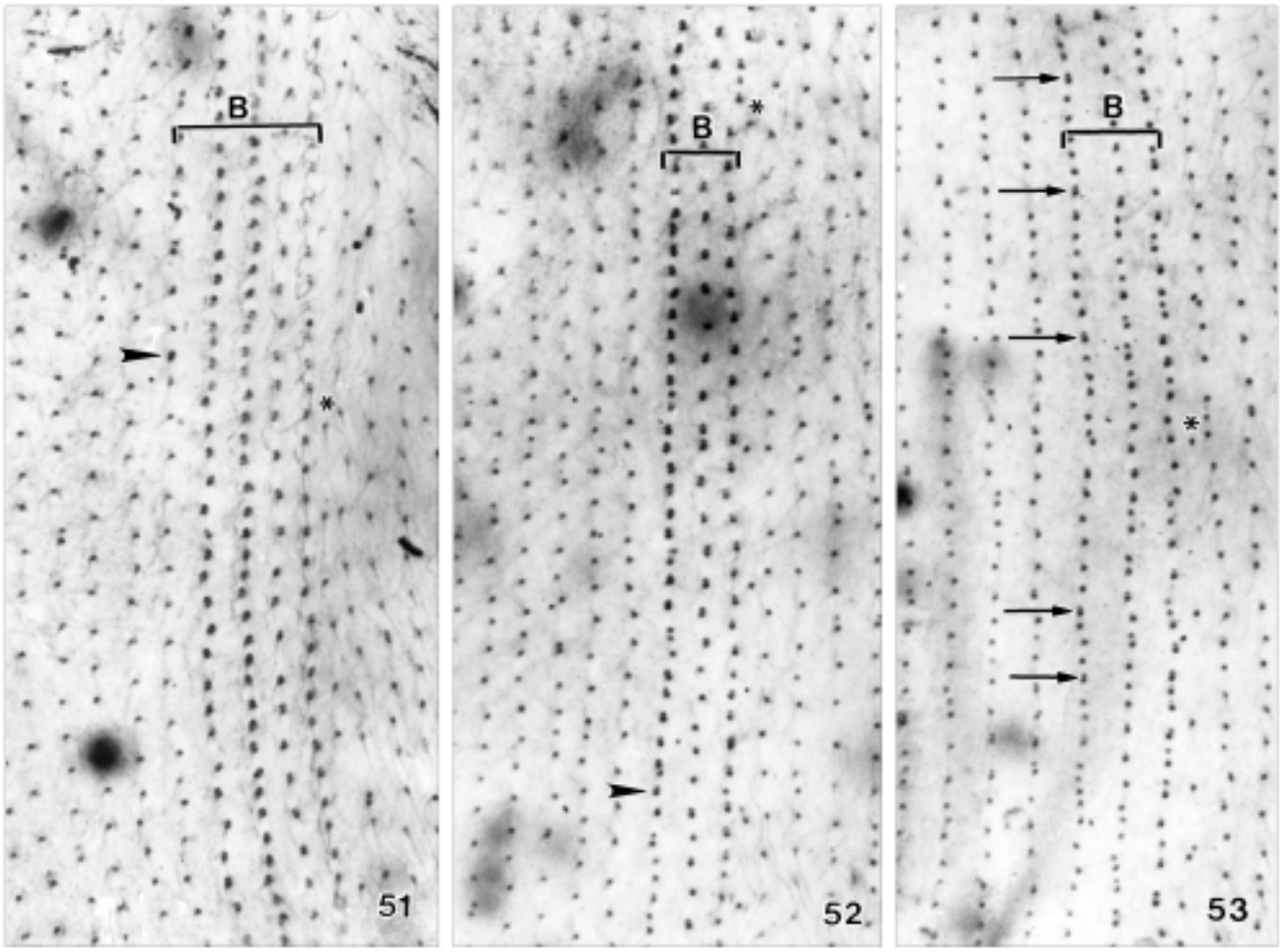

Figs 51-53. *Myriokaryon lieberkuehnii*, dorsal brush after protargol impregnation. The figures are from the same specimen as shown in figure 49, but demonstrate the middle (51) and posterior (52) region, where the brush, due to successive shortening of the rows from left to right (arrowheads), consist of only five, respectively, three rows. Figure 53 shows the post-brush area, where kinetids are slightly narrower spaced and some dikinetids (arrows) are interspersed in the basically monokinetidal rows extending to rear body end as ordinary somatic kineties. Kineties are successively inserted along the left brush margin (asterisks). Thus and due to the successive addition of kineties along the right mouth margin (Figs 37, 40, 44), kinety number is higher in mid-body than in the oral area. B - dorsal brush.

must be confirmed by more detailed investigations. Indeed, *M. lieberkuehnii* has been confused with other large, likely not yet described species, for instance, by Kahl (1930a; the small form, Fig. 99) and Al-Rasheid (2000), whose identification did not withstand a thorough reinvestigation (slide kindly provided by Dr. K. Al-Rasheid). The specimen illustrated (Fig. 100) and some others contained in the slide are insufficiently impregnated, but observation with interference contrast optics reveals a three-rowed polykinetid along the long and narrow mouth, indicating that it might be a poorly preserved geleiid. These data suggest that misidentifications are common and several not yet described or recognized *Myriokaryon* or *Myriokaryon*-like ciliate species exist, such as *Cranotheridium elongatum* Penard, 1922 and the new genus described below.

Myriokaryon lieberkuehnii is likely restricted to freshwater, occurring in ponds and pond-like habitats (Kahl 1930a; present study) or the lentic zones of running waters (Buck 1961, Dragesco 1972). Only Jankowski (1973) found it in plankton of ponds and in a lake near Leningrad. He observed up to 10 specimens in 1l lake water, where they hanged vertically in the water

column, indicating negative geotaxis. The records available show that *M. lieberkuehnii* has a wide ecological range from clean lake water to microaerobic bog environment (present record); it is thus surprising that it is so rare.

Detailed data on food and environmental requirements are unknown, although Buck (1961) classified *M. lieberkuehnii* as a beta-mesosaprobic indicator species in rivers of Germany. Like me, Jankowski (1973) observed bacteria, organic debris, small diatoms, and chrysomonads in the food vacuoles. *Colpidium*, when added in mass, was not ingested; thus, pure cultures failed. Jankowski (1973) observed globular inclusions 3-6 µm across, possibly endosymbionts.

Cephalospatula gen. n.

Diagnosis: vermiform Myriokaryonidae with long mouth on golfclub-shaped anterior (oral) body portion and 3 isomorphic dorsal brush rows. Extrusomes bundled in inflated anterior portion of oral bulge. At left side of circumoral kinety few oblique kinetofragments more or less distinctly connected with left side ciliary rows (basically *Spathidium* pattern).

Type species: *Cephalospatula brasiliensis* sp. n.

Etymology: composite of the Greek noun *cephalo* (head) and the Latin generic name *Spathidium* (spatulate organism), referring to both, the inflated anterior end and the similarity with members of the family Spathidiidae. Feminine gender.

Description of *Cephalospatula brasiliensis* sp. n. (Figs 54-90; Table 2)

Diagnosis: size about 350 x 35 µm *in vivo*. Rod-shaped with flat, inconspicuous oral bulge extending about one third of body length. Macronucleus filiform. On average 4 contractile vacuoles in line with dorsal brush. Two types of extrusomes: type I acicular and about 10 x 1 µm *in vivo*; type II rod-shaped and 3 µm long. On average 37 ciliary rows and about 50 dikinetids in each brush row.

Type location: floodplain soil of Paraná River in Brazil, near the town of Maringá, 53°15'W 22°40'S.

Etymology: named after the native country.

Type material: 1 holotype slide and 4 paratype slides with protargol-impregnated specimens from type location and 6 voucher slides with protargol-impregnated specimens from the other populations have been deposited in the Biologiezentrum of the Oberösterreichische Landesmuseum in Linz (LI). Relevant specimens are marked by a black ink circle on the cover glass.

Description: I studied 3 populations of this species. However, only few specimens were found, altogether 16 cells. Thus, morphometry of the individual populations is incomplete (Table 2). A closer analysis of the data shows that the two Brazilian populations tend to be more similar to each other than to the Venezuelan specimens, indicating some biogeographic specialization. However, variability of most characters is high, as usual in long and slender ciliates, suggesting that morphometric differences should not be over-interpreted. Nonetheless, I base the diagnosis and description only on the two Brazilian populations. The Venezuelan specimens are considerably longer and thinner than the Brazilian ones (439 x 27 µm *vs*. 375 x 31 µm and 287 x 32 µm) and have also fewer ciliary rows (32 *vs.* 36-38). All other main features, viz., the nuclear apparatus and extrusome size, shape, and location are very similar.

Size 200-500 x 20-45 µm *in vivo*, depending on population, Brazilian specimens frequently near 250 x 35 µm and distinctly stouter than Venezuelan cells (Table 2). Usually rod-shaped and slightly curved, rarely vermiform; unflattened and acontractile. Anterior body end obliquely truncate and slightly inflated, especially in protargol preparations, inflation ("head") and oblique truncation difficult to recognize *in vivo* because specimens are very flexible and restless; posterior end narrowly rounded, widest near or in mid-body (Figs 54, 68, 78, 83, 86, 90). Nuclear apparatus usually in posterior two thirds of cell. Macronucleus filiform, tortuous, often somewhat spiralized and nodulated, ribbon-like flattened (2:1) in most specimens from type location and in some cells from the other populations, a conspicuous feature found also in several slender spathidiids (Foissner *et al*. 2002); nucleoli scattered, small, inconspicuous. On average 18 globular to broadly ellipsoidal micronuclei attached to or near macronuclear strand, some scattered (Figs 54, 67, 69, 80, 83, 86). Three to eight, usually three to five contractile vacuoles in line with dorsal brush, first vacuole, occasionally also second within brush rows; each vacuole with several closely spaced, interkinetal excretory pores in line, except of scattered pores of last vacuole in posterior body end (Figs 54, 57, 66, 68, 71). Cortex rather thick, contains about three rows of pale, 0.8-1 x 0,4 µm-sized granules between each two ciliary rows; granules form short, transverse rows (type location) or arrow-like pattern (other populations) in cortex of oral bulge (Figs 55, 56, 59, 60, 64). Two shape and size types of extrusomes scattered in cytoplasm and assembled to highly conspicuous bundle in inflated anterior portion of oral bulge, definitely lacking in ventral bulge

Table 2. Morphometric data on three populations of *Cephalospatula brasiliensis.*

Characteristics[a]	Pop[b]	x	M	SD	SE	CV	Min	Max	n
Body, length	BRP	375.0	390.0	101.9	38.5	27.2	195.0	500.0	7
	BRR	287.5	310.0	59.7	29.8	20.8	200.0	330.0	4
	VEN	439.0	435.0	95.2	42.6	27.7	300.0	550.0	5
	TOT	373.1	380.0	103.4	25.8	21.7	195.0	550.0	16
Body, maximum width	BRP	31.0	31.0	5.0	1.9	16.1	22.0	36.0	7
	BRR	32.0	30.0	5.4	2.7	16.9	28.0	40.0	4
	VEN	26.8	28.0	4.4	2.0	16.6	20.0	31.0	5
	TOT	29.9	30.0	5.1	1.3	17.1	20.0	40.0	16
Body length:width, ratio	BRP	11.9	12.3	1.9	0.7	16.1	8.9	14.7	7
	BRR	9.2	9.3	2.4	1.2	26.2	6.7	11.4	4
	VEN	16.5	15.0	3.5	1.6	21.1	13.7	17.9	5
	TOT	12.7	12.6	3.8	0.9	29.9	6.7	22.0	16
Mouth, length (anterior body end to	BRP	108.0	115.0	29.0	11.0	26.9	55.0	140.0	7
proximal end of circumoral kinety, distance)	BRR	98.5	107.5	21.2	10.6	21.5	67.0	112.0	4
	VEN	128.2	125.0	42.4	19.0	33.1	70.0	180.0	5
	TOT	111.9	111.0	32.4	8.1	29.0	55.0	180.0	16
Body length:mouth length, ratio	BRP	3.5	3.5	0.2	0.1	5.6	3.1	3.7	7
	BRR	2.9	3.0	0.1	0.1	4.9	2.7	3.0	4
	VEN	3.6	3.5	0.5	0.2	15.1	2.8	4.3	5
	TOT	3.4	3.5	0.4	0.1	13.4	2.7	4.3	16
Mouth, anterior width (distance between	BRP	12.0	-	-	-	-	9.0	15.0	2
circumoral kinety in head area)	BRR	14.5	-	-	-	-	12.0	17.0	2
	VEN	12.5	-	-	-	-	12.0	13.0	2
	TOT	13.0	12.5	2.8	1.1	21.2	9.0	17.0	16
Mouth, mid-region width (distance between	BRP	4.7	5.0	-	-	-	4.0	5.0	6
circumoral kinety)	BRR	5.3	4.5	1.9	1.0	36.1	4.0	8.0	4
	VEN	4.0	4.0	-	-	-	4.0	4.0	3
	TOT	4.7	1.1	0.3	23.6	4.0	4.0	8.0	13
Anterior body end to macronucleus, distance	BRP	117.9	125.0	30.7	11.6	26.0	65.0	150.0	7
	BRR	110.5	122.5	34.4	17.2	31.1	60.0	137.0	4
	VEN	147.6	138.0	31.3	14.0	21.2	120.0	190.0	5
	TOT	125.3	125.0	33.5	8.4	26.8	60.0	190.0	16
Macronuclear figure, length	BRP	209.2	200.0	73.9	30.2	35.3	95.0	290.0	6
	BRR	143.0	147.5	38.8	19.4	27.1	92.0	185.0	4
	VEN	232.0	240.0	71.8	32.1	31.0	125.0	310.0	5
	TOT	199.1	190.0	71.3	18.4	35.8	92.0	310.0	15
Macronucleus spread, length (uncoiled but	BRP	270.0	270.0	-	-	-	110.0	400.0	7
not despiralized, very approximate values)	BRR	176.3	180.0	-	-	-	110.0	235.0	4
	VEN	266.0	295.0	-	-	-	125.0	360.0	5
	TOT	245.3	255.0	-	-	-	110.0	400.0	16
Macronucleus, width	BRP	8.7	9.0	1.4	0.5	15.8	7.0	10.0	7
	BRR	6.0	6.0	0.8	0.4	13.6	5.0	7.0	4
	VEN	7.6	8.0	1.5	0.7	20.0	5.0	9.0	5
	TOT	7.7	8.0	1.7	0.4	21.6	5.0	10.0	16
Macronucleus, number (in 2 out of 16	BRP	1.0	1.0	0.0	0.0	0.0	1.0	1.0	5
specimens broken into two long pieces)	BRR	1.0	1.0	0.0	0.0	0.0	1.0	1.0	4
	VEN	1.0	1.0	0.0	0.0	0.0	1.0	1.0	5
	TOT	1.0	1.0	0.0	0.0	0.0	1.0	1.0	14
Micronuclei, diameter	BRP	3.6	3.5	-	-	-	3.0	4.0	7
	BRR	3.5	3.5	-	-	-	3.0	4.0	3
	VEN	3.5	3.5	-	-	-	3.0	4.0	5
	TOT	3.6	3.5	-	-	-	3.0	4.0	16
Micronuclei, number	BRP	19.3	20.0	2.9	1.1	15.2	14.0	23.0	7
	BRR	17.8	17.5	5.7	2.8	32.0	12.0	24.0	4
	VEN	19.0	17.0	4.0	1.8	21.1	15.0	25.0	5
	TOT	18.8	19.0	3.8	1.0	20.3	12.0	25.0	16

Table 2. (contd)	Pop[b]	x	M	SD	SE	CV	Min	Max	n
Contractile vacuoles, number	BRP	5.3	5.0	1.8	0.7	34.0	3.0	8.0	7
	BRR	3.0	3.0	0.0	0.0	0.0	5.0	5.0	3
	VEN	5.0	5.0	1.2	0.6	24.5	3.0	6.0	5
	TOT	5.1	5.0	1.4	0.4	26.4	3.0	8.0	15
Somatic kineties, total number in mid-body	BRP	35.9	36.0	4.5	1.7	12.4	29.0	41.0	7
	BRR	37.8	38.0	2.9	1.4	7.6	34.0	41.0	4
	VEN	31.6	32.0	2.5	1.1	7.9	28.0	35.0	5
	TOT	35.0	34.5	4.2	1.0	11.9	28.0	41.0	16
Ciliated kinetids in a lateral kinety, number	BRP	121.4	130.0	33.0	12.5	27.2	60.0	155.0	7
	BRR	109.3	110.0	29.0	16.8	26.5	80.0	138.0	3
	VEN	154.0	170.0	36.0	16.1	23.4	95.0	183.0	5
	TOT	129.9	138.0	35.9	9.3	27.7	60.0	183.0	15
Dorsal brush rows, number	BRP	3.0	3.0	0.0	0.0	0.0	3.0	3.0	7
	BRR	3.0	3.0	0.0	0.0	0.0	3.0	3.0	3
	VEN	3.0	3.0	0.0	0.0	0.0	3.0	3.0	4
	TOT	3.0	3.0	0.0	0.0	0.0	3.0	3.0	14
Dorsal brush row 1, length (distance circumoral kinety to last dikinetid)	BRP	113.9	100.0	38.5	14.6	33.8	67.0	170.0	7
	BRR	113.3	115.0	2.9	1.7	2.6	110.0	115.0	3
	VEN	157.5	175.0	49.2	24.6	31.3	85.0	195.0	4
	TOT	126.2	115.0	40.8	10.9	32.4	67.0	195.0	14
Dorsal brush row 1, number of dikinetids	BRP	43.9	39.0	14.2	5.4	32.4	26.0	67.0	7
	BRR	40.7	42.0	10.1	5.8	24.8	30.0	50.0	3
	VEN	51.0	55.5	16.0	8.0	31.3	28.0	65.0	4
	TOT	45.2	46.0	13.6	3.6	30.0	26.0	67.0	14
Dorsal brush row 2, length (distance circumoral kinety to last dikinetid)	BRP	123.9	130.0	35.3	13.3	28.5	67.0	170.0	7
	BRR	121.7	120.0	7.6	4.4	6.3	115.0	130.0	3
	VEN	163.8	185.0	53.6	26.8	32.7	85.0	200.0	4
	TOT	134.8	130.0	40.1	10.7	29.8	67.0	200.0	14
Dorsal brush row 2, number of dikinetids	BRP	57.6	55.0	21.8	8.2	37.8	18.0	80.0	7
	BRR	54.0	55.0	13.5	7.8	25.1	40.0	67.0	3
	VEN	57.0	67.0	19.1	11.0	33.5	35.0	69.0	3
	TOT	56.6	55.0	18.2	5.0	32.1	18.0	80.0	13
Dorsal brush row 3, length (distance circumoral kinety to last dikinetid)	BRP	133.1	130.0	41.1	15.5	30.9	67.0	190.0	7
	BRR	125.0	125.0	5.0	2.9	4.0	120.0	130.0	3
	VEN	163.8	182.5	46.6	23.3	28.5	95.0	195.0	4
	TOT	140.1	130.0	39.2	10.5	28.0	67.0	195.0	14
Dorsal brush row 3, number of dikinetids	BRP	49.1	50.0	14.4	5.4	29.3	27.0	70.0	7
	BRR	49.0	50.0	10.5	6.1	21.5	38.0	59.0	3
	VEN	49.8	51.5	12.5	6.2	25.1	33.0	63.0	4
	TOT	49.3	50.0	12.2	3.3	24.7	27.0	70.0	14

[a] Data based on mounted, protargol-impregnated (Foissner's method), morphostatic specimens from non-flooded Petri dish cultures. Measurements in µm. CV - coefficient of variation in %, M - median, Max - maximum, Min - minimum, n - number of individuals investigated, SD - standard deviation, SE - standard error of arithmetic mean, x - arithmetic mean. [b] Populations: BRP - Brazil, Paraná floodplain type population; BRR - Brazil, Restingha region (Mata Atlantica) near Rio de Janeiro; VEN - Venezuela, Laja (rock pool) at Puerto Ayacucho airport; TOT - all three populations combined.

portion of all populations and specimens investigated (Figs 54, 57, 58, 61-63, 79, 81, 82, 90): type I extrusomes conspicuous because acicular, slightly curved and 12 x 1 µm in size (9-11 x 1 µm in second Brazilian population, 12-14 x 1 µm in Venezuelan specimens), rarely faintly impregnate with the protargol method used; type II extrusomes rod-shaped, inconspicuous because fine and only 3-4 µm long. Exploded type I extrusomes 25-35 x 1 µm in size, of typical toxicyst structure (Figs 62, 79, 82). Cytoplasm colourless, usually crammed with lipid droplets 1-2 µm across and food vacuoles containing remnants of rotifers and oral baskets of small ciliates, likely *Drepanomonas* (Figs 54, 55, 68). Swims rather rapidly by rotation about main body axis, showing great flexibility.

Cilia about 8 µm long *in vivo*, loosely spaced in oral area, arranged in an average of 37 (32 in Venezuelan specimens) ordinarily and equidistantly spaced rows abutting on circumoral kinety in *Spathidium* pattern, that is, in steep angles on right side and at almost right angles

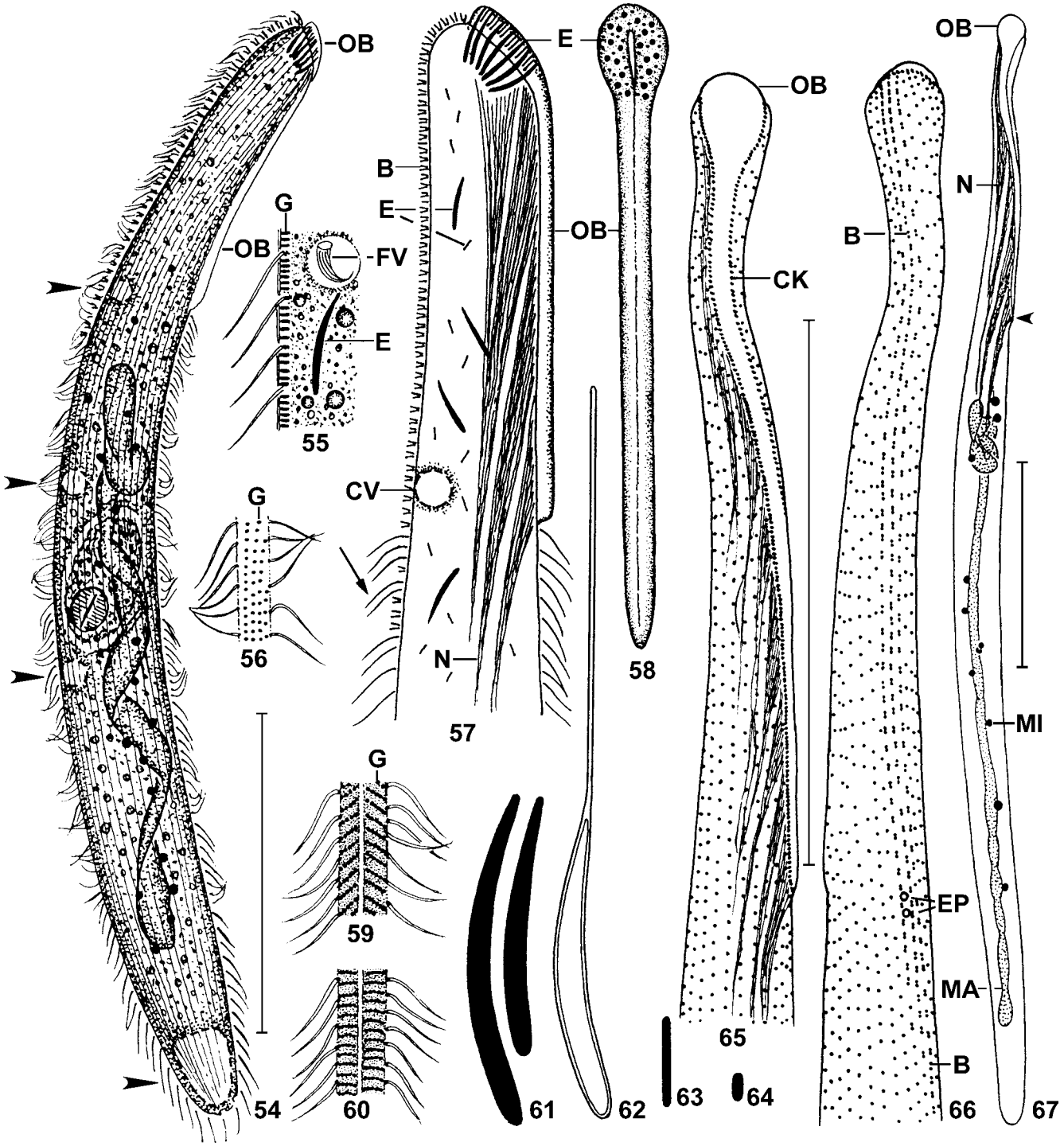

Figs 54-67. *Cephalospatula brasiliensis* from life (54-64) and after protargol impregnation (65-67). **54 -** right side view of a representative specimen from type location. Note the large food vacuole with a decomposing rotifer in mid-body. Arrowheads mark contractile vacuoles; **55, 56 -** optical section and surface view of cortex. Note food vacuole with a decomposing oral basket of a microthoracid ciliate; **57, 58 -** lateral and frontal view of oral area, showing the conspicuous, spoon-shaped oral bulge containing extrusomes only in the anterior inflation. Arrow marks posterior brush region, where bristles and ordinary cilia alternate; **59, 60 -** cortical granulation of oral bulge in a Venezuelan (59) and Brazilian (60) specimen; **61-63 -** resting (61, 63) and exploded (62) type I (61, 62) and type II (63) oral bulge extrusomes, drawn to scale, length 9-12 µm, 25 µm, 3-4 µm; **64 -** cortical granule, about 0.8-1 x 0.4 µm; **65, 66 -** ventral and dorsal view of ciliary pattern in oral body portion of a Venezuelan specimen; **67 -** ventrolateral view of a Venezuelan specimen with almost straight macronucleus. Arrowhead marks end of oral bulge. B - dorsal brush; CK - circumoral kinety; CV - contractile vacuole; E - extrusomes; EP - excretory pores; FV - food vacuole; G - cortical granules; MA - macronucleus; MI - micronucleus; N - nematodesmata; OB - oral bulge. Scale bars 100 µm.

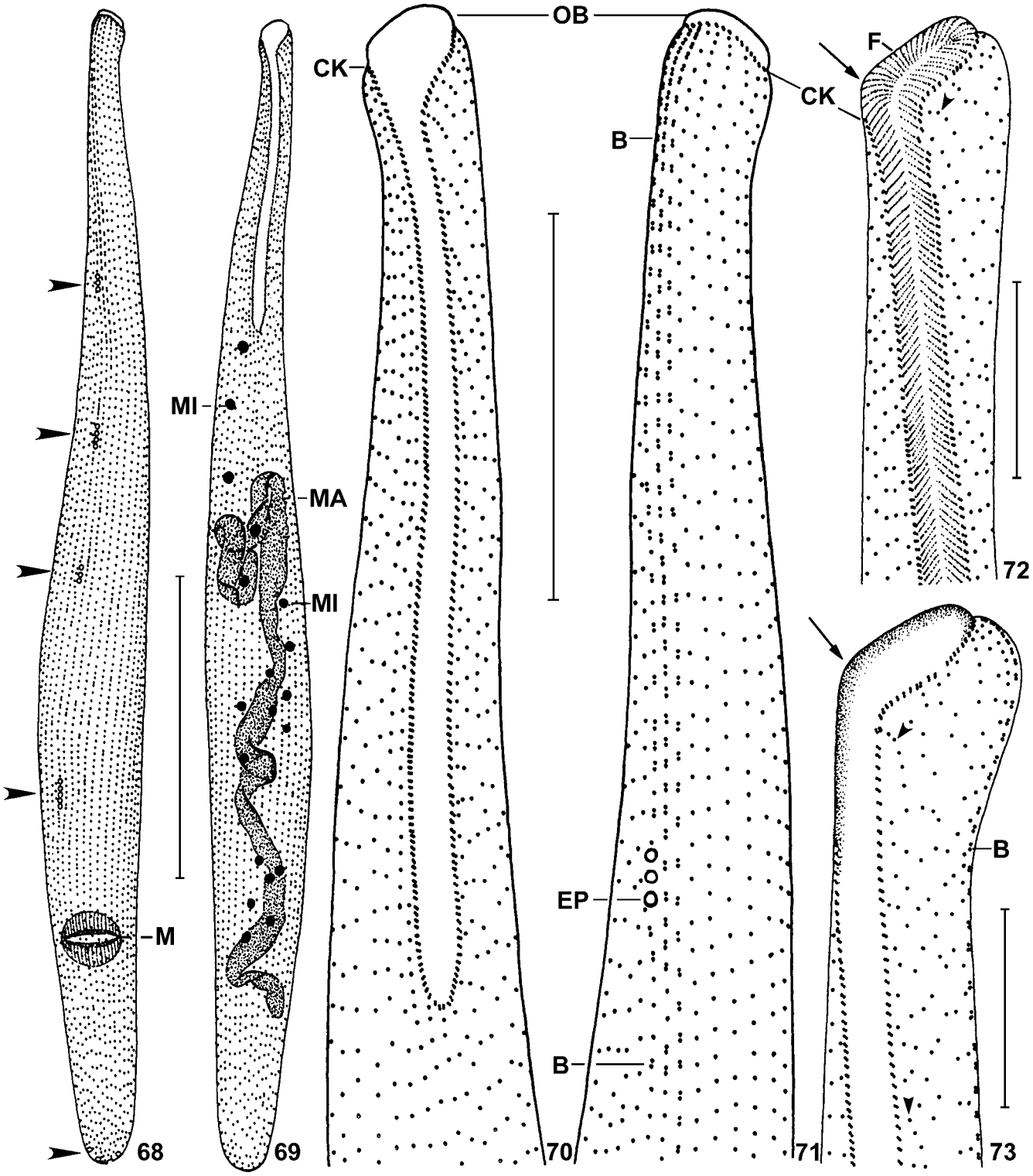

Figs 68-73. *Cephalospatula brasiliensis*, ciliary pattern after protargol impregnation. **68, 69** - dorsal and ventral view of holotype specimen. Arrowheads mark excretory pores of the contractile vacuoles; **70, 71** - ventral and dorsal view of oral body portion of holotype specimen; **72, 73** - left side view of anterior body portion of two other specimens from type location. Note the sharp angle in the oral bulge (arrows) and circumoral kinety caused by the oblique truncation of the body end. Arrowheads mark indistinct left side kinetofragments. B - dorsal brush; CK - circumoral kinety; EP - excretory pores; F - oral bulge fibres; M - mastax of a rotifer; MA - macronucleus; MI - micronuclei; OB - oral bulge. Scale bars 100 µm (68, 69); 40 µm (70, 71); 20 µm (72, 73).

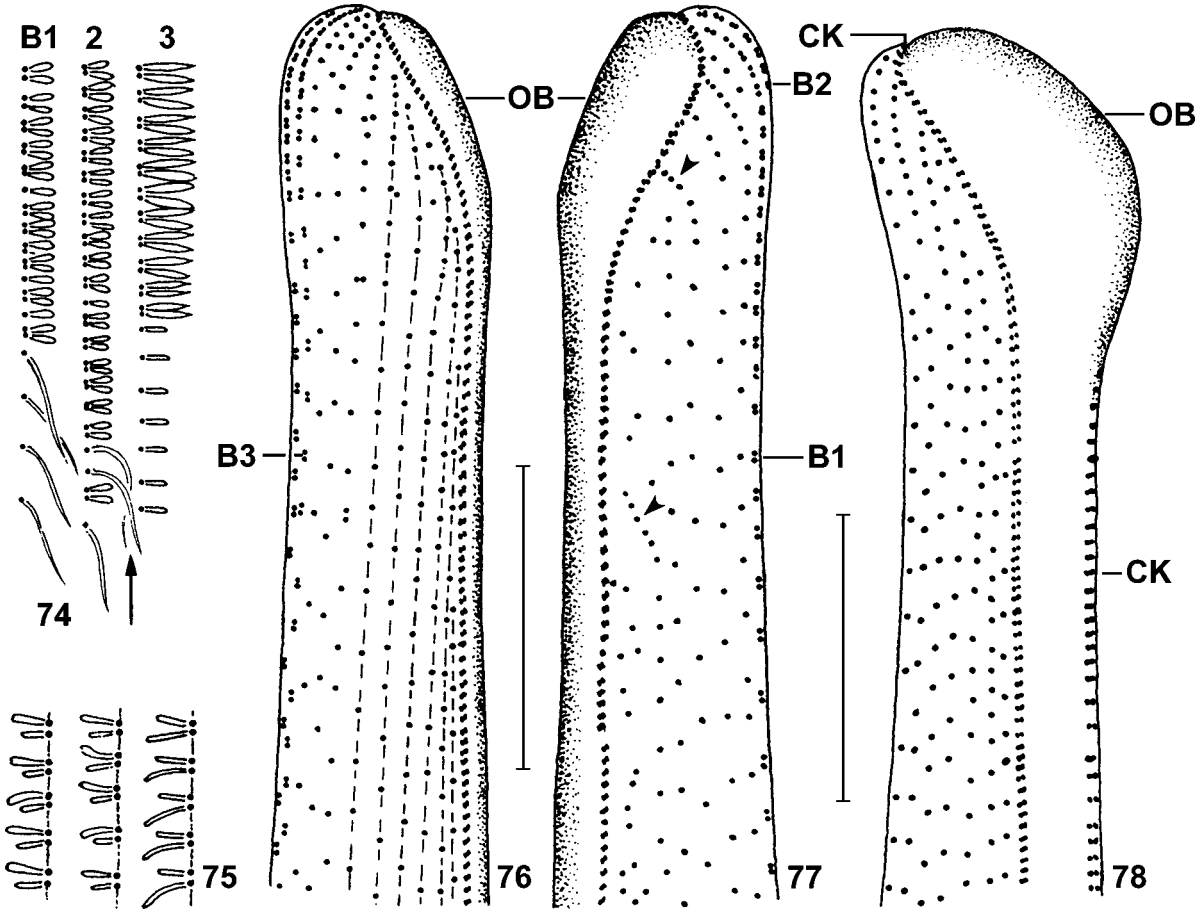

Figs 74-78. *Cephalospatula brasiliensis* from life (74) and after protargol impregnation (75-78). **74, 75 -** posterior portion of dorsal brush in a specimen from Brazilian type location *in vivo* (74) and middle brush region of a Venezuelan specimen after protargol impregnation. Arrow denotes ordinary cilia between brush bristles. Note monokinetidal bristle tail of row 3; **76, 77 -** right and left side ciliary pattern of anterior body portion in a Venezuelan specimen. The ciliary rows (basal bodies connected by lines) abut on the right branch of the circumoral kinety at very steep angles (*Arcuospathidium*/*Myriokaryon* pattern), while at left side an indistinct *Myriokaryon* pattern occurs, as indicated by some oblique kinetofragments (arrowheads); **78 -** ventrolateral view of anterior portion of a specimen from Brazilian population II. Note the strong inflation of the anterior body end, respectively, of the oral bulge. B1-3 - dorsal brush rows; CK - circumoral kinety; OB - oral bulge. Scale bars 20 µm.

on left; left side pattern, however, distinct only in apical region, where cilia form kinetofragment-like condensations (Figs 54, 65, 68-73, 76-78, 83-85, 87, 88; Table 2). Three dorsolateral ciliary rows anteriorly differentiated to dorsal brush occupying 35% of body length on average; brush, however, inconspicuous *in vivo* because bristles merely up to 4 µm long; dikinetidal and monokinetidal bristles irregularly alternate in posterior region of brush, and some monokinetids are interspersed in whole length of brush (Figs 54, 57, 66, 68, 71, 76, 77, 89; Table 2). Brush rows 1 and 2 of very similar structure, that is, composed of about 2 µm long, paired, inflated bristles, row 2 slightly longer than rows 1 and 3; row 3 composed of 3-4 µm long, fusiform bristles and a monokinetidal tail extending to second body third with about 3 µm long bristles; rarely, brush rows have a short, monokinetidal tail anteriorly (Figs 54, 57, 74, 75).

Mouth extends on anterior third of body, indistinct, except of inflated anterior portion containing the conspicuous extrusome bundle, due to the flat, hardly projecting oral bulge. Oral bulge distinctly spoon-shaped, conspicuous when viewed ventrally, both *in vivo* and protargol preparations, due to the anterior inflation; contains fine, short fibres originating from circumoral dikinetids and extending obliquely anteriorly. Circumoral kinety composed of comparatively widely spaced, oblique dikinetids having ciliated only one basal body; of same shape as oral bulge, shows highly characteristic,

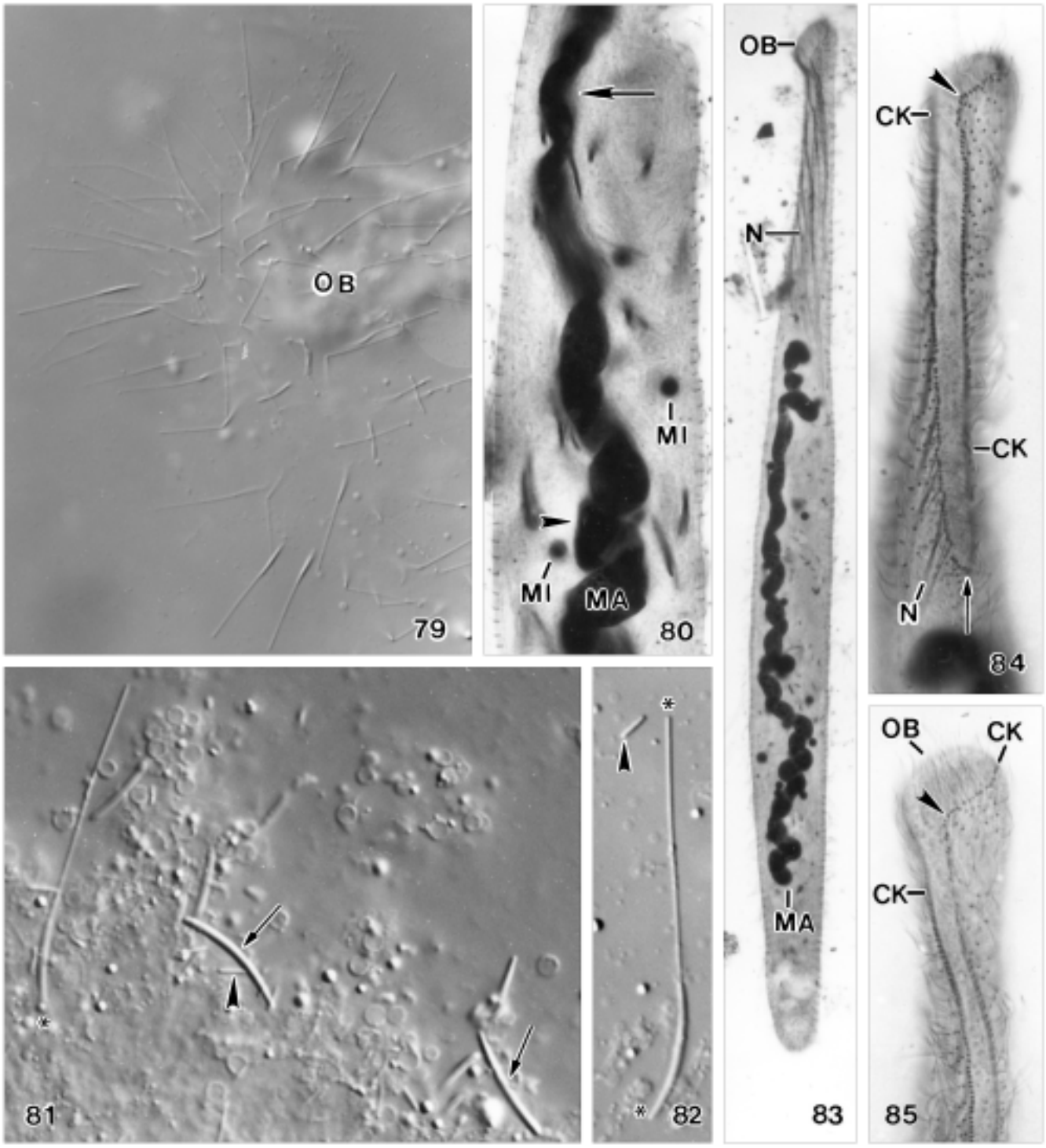

Figs 79-85. *Cephalospatula brasiliensis* from life (79, 81, 82) and after protargol impregnation (80, 83-85). **79 -** anterior body (oral bulge) end of a squashed specimen with released type I extrusomes, which have typical toxicyst structure and are about 25 µm long; **80 -** middle portion of nuclear apparatus. The macronucleus is spiralized and ribbon-like flattened showing either the broad (arrowhead) or narrow (arrow) side; **81, 82 -** resting (arrows) and extruded (asterisks) type I extrusomes and resting type II extrusomes (arrowheads), which are 3-4 µm long; **83 -** overview showing some main features, such as the obliquely truncated anterior end and the spiralized macronucleus; **84, 85 -** ventral views of anterior body portion showing the sharp bend (arrowheads) in the oral bulge and circumoral kinety, a main feature of the family Myriokaryonidae. Arrow denotes proximal end of mouth (circumoral kinety). CK - circumoral kinety; MA - macronucleus; MI - micronuclei; N - nematodesmata; OB - oral bulge.

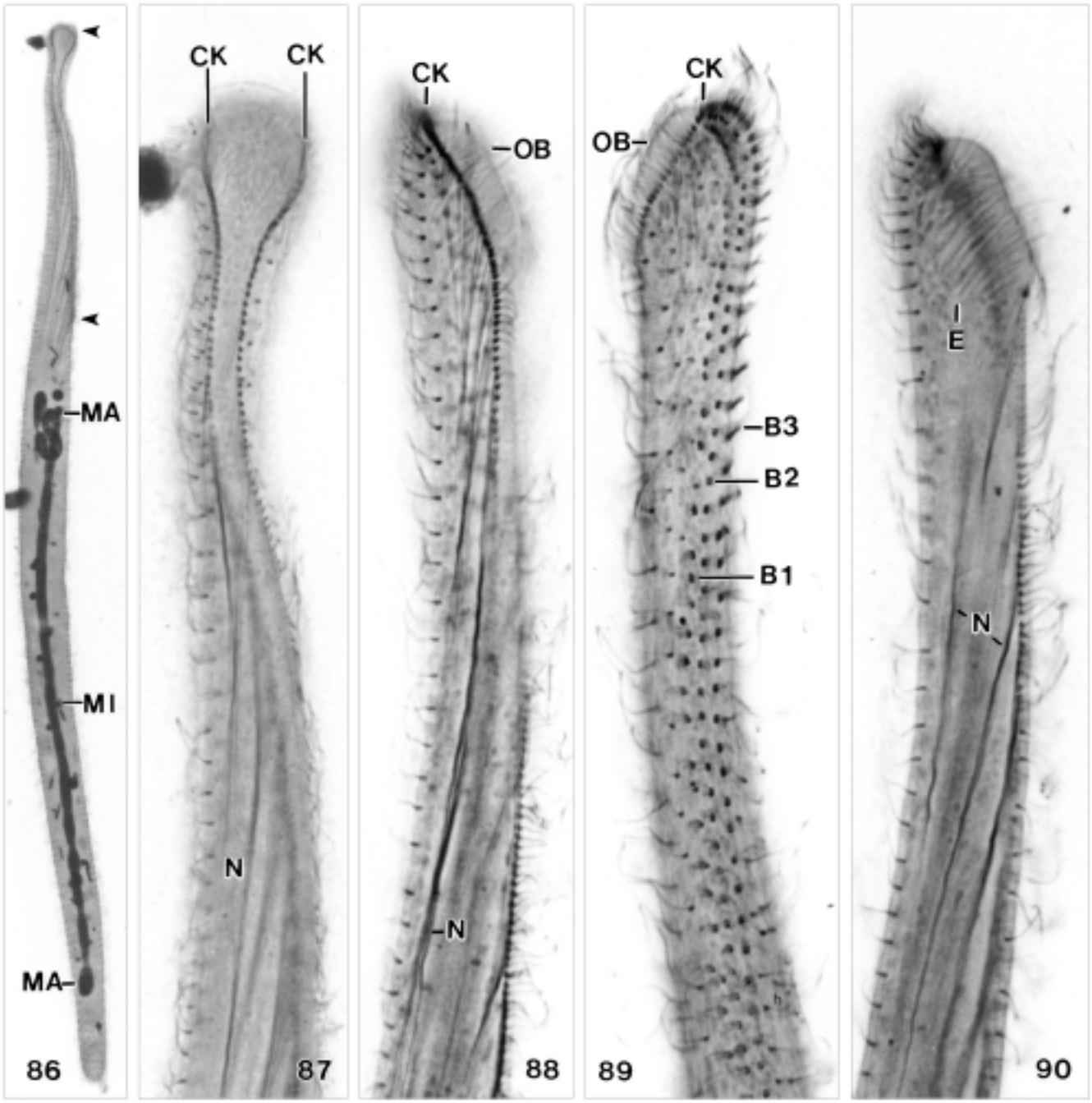

Figs 86-90. *Cephalospatula brasiliensis* after protargol impregnation. **86, 87 -** overview and oral detail of a slender specimen. Arrowheads mark the mouth, respectively, oral bulge, which is hardly set off from body proper proximally, and thus difficult to recognize *in vivo*. Note the conspicuous widening of oral bulge and circumoral kinety in the truncated anterior body end, a main feature of the family; extrusomes are contained only in the widened area, a main feature of the genus (Figs 57, 90); **88-90 -** right (88) and left (89) side view of ciliary pattern and optical section (90) of a laterally oriented specimen showing details of oral area, viz., the anteriorly distinctly curved dikinetidal circumoral kinety associated with conspicuous nematodesmata; the three-rowed dorsal brush; and the extrusomes in the anterior widening of the oral bulge. B1-3 - dorsal brush rows; CK - circumoral kinety; E - extrusomes; MA - macronucleus; MI - micronucleus; N - nematodesmata (oral basket rods); OB - oral bulge.

sharp bend subapically, that is, in the transition zone of oblique anterior and straight ventral portion. Oral basket conspicuous because of long nematodesma bundles originating from circumoral dikinetids (Figs 54, 57, 58, 65-73, 76-78, 83-90; Table 1).

Occurrence and ecology: as yet found only at three sites in South America, as described in the material and methods section, although I investigated similar biotopes worldwide (Foissner 1998, Foissner *et al*. 2002, and unpubl. data), suggesting that this conspicuous ciliate might be restricted to South America and/or Gondwana. Two of the three sites, and to a certain extent also the Restingha area, are definitely semiterrestrial (floodplain soil, mud and soil from a rock-pool), indicating that *C. brasiliensis* might occur also in ordinary freshwaters, although the slender shape suggests a preference for soil (Foissner 1987).

DISCUSSION

Myriokaryonidae fam. n.

Diagnosis: Spathidiina with spoon-shaped oral bulge (circumoral kinety) and oblique to transverse-truncate anterior body end, causing a more or less sharp bend in oral bulge and circumoral kinety.

Type genus: *Myriokaryon* Jankowski, 1973.

Nomenclature: Jankowski (1975) already erected a family Myriokaryonidae, but without any characterization. Thus, it is a nomen nudum.

Suprafamiliar classification: *Myriokaryon* and related genera belong to the gymnostomatous holotrichs, as defined by Corliss (1979), Grain (1994), and Lynn and Small (2002), because they have a holotrichous ciliature composed of monokinetids, a rhabdos-type oral ciliature, a dorsal brush, and toxicysts. Today, this assemblage is usually ranked as a class, viz., Litostomatea or Gymnostomatea (Foissner *et al*. 2002). Many distinct groups are recognizable within this large clade, which contains about 1000 described and many undescribed species (Foissner *et al*. 2002). Unfortunately, within-class classification differs considerably, likely because few detailed data are available on ultrastructure, character states (plesiomorphies, apomorphies), and gene sequences (Corliss 1979, Foissner and Foissner 1988, Grain 1994, Lynn and Small 2002). My own cladistic attempts (unpubl., Hennig's method) failed because I could not unequivocally determine the state of most characters. Similarly, the cladistic analysis by Lipscomb and Riordan (1990) obviously confused character states because spathidiids and pleurostomatids form a clade, which is, in my opinion, unlikely. Gene sequence data are available only from few species and thus cannot be used in the present context. Thus, my classification of the Myriokaryonidae follows the system of Foissner and Foissner (1988), which is based on light microscopical and ultrastructural data. However, I emphasize that any classification must be considered as preliminary at the present state of knowledge.

In spite of these problems, most recent authors agree that *Myriokaryon* belongs to the group which contains *Spathidium* and related genera. This is in accordance with the present results, which suggest that the Myriokaryonidae should be classified as a family of the order Spathidiida Foissner and Foissner (1988): "Cytostome apical, round or slit-like, in suborder Didiniina on top of cone-like proboscis; rhabdos made of three microtubular components: transverse ribbons originating from the nonciliated kinetosomes of the oral dikinetids, nematodesmal bundles originating exclusively from the same source, and bulge microtubules; somatic ciliation uniform or limited to dense bands which, however, rest within longitudinally running kineties composed of nonciliated kinetids; dorsal brush composed of two to many kineties; toxicysts localized, typically in or near oral area; free-living". Foissner and Foissner (1988) distinguish three suborders within the Spathidiida, viz., the Belonophryina (mainly *Actinobolina* and related genera), the Didiniina (*Didinium* and related genera), and the Spathidiina, which they define as follows: "Cytostome apical, round, oval or slit-like, in some genera covering the ventral body margin; somatic ciliation usually uniform". Obviously, the Myriokaryonidae match this definition.

Comparison with related families: the Myriokaryonidae are established to include *Myriokaryon* Jankowski, 1973 and three new genera, viz., *Cephalospatula*, *Berghophrya*, and *Kahlophrya*. The key features uniting these genera, viz., the transverse-truncate anterior body end and the spoon-like anterior widening of the circumoral kinety and oral bulge are, unfortunately, difficult to recognize because the truncated part, viz., the spoon-shovel, is small and the oral bulge flat (Figs 1, 5, 13, 20, 40, 48, 54, 57, 70, 76-78, 83-85). The truncation of the body end causes a highly characteristic bend of the oral bulge and circumoral kinety in the transition zone of spoon-shovel and spoon-handle, that is, the region where the oral bulge and the circumoral kinety enter the ventral side of the cell (Figs 15, 26-28, 57, 72, 73, 76, 84,

85, 87, 88); again, the bend is not easily recognized neither *in vivo* or silver preparations, especially in the elliptical species, viz., *Bergophrya* and *Kahlophrya* (Figs 102, 103, 107, 109-111).

As discussed above, the Myriokaryonidae match the diagnosis of the suborder Spathidiina, which contains the families Spathidiidae, Lacrymariidae, Homalozoonidae, and Trachelophyllidae; the latter family was raised to subordinal rank recently (Foissner *et al*. 2002). Within this assemblage, the Myriokaryonidae are obviously most closely related to the Spathidiidae, as shown by the general body plan and ciliary pattern, which basically match those of "classical" spathidiids, such as *Spathidium* and *Arcuospathidium*, as described by Foissner (1984) and Foissner *et al*. (2002). Interestingly, most generic patterns found in the Spathidiidae occur also in the Myriokaryonidae, indicating highly convergent evolution.

Admittedly, the features separating the Myriokaryonidae from the Spathidiidae (preliminary characterization: Spathidiina with roundish to elongate elliptical oral bulge and circumoral kinety) are rather inconspicuous. However, this must be considered under a more general view, viz., that haptorid gymnostomes have, compared with hypotrichs for instance, fewer distinct features, which, additionally, are more difficult to recognize and reveal.

Kahl (1930a) classified *Myriokaryon lieberkuehnii* in *Pseudoprorodon* (now *Prorodon* for nomenclatural reasons, see Aescht 2001 and Foissner *et al*. 1994), a still poorly known genus of unclear affinities. However, if the redescription of the type species, *P. niveus*, by Grolière (1977) is accepted, then *Prorodon* is highly different from *Myriokaryon* and, likely, also from the spathidiids. This is emphasized by *Pseudoprorodon* (now *Prorodon*) *arenicola*, which, at first glance, looks like a myriokaryonid (Dragesco 1960), but has a prorodontid oral basket (Kattar 1972).

Based on a reinvestigation, Jankowski (1973) classified *Prorodon lieberkuehnii* into a new genus, *Myriokaryon*, which he assigned to the Tracheliidae because of the supposed dileptid oral ciliary pattern. This was not accepted by Lynn and Small (2002), who classified *Myriokaryon* in the Spathidiidae, a relationship also discussed by Jankowski (1973). My investigations show that the short, transverse kineties at the left side of the circumoral kinety are not dileptid preoral ciliary rows, as supposed by Jankowski (1973), but the polymerized anterior end of the left side somatic kineties. Such polymerization is frequent in spathidiids (Foissner 1984, Foissner *et al*. 2002).

Cranotheridium foliosum (Foissner, 1983), as redescribed by Wirnsberger *et al*. (1984), has very similar generic features as *Myriokaryon*, viz., a slightly spoon-shaped oral bulge and many isomorphic dorsal brush rows. However, I hesitate to transfer it to *Myriokaryon* because it is a small (length near 80 µm), *Spathidium*-shaped species and thus quite dissimilar to *M. lieberkuehnii*. Possibly, *C. foliosum* evolved convergently and belongs to the Spathidiidae, as proposed by Wirnsberger *et al*. (1984). Unfortunately, details of the oral and somatic ciliary pattern of *Cranotheridium taeniatum*, type of the genus, are unknown. However, if the observations of Schewiakoff (1893) are correct, *Cranotheridium* likely neither belongs to the Myriokaryonidae nor Spathidiidae because it has a distinct, prostomatid or nassulid pharyngeal basket. Indeed, very recent observations on a *Cranotheridium foliosum*-like ciliate from soil suggest that such species represent a new spathidiid genus different from *Cranotheridium* Schewiakoff, 1893.

Myriokaryon lieberkuehnii

My population of *M. lieberkuehnii* basically matches the original figure by Bütschli (1889) and several redescriptions (Kahl 1930a, Dragesco 1972, Jankowski 1973, Dragesco and Dragesco-Kernéis 1986), especially in having a large, slender body with a minute, transverse truncation anteriorly; more than 2000 macronuclear nodules; many contractile vacuoles; long, fine extrusomes; and about 100 ciliary rows. Thus, identification is beyond reasonable doubts.

However, more or less pronounced differences are found in details, all likely caused by incomplete and/or incorrect observations of the above mentioned authors. I shall not discuss all these mistakes, but some must be mentioned for the sake of identification and taxonomic classification; a few doubtful identifications and synonymies are mentioned in Kahl (1930a) and the distribution and ecology section.

Bütschli (1889) and Kahl (1930a) illustrated a sort of conical oral basket at the anterior end of the organisms (Figs 91, 97, 99). Such basket is definitely absent in my specimens. I do not have any explanation for this difference, except of that these are different species, which is, however, unlikely considering that many other features match well. Jankowski (1973) suggests that previous authors misinterpreted the apical extrusome bundles ("trichites") as a nematodesmal apparatus. Dragesco (1972) and Dragesco and Dragesco-Kernéis (1986), whose *in vivo* observations match my data, did

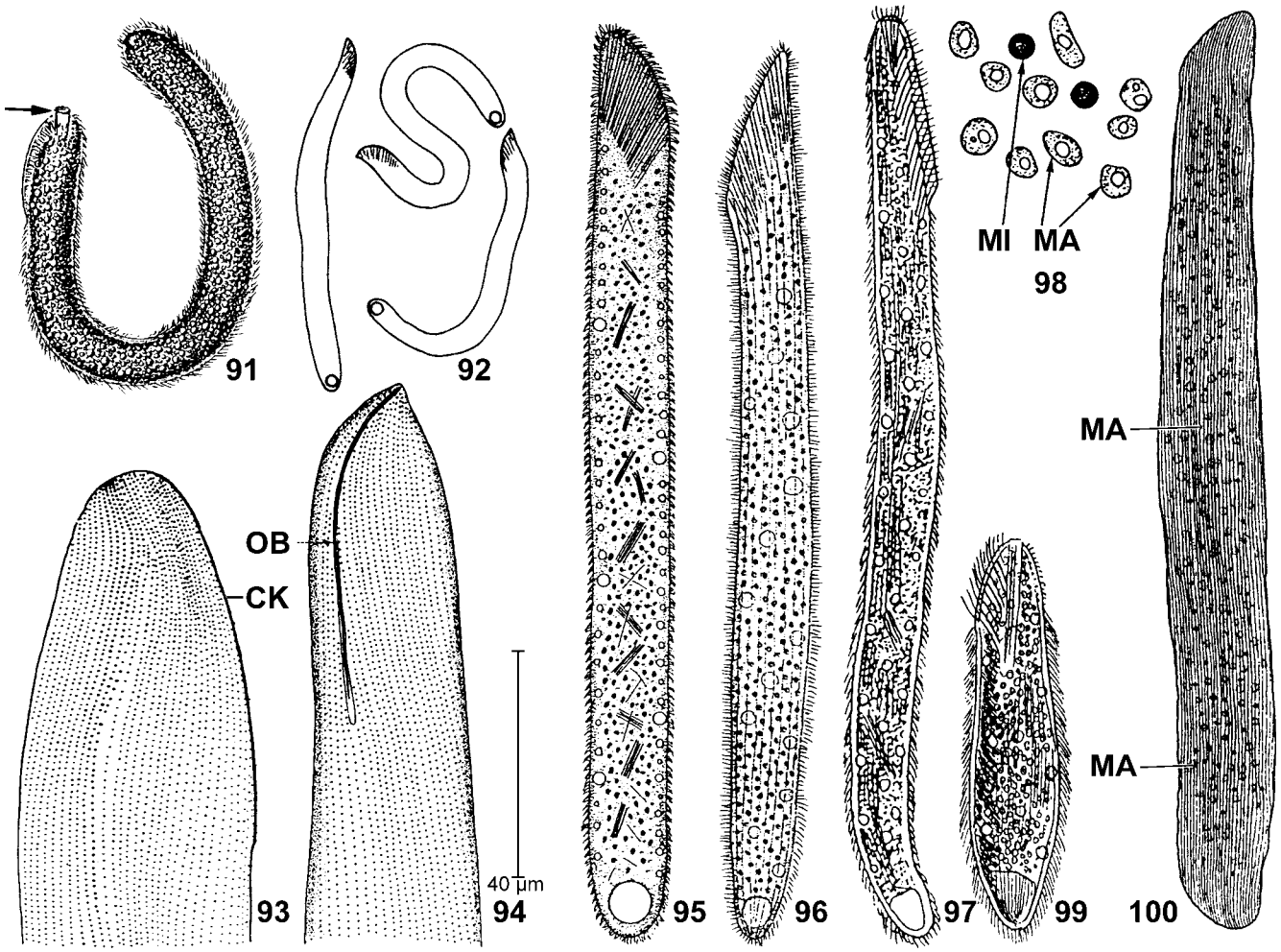

Figs 91-100. *Myriokaryon lieberkuehnii*, figures from literature. **91** - from Bütschli (1889), length 1250 µm. Arrow marks tubular "mouth"; **92, 93, 95, 98** - from Dragesco (1972), shape variability from life (92), ciliary pattern in anterior body region after protargol impregnation (93), general *in vivo* view, length 1100 µm (95), and nuclear pattern after Feulgen reaction (98); **94** - from Dragesco and Dragesco-Kernéis (1986), ciliary pattern of ventral side after protargol impregnation; **96** - from Cunha (1914), general *in vivo* view, length 600-800 µm; **97** - from Kahl (1930a), general *in vivo* view of an ordinary specimen, length 1100 µm; **99** - from Kahl (1930a), general *in vivo* view of a small specimen, length 600 µm (likely a misidentification); **100** - from Al-Rasheid (2000), left lateral view after protargol impregnation, length 600-800 µm (misidentification, see discussion). CK - circumoral kinety; MA - macronuclear nodules; MI - micronucleus, OB - oral bulge.

not see the dorsal brush and the special ciliary pattern at the left side of the circumoral kinety, although they used protargol impregnation (Figs 92-95). Likely, their preparations were too weak. The data of Jankowski (1973) are much better than those of Dragesco, although he misinterpreted the whole mouth organization, possibly because he related *Myriokaryon* to the dileptids (Fig. 101). Specifically, he did not observe the circumoral kinety and the very fine nematodesmata. Thus, he interpreted the narrow, central mouth slit as "mouth free of any nematodesmal armature". Further, he misinterpreted the densely ciliated anterior end of the left side ciliary rows as tracheliid preoral kineties, and the long toxicysts as "trichites". On the other hand, Jankowski (1973) recognized, inter alia, the widened anterior end of the oral bulge, the polymerized anterior end of the left side kineties, and the high number (about 10) of dorsal brush rows (thigmotactic stripe).

Cephalospatula brasiliensis as a new genus and species

Cephalospatula is obviously related to *Myriokaryon*, as shown by distinct similarities in shape of body and oral bulge and the kinetofragments along the left margin of the circumoral kinety, although these are less conspicuous. On the other hand, there are also considerable differences, mainly in the number of dorsal brush rows (three *vs.* many) and the arrangement of the oral

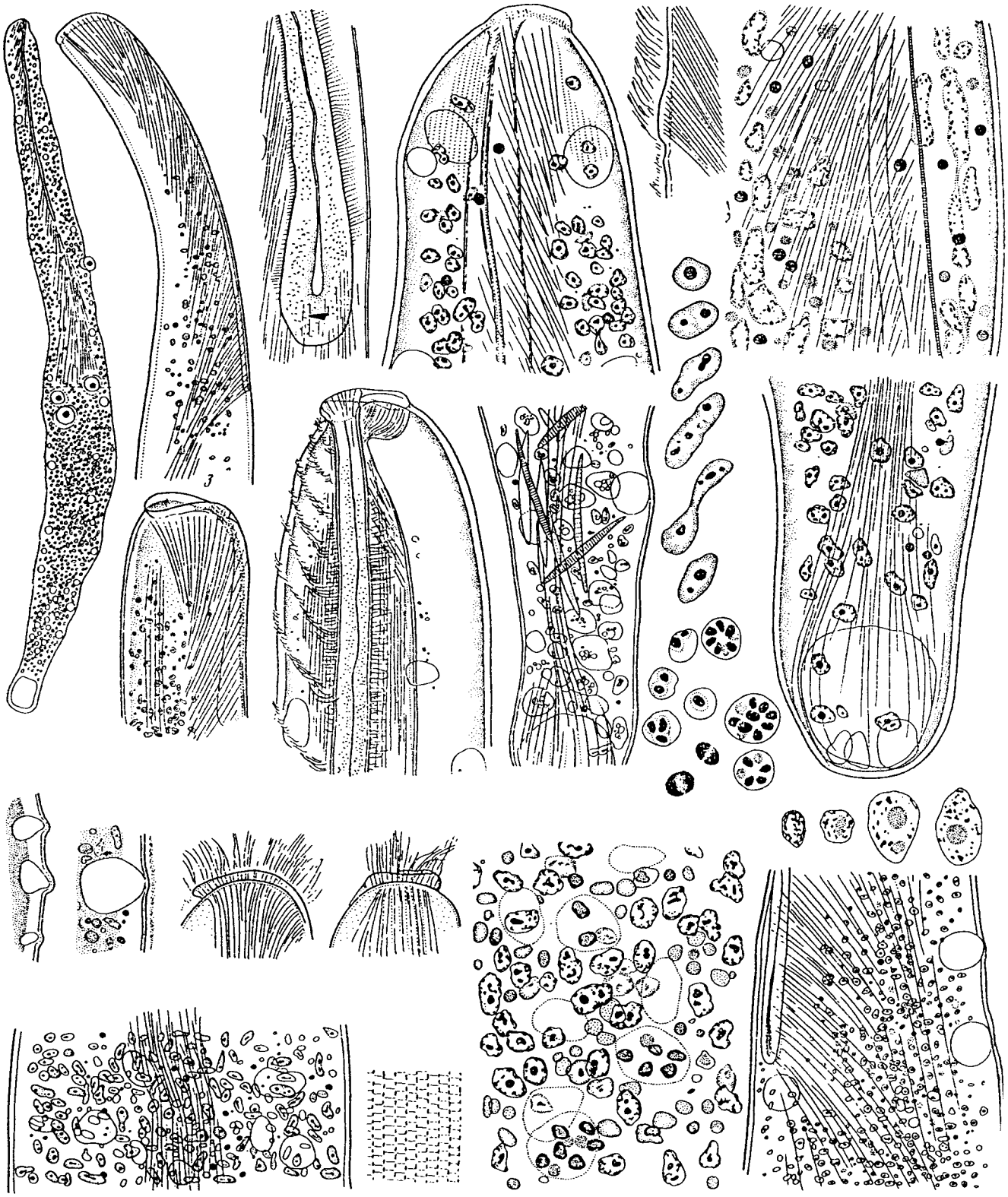

Fig. 101. *Myriokaryon lieberkuehnii*, Russian neotype population investigated by Jankowski (1973). Figures without scale bars and explained in text. Thus, the reader is referred to the original publication (English translation available from Foissner).

extrusomes (single apical bundle *vs.* scattered in whole bulge). Three brush rows are the usual brush pattern in haptorid gymnostomes and are thus likely the plesiomorphic state of this important specialization (Foissner and Foissner 1988, Foissner *et al*. 2002). Thus, any deviation from this pattern, as in *Myriokaryon*, should be rated rather high, viz., at genus level. Likewise, the extrusome pattern is widely used for separation of genera and even families, for instance, in the spathidiid genera *Legendrea* and *Cranotheridium* (see Kahl 1930a for literature), and the definition of the family Pleuroplitidae Foissner, 1996.

There is only one species in the literature, viz., *Spathidium vermiforme* Penard, 1922, bearing some resemblance to *C. brasiliensis*. However, *S. vermiforme* is leaf-like flattened and has the extrusomes scattered in the short, oblique oral bulge. Thus, *C. brasiliensis* is a very distinct species easy to recognize by the large, slender body; the extrusome bundle in the widened apical end; the filiform macronucleus; and the dorsal row of contractile vacuoles.

Berghophrya gen. n. (Figs 102-109)

Diagnosis: ellipsoidal Myriokaryonidae with short mouth on obliquely truncated anterior body end and 3 dorsal brush rows accompanied by 3 rows of papillae. Extrusomes scattered in oral bulge and postoral bundles. Infraciliature likely in *Arcuospathidium* pattern.

Type species: *Holophrya Emmae* Bergh, 1896.

Dedication: I dedicate this genus to Dr. R. S. Bergh, the Danish protozoologist who discovered and described the type species so well that the data are useful even today. *Berghophrya* is a composite of *Bergh* and the Greek noun *ophrya* (eyebrow ~ cilia ~ ciliate). Feminine gender.

Comparison with related genera: the excellent observations of Bergh (1896) were confirmed and supplemented by Kahl (1930a). They show that *Holophrya emmae* has the same main generic feature as *Myriokaryon lieberkuehnii* and *Cephalospatula brasiliensis*, viz., a spoon-like oral bulge (Figs 102-109). Kahl (1930a) even recognized the similarity with *M. lieberkuehnii* and classified both in *Pseudoprorodon*. Accordingly, the redescription of *H. emmae* by Song and Wilbert (1989), which shows a ciliate with a circular oral bulge, is based on a misidentification (see the new genus *Songophrya* below). *Holophrya emmae* is sufficiently different in details of the dorsal brush and extrusome pattern to be transferred to a new genus: *Berghophrya emmae* (Bergh, 1896) comb. n.

Details of the infraciliature from silver-impregnated *B. emmae* are not available. However, Kahl (1930a) shows that it likely has an *Arcuospathidium* pattern, like *Kahlophrya armata*, that is, the ciliary rows abut on the circumoral kinety at steep angles at both sides of the oral bulge (Fig 107).

Kahlophrya gen. n. (Figs 110-112)

Diagnosis: elongate Myriokaryonidae with short mouth on obliquely truncated anterior body end and many (more than 3) dorsal brush rows, most of which are heteromorphic. Extrusomes scattered in oral bulge and equidistant body stripes. Infraciliature in *Arcuospathidium* pattern.

Type species: *Pseudoprorodon armatus* Kahl, 1930a.

Dedication: I dedicate this genus to Alfred Kahl (1877-1946), the famous German ciliate taxonomist, whose detailed observations greatly facilitated the present study. *Kahlophrya* is a composite of *Kahl* and the Greek noun *ophrya* (eyebrow ~ cilia ~ ciliate). Feminine gender.

Comparison with related genera: *Kahlophrya* is based on the redescription of *Pseudoprorodon armatus* Kahl, 1930a by Foissner (1997). This study shows the features mentioned in the genus diagnosis and the spoon-shaped oral bulge characteristic for the family (Figs 110-112). Thus, *Pseudoprorodon armatus* Kahl, 1930a and *Prorodon armatides* Foissner, 1997 are combined to *Kahlophrya armata* (Kahl, 1930a) comb. n. The main generic feature of *Kahlophrya* is the dorsal brush, which consists of about 20 rows. This resembles *Myriokaryon*, whose rows are, however, isomorphic, that is, consist of dikinetids with short cilia (bristles). *Kahlophrya* has only one isomorphic brush row, all others are heteromorphic, that is, composed of irregularly alternating monokinetids with ordinary cilia and dikinetids with short bristles. A tendency for heteromorphy is recognizable also in the posterior region of the brush rows of *Myriokaryon* and *Cephalospatula* (Figs 51-53, 57). Another important feature of *Kahlophrya* are the about 20 stripes of body extrusomes not found in any other genus of the family, although the genus *Berghophrya* shows such a tendency (see above); further, somatic extrusome stripes occur in several genera of related families, viz., in *Apospathidium* of the family Spathidiidae and in *Apobryophyllum* of the family Bryophyllidae (Foissner *et al*. 2002). The ciliary pattern of *Kahlophrya* is as in the spathidiid genus

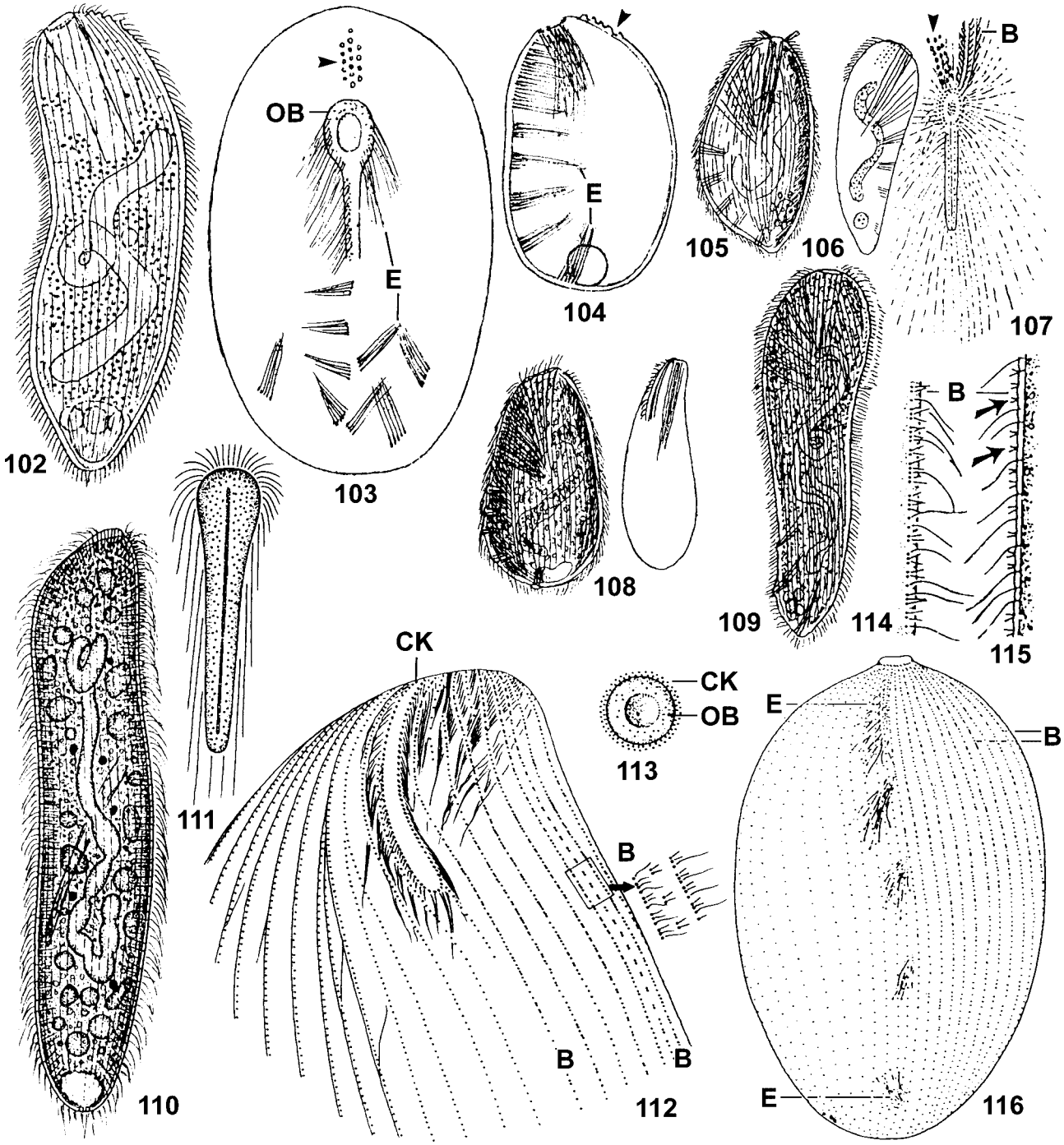

Figs 102-109. *Berghophrya emmae* from life, according to Bergh 1896 (102-104) and Kahl 1930a (105-109). **102 -** general left side view, length up to 200 µm; **103, 104 -** ventral and lateral view of squashed specimens showing the spoon-shaped oral bulge, the dorsal papillae (arrowheads), and postoral extrusome bundles; **105-107 -** small variety (length 160 µm), lateral, dorsal, and frontal view of oral area with dorsal papillae marked by arrowhead; **108 -** medium-sized variety, length 300 µm; **109 -** vermiform variety, length 320 µm.

Figs 110-112. *Kahlophrya armata* from life (110, 111) and after protargol impregnation (112), according to Foissner (1997). **110-111 -** general left side view (length 210 µm) and frontal view of oral area; **112 -** ciliary pattern of anterior ventral side. Note the complicated dorsal brush composed of many rows with bristles and ordinary cilia.

Figs 113-116. *Songophrya armata* from life (114) and after protargol impregnation (113, 115, 116), according to Song and Wilbert (1989). This species has a circular oral bulge (113) and is thus highly different from *Berghophrya emmae*, which has a spoon-shaped oral bulge (103, 107). *Songophrya armata* has a size of 90-200 x 60-120 µm and the same brush type as *Kahlophrya armata*, that is, many rows composed of short, paired bristles (arrows) alternating with ordinary cilia (112, 114-116). B - dorsal brush; CK - circumoral kinety; E - extrusomes; OB - oral bulge.

Arcuospathidium and the myriokaryonid genus *Berghophrya* (see above), that is, the somatic ciliary rows abut on the circumoral kinety in steep angles at both sides of the oral bulge.

***Songophrya* gen. n. (Figs 113-116)**

Diagnosis: Pseudoholophryidae with circular oral opening and a row of extrusome bundles extending from anterior to posterior body end.

Type species: *Songophrya armata* sp. n.

Dedication: I dedicate this genus to Prof. Dr. Weibo Song (Ocean University of China), an eminent Chinese protozoologist, who significantly contributes to ciliate alpha-taxonomy since 15 years and discovered the type species. *Songophrya* is a composite of *Song* and the Greek noun *ophrya* (eyebrow ~ cilia ~ ciliate). Feminine gender.

Comparison with related genera: Foissner and Gschwind (1998) and Foissner *et al*. (2002) suggested that *Pseudoprorodon emmae* Bergh, 1896, as redescribed by Song and Wilbert (1989), is likely another species and the representative of a new genus belonging to the family Pseudoholophryidae, as redefined by Foissner *et al*. (2002). With the new knowledge available from *Myriokaryon* and *Cephalospatula*, it is evident that the species described by Song and Wilbert (1989) is not *Holophrya emmae* Bergh, 1896 because it has a simple, circular oral bulge, while that of *H. emmae* is conspicuously spoon-shaped (Figs 103, 113). Unfortunately, Song and Wilbert (1989) did not discuss this important difference, and thus their identification remains obscure; possibly, they did not know Bergh's original description. Within the family Pseudoholophryidae, which contains the genera *Pseudoholophrya*, *Paraenchelys*, and *Ovalorhabdos*, *Songophrya* is unique in having a row of extrusome bundles. Further, the ciliary rows extend almost meridionally, while distinctly spirally in the other genera. As concerns the oral bulge, it is circular in *Songophrya*, *Pseudoholophrya* and *Paraenchelys*, while distinctly elliptical in *Ovalorhabdos* (Foissner 1984, Foissner and Gschwind 1998, Foissner *et al*. 2002). The extrusomes, which distinguish the genera *Pseudoholophrya* and *Paraenchelys* (basically rod-shaped *vs.* basically drumstick-shaped), were not studied *in vivo* by Song and Wilbert (1989). Likely, they are filiform, but it cannot be excluded that a second fusiform type is present, which would be a further important genus character.

***Songophrya armata* sp. n.**

Diagnosis: size 90-200 x 60-120 µm *in vivo*; ellipsoidal. Macronucleus filiform. Extrusome row composed of 5-7 (x 5.3) bundles. On average 102 ciliary rows, more than 20 differentiated to dorsal brush in anterior half.

Type location: pond (Poppelsdorfer Weiher) in Bonn, Germany (7°E 51°N).

Etymology: the Latin adjective *armata* (armed) refers to the conspicuous extrusomes.

Description: see Song and Wilbert (1989) and figures 113-116.

Acknowledgements. The technical assistance of Dr. B. Moser and Dr. E. Herzog is gratefully acknowledged. Financial support was provided by the Austrian Science Foundation (FWF-Project P-15017).

REFERENCES

Aescht E. (2001) Catalogue of the generic names of ciliates (Protozoa, Ciliophora). *Denisia*, Linz **1:** 1-350

Al-Rasheid K. A. S. (2000) Some marine interstitial Prostomatida and Haptorida (Ciliata) from the Jubail Marine Wildlife Sanctuary on the Saudi Arabian Gulf shore. *Fauna of Arabia* **18:** 5-22

Bergh R. S. (1896) Über Stützfasern in der Zellsubstanz einiger Infusorien. *Anat. Hefte* **7:** 103-113

Buck H. (1961) Zur Verbreitung der Ciliaten in den Fließgewässern Nordwürttembergs. *Jh. Ver. vaterl. Naturk. Württ.* **116:** 195-217

Bütschli O. (1887-1889): Protozoa. Abt. III. Infusoria und System der Radiolaria. In: Klassen und Ordnungen des Thier-Reichs, (Ed. H. G. Bronn). C. F. Winter, Leipzig, **1:** 1098-2035.

Corliss J. O. (1979) The Ciliated Protozoa. Characterization, Classification and Guide to the Literature. 2nd ed. Pergamon Press, Oxford, New York, Toronto, Sydney, Paris, Frankfurt

Cunha A. M. da (1914) Contribuição para o conhecimento da fauna de protozoarios do Brazil. [Beitrag zur Kenntnis der Protozoenfauna Brasiliens.] *Mém. Inst. Osw. Cruz* **6:** 169-179 (in Portuguese and German)

Dragesco J. (1960) Ciliés mésopsammiques littoraux. Systématique, morphologie, écologie. *Trav. Stn biol. Roscoff* (N.S.) **12:** 1-356

Dragesco J. (1972) Ciliés libres de la cuvette tchadienne. *Annls. Fac. Sci. Univ. féd. Cameroun* **11:** 71-91

Dragesco J., Dragesco-Kernéis A. (1986) Ciliés libres de l'Afrique intertropicale. Introduction à la connaissance et à l'étude des ciliés. *Faune tropicale* **26:** 1-559

Fauré-Fremiet E., André J. (1968) L'organisation corticale des Ciliata. *C. r. hebd. Séanc. Acad. Sci., Paris* **266:** 487-490

Foissner W. (1983) Taxonomische Studien über die Ciliaten des Großglocknergebietes (Hohe Tauern, Österreich) I. Familien Holophryidae, Prorodontidae, Plagiocampidae, Colepidae, Enchelyidae und Lacrymariidae nov. fam. *Annln naturh. Mus. Wien* **84B:** 49-85

Foissner W. (1984) Infraciliatur, Silberliniensystem und Biometrie einiger neuer und wenig bekannter terrestrischer, limnischer und mariner Ciliaten (Protozoa: Ciliophora) aus den Klassen Kinetofragminophora, Colpodea und Polyhymenophora. *Stapfia*, Linz **12:** 1-165

Foissner W. (1987) Soil protozoa: fundamental problems, ecological significance, adaptations in ciliates and testaceans, bioindicators, and guide to the literature. *Progr. Protistol.* **2:** 69-212

Foissner W. (1991) Basic light and scanning electron microscopic methods for taxonomic studies of ciliated protozoa. *Europ. J. Protistol.* **27:** 313-330

Foissner W. (1996) Faunistics, taxonomy and ecology of moss and soil ciliates (Protozoa, Ciliophora) from Antarctica, with description of new species, including *Pleuroplitoides smithi* gen. n., sp. n. *Acta Protozool*. **35:** 95-123

Foissner W. (1997) Faunistic and taxonomic studies on ciliates (Protozoa, Ciliophora) from clean rivers in Bavaria (Germany), with descriptions of new species and ecological notes. *Limnologica* **27:** 179-238

Foissner W. (1998) An updated compilation of world soil ciliates (Protozoa, Ciliophora), with ecological notes, new records, and descriptions of new species. *Europ. J. Protistol.* **34:** 195-235

Foissner W., Foissner I. (1988) The fine structure of *Fuscheria terricola* Berger *et al*., 1983 and a proposed new classification of the subclass Haptoria Corliss, 1974 (Ciliophora, Litostomatea). *Arch. Protistenk.* **135:** 213-235

Foissner W., Gschwind K. (1998) Taxonomy of some freshwater ciliates (Protozoa: Ciliophora) from Germany. *Ber. nat.-med. Ver. Salzburg* **12:** 25-76

Foissner W., Berger H., Kohmann F. (1994) Taxonomische und ökologische Revision der Ciliaten des Saprobiensystems - Band III: Hymenostomata, Prostomatida, Nassulida. *Informationsberichte des Bayer. Landesamtes für Wasserwirtschaft* **1/94:** 1-548

Foissner W., Agatha S., Berger H. (2002) Soil ciliates (Protozoa, Ciliophora) from Namibia (Southwest Africa), with emphasis on two contrasting environments, the Etosha region and the Namib Desert. *Denisia*, Linz **5:** 1-1459

Grain J. (1994) Classe des Litostomatea Small et Lynn, 1981. *Traite Zool.* **2**(2)**:** 267-310

Grolière C.-A. (1977) Contribution a l'etude des cilies des sphaignes et des etendues d'eau acides. I - Description de quelques especes de gymnostomes, hypostomes, hymenostomes et heterotriches. *Annls Stn limnol. Besse* **10** (years 1975/1976)**:** 265-297

Jankowski A. W. (1973) Free-living Ciliophora. 1. *Myriokaryon* gen. n., giant planktonic holotrich. *Zool. Zh.* **52:** 424-428 (in Russian with English summary; I am indebted to Dr. Jankowski for the English translation of the full paper; it is available from me on request)

Jankowski A. W. (1975) A conspectus of the new system of subphylum Ciliophora Doflein, 1901. In: Account of Scientific Sessions on Results of Scientific Work, year 1974: Abstracts of Reports, (Ed. U. S. Balashov). Tezisy Dokladov, Zoologickekii Institut, Akad. Nauk SSR, Leningrad, 26-27 (in Russian)

Kahl A. (1926) Neue und wenig bekannte Formen der holotrichen und heterotrichen Ciliaten. *Arch. Protistenkd.* **55:** 197-438

Kahl A. (1930a) Urtiere oder Protozoa I: Wimpertiere oder Ciliata (Infusoria) 1. Allgemeiner Teil und Prostomata. *Tierwelt Dtl.* **18:** 1-180

Kahl A. (1930b) Neue und ergänzende Beobachtungen holotricher Infusorien. II. *Arch. Protistenkd.* **70:** 313-446

Kattar M. R. (1972) Quelques aspects de l'ultrastructure du cilié *Pseudoprorodon arenicola* Kahl, 1930. *Protistologica* **8:** 135-141

Lipscomb D. L., Riordan G. P. (1990) The ultrastructure of *Chaenea teres* and an analysis of the phylogeny of the haptorid ciliates. *J. Protozool.* **37:** 287-300

Lynn D. H., Small E. B. (2002) Phylum Ciliophora Doflein, 1901. In: An Illustrated Guide to the Protozoa, 2nd ed., (Eds. J. J. Lee, G. F. Leedale, P. Bradbury). Society of Protozoologists, Lawrence, **1:** 371-656 (printed in year 2000, but available only in year 2002)

Penard E. (1922) Études sur les Infusoires d'Eau Douce. Georg & Cie, Genève

Schewiakoff W. (1893) Über die geographische Verbreitung der Süsswasser-Protozoën. Zap. imp. Akad. Nauk SSSR (Series 7) **41:** 1-201

Song W., Wilbert N. (1989) Taxonomische Untersuchungen an Aufwuchsciliaten (Protozoa, Ciliophora) im Poppelsdorfer Weiher, Bonn. *Lauterbornia* **3:** 2-221

Stein F. (1859) Der Organismus der Infusionsthiere nach eigenen Forschungen in sytematischer Reihenfolge bearbeitet. I. Abtheilung. Allgemeiner Theil und Naturgeschichte der hypotrichen Infusionsthiere. W. Engelmann, Leipzig

Wirnsberger E., Foissner W., Adam H. (1984) Morphologie und Infraciliatur von *Perispira pyriformis* nov. spec. *Cranotheridium foliosus* (Foissner, 1983) nov. comb. und *Dileptus anser* (O. F. Müller, 1786) (Protozoa, Ciliophora). *Arch. Protistenkd.* **128:** 305-317

Received on 2nd September, 2002: revised version on 11th November, 2002; accepted on 19th February, 2003

Acta Protozool. (2003) 42: 145 - 159

ACTA
PROTOZOOLOGICA

Two Remarkable Soil Spathidiids (Ciliophora: Haptorida), *Arcuospathidium pachyoplites* sp. n. and *Spathidium faurefremieti* nom. n.

Wilhelm FOISSNER

Universität Salzburg, Institut für Zoologie, Salzburg, Austria

Summary. This paper continues a series of studies on spathidiids, a group of free-living, rapacious ciliates with a high biodiversity. *Arcuospathidium pachyoplites* sp. n. was discovered in saline coastal soil from the Henry Pittier National Park in Venezuela, South America. *Spathidium faurefremieti*, originally described by Tucolesco (1962) from Rumanian cave water, was rediscovered in savannah soil from the Shimba Hills National Reserve in Kenya (Africa) and in floodplain soils of Brazil (South America) and Australia. The morphology of these species was investigated using live observation and protargol impregnation. The South American *A. pachyoplites* differs from the African *A. vlassaki*, possibly the nearest relative, mainly by the extrusomes and dorsal brush. *Spathidium faurei* Tucolesco, 1962 is an objective homonym of *Spathidium faurei* Kahl, 1930 and thus re-named: *Spathidium faurefremieti* nom. n. This species is remarkable in having a second contractile vacuole in anterior body half. However, conspecificity of the European and Kenyan populations is questionable; likewise, the Kenyan and Brazilian populations differ considerably, suggesting that further research might prove that all are different subspecies or even species. The present study shows that (i) an increased number of contractile vacuoles likely evolved independently three times, viz., in *Spathidium*, *Arcuospathidium*, and *Supraspathidium*, and (ii) the bivacuolate species should be separated from the polyvacuolate species, which can be referred to the genus *Supraspathidium*.

Key words: Australia, biodiversity, Brazil, Kenya, *Supraspathidium*, terrestrial Protozoa, Venezuela.

INTRODUCTION

This paper continues a series of studies on spathidiid and *Spathidium*-like ciliates, whose full diversity is still not known (Buitkamp 1977; Dragesco and Dragesco-Kernéis 1979; Foissner 1984, 2000, 2003a; Foissner *et al*. 2002). The two species described here are remarkable in several ways. *Arcuospathidium pachyoplites* from a saline site in Venezuela is rather similar to *A. vlassaki* Foissner, 2000 and *A. etoschense* Foissner *et al*. 2002 from saline inland habitats of Africa. These species might be examples for post-Gondwanan speciation. The second species, *Spathidium faurefremieti* is outstanding in having two contractile vacuoles, a feature which, however, obviously evolved independently at least twice because it is found in spathidiids with either an *Arcuospathidium* or *Spathidium* ciliary pattern, viz., in *A. bulli* Foissner, 2000 and *S. faurefremieti* redescribed here.

Both species are very slender showing that many soil ciliates have the same main morphological adaptation as many metazoan soil inhabitants, viz., a worm-like body.

Address for correspondence: Wilhelm Foissner, Universität Salzburg, Institut für Zoologie, Hellbrunnerstrasse 34, A-5020 Salzburg, Austria; Fax. ++43 (0) 662 8044 5698

Further, they are able to produce dormant stages (resting cysts) to survive periods of dryness, a main physiological adaptation of soil organisms in general (Foissner 1987).

MATERIALS AND METHODS

See type locations and distribution sections for collectors and detailed site descriptions. The samples were air-dried in the Salzburg laboratory and stored in plastic bags until investigation. The ciliates were reactivated from the resting cysts by the non-flooded Petri dish method, as described in Foissner (1987) and Foissner *et al.* (2002). Briefly, this simple method involves placing soil in a Petri dish (10-20 cm wide, 2-3 cm high) and saturating, but not flooding it, with distilled water. These cultures were analyzed for ciliates by inspecting about 2 ml of the run-off (soil percolate) on days 2, 7, 14, 21, and 28. The descriptions of the species are based on material obtained from such cultures, i.e. no clones were set up.

Morphological methods followed those used in our previous studies (e.g. Foissner 1984, 1991; Foissner *et al*. 2002), and thus need not to be detailed here. Briefly, live specimens were studied in bright field and interference contrast, and permanent preparations were made with protargol (Protocol A in Foissner 1991).

RESULTS

Description of *Arcuospathidium pachyoplites* sp. n. (Figs 1-16, 23-25, 27-34, 37-43; Table 1)

Diagnosis: size about 170 x 20 µm *in vivo*. Knife-shaped with steep, slightly cuneate oral bulge occupying about 22% of body length. Macronucleus tortuous, figure formed about 80 µm long. Extrusomes conspicuous because lanceolate and 7 x 1.4 µm in size, scattered in both sides of oral bulge and attached to bulge cortex with narrowed anterior end. On average 10 ciliary rows; dorsal brush inconspicuous, occupies 17% of body length on average.

Type location: saline coastal soil in the surroundings of the village of Choroni (67°45'W 10°15'N), Henry Pittier National Park, north coast of Venezuela, South America.

Etymology: apposite noun composed of the Greek words pachy (thick) and (h) oplites (soldier ~ extrusome), referring to the conspicuous extrusomes.

Table 1. Morphometric data on *Arcuospathidium pachyoplites.*

Characteristics[a]	x	M	SD	SE	CV	Min	Max	n
Body, length	158.9	160.0	25.5	5.6	16.1	115.0	210.0	21
Body, width	19.3	18.0	6.1	1.3	31.6	12.0	38.0	21
Body length:width, ratio	9.0	8.2	3.3	0.7	36.7	4.8	17.5	21
Oral bulge, length	34.4	35.0	6.2	1.4	18.0	21.0	44.0	21
Body length:oral bulge length, ratio	4.7	4.6	0.7	0.2	15.4	3.2	6.2	21
Oral bulge, width	4.6	4.5	0.7	0.1	14.6	3.0	5.5	21
Oral bulge, height at anterior end	2.0	2.0	-	-	-	1.5	3.0	21
Circumoral kinety to end of brush row 1, distance	17.2	18.0	3.2	0.7	18.5	11.0	23.0	21
Circumoral kinety to end of brush row 2, distance	27.2	27.0	4.8	1.0	17.6	18.0	38.0	21
Circumoral kinety to end of brush row 3, distance	17.0	18.0	3.8	0.8	21.2	12.0	27.0	21
Anterior body end to macronucleus, distance	57.1	56.0	10.6	2.3	18.5	43.0	84.0	21
Macronucleus figure, length	72.4	72.0	14.0	3.0	19.3	52.0	98.0	21
Macronucleus, length (spread)[b]	111.3	110.0	-	-	-	80.0	150.0	21
Macronucleus, width in middle	4.2	4.0	0.8	0.2	18.3	3.0	5.0	21
Somatic kineties, number (including brush)	10.0	10.0	0.9	0.2	8.7	9.0	12.0	21
Ciliated kinetids in a lateral kinety, number	56.2	56.0	10.8	2.4	19.2	36.0	78.0	21
Dorsal brush rows, number[c]	3.0	3.0	0.0	0.0	0.0	3.0	3.0	21
Dikinetids in brush row 1, number	11.4	11.0	2.2	0.5	18.9	7.0	15.0	21
Dikinetids in brush row 2, number	28.0	28.0	5.7	1.2	20.4	18.0	38.0	21
Dikinetids in brush row 3, number	13.3	13.0	2.0	0.4	14.7	11.9	19.0	21

[a]Data based on mounted, protargol-impregnated, selected (see description of species) specimens from a non-flooded Petri dish culture. [b]Very approximate values. [c]Only full rows counted. Measurements in µm. CV - coefficient of variation in %, M - median, Max - maximum, Min - minimum, n - number of individuals investigated, SD - standard deviation, SE - standard error of arithmetic mean, x - arithmetic mean.

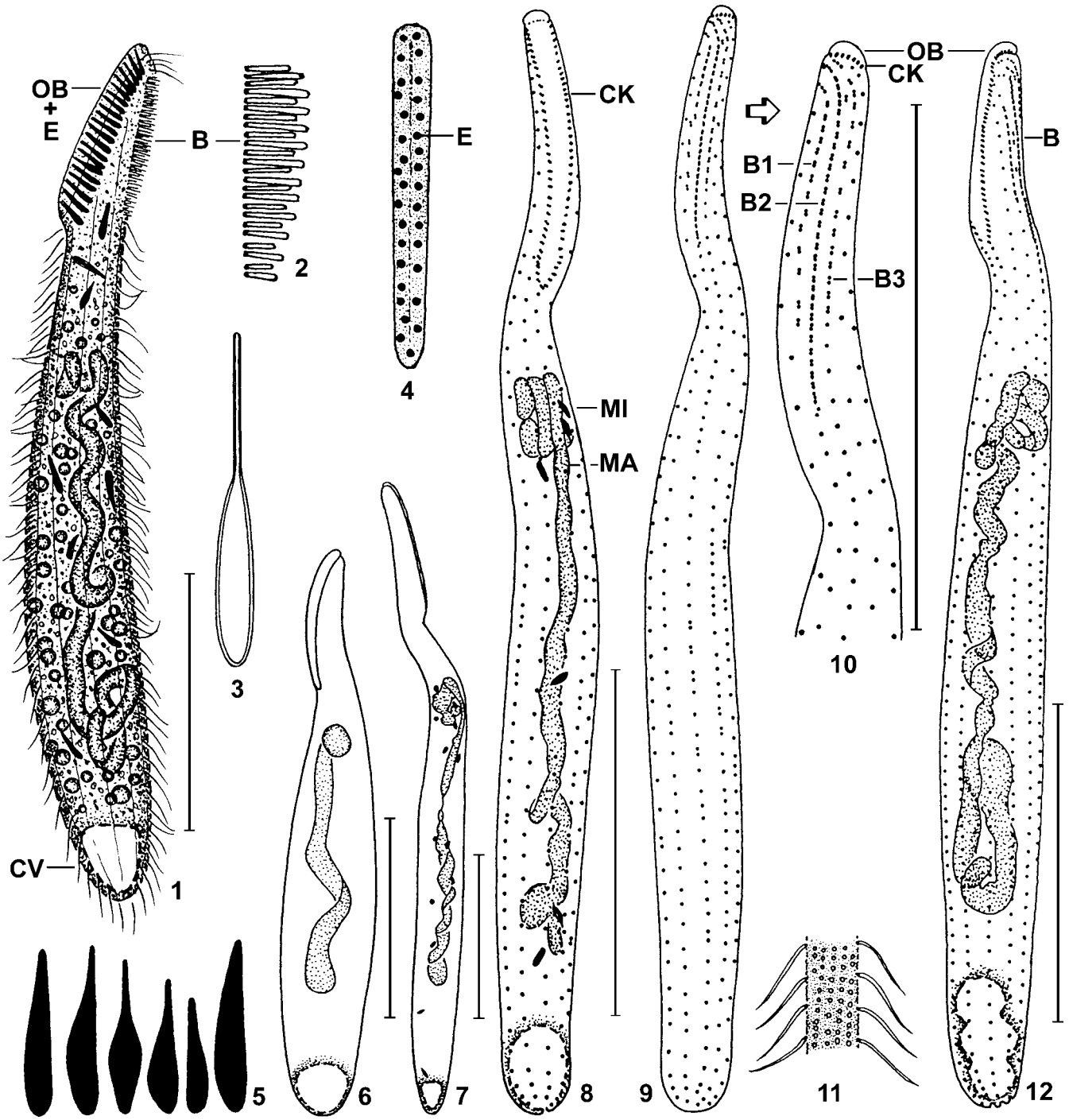

Figs 1-12. *Arcuospathidium pachyoplites* from life (1-5, 11) and after protargol impregnation (6-10, 12). **1 -** left side view of a representative specimen, i.e., "constructed" from live observations and morphometric data shown in table 1. The oral bulge is very conspicuous due to the massive extrusomes contained; **2 -** posterior half of brush row 2, longest bristles 4 µm; **3 -** exploded toxicyst, length 20 µm; **4 -** frontal view of the indistinctly cuneate oral bulge studded with extrusomes; **5 -** oral bulge extrusomes, length 6-8 µm; **6, 7 -** a broad and a slender specimen; note variability of macronucleus; **8-10 -** ciliary pattern of ventral and dorsal side and nuclear apparatus of holotype specimen. Note the oblong circumoral kinety and the dorsal brush dikinetids, which are much more closely spaced in middle row 2 than in rows 1 and 3; **11 -** surface view showing cortical granulation; **12 -** left side view of another specimen with rather distorted dorsal brush and typical macronucleus with coiled and inflated ends. B - dorsal brush, B1-3 - dorsal brush rows, CK - circumoral kinety, CV - contractile vacuole, E - extrusomes, MA - macronucleus, MI - micronucleus, OB - oral bulge. Scale bars - 50 µm.

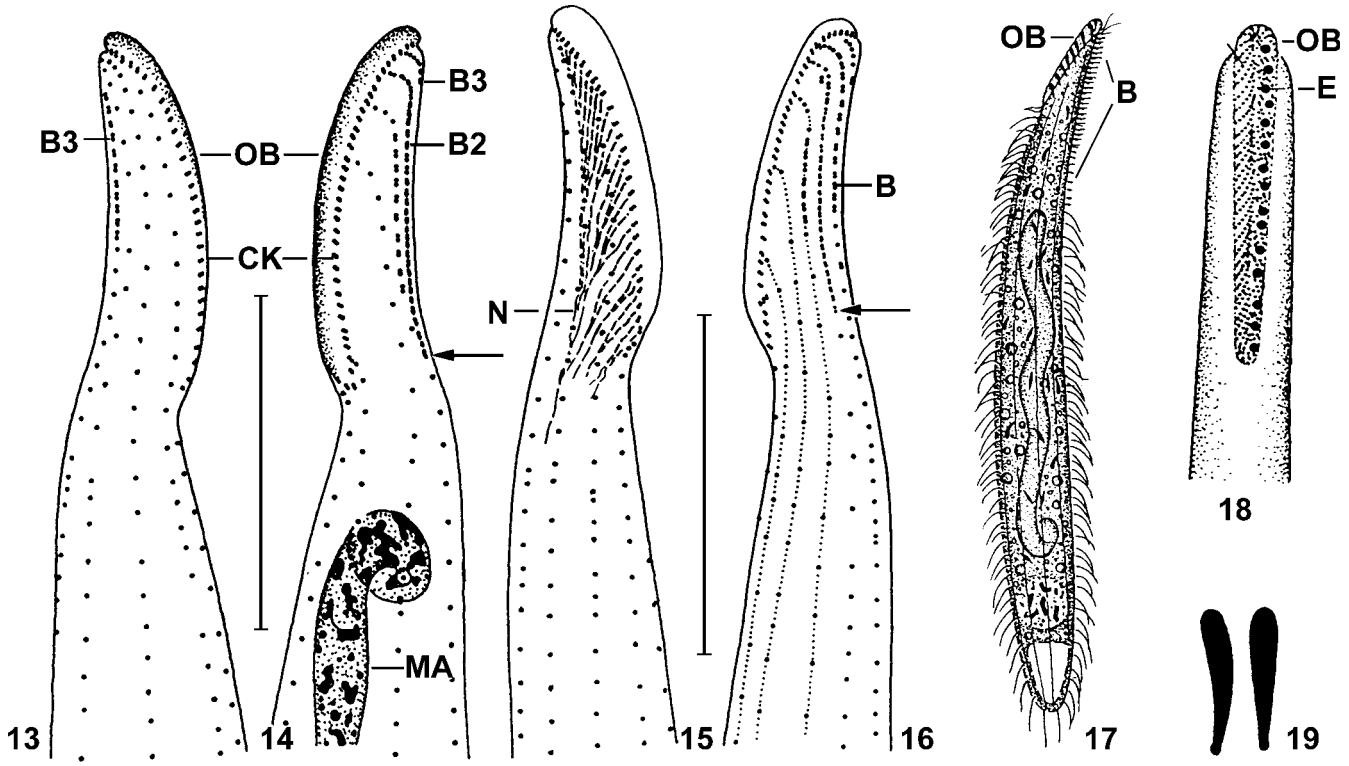

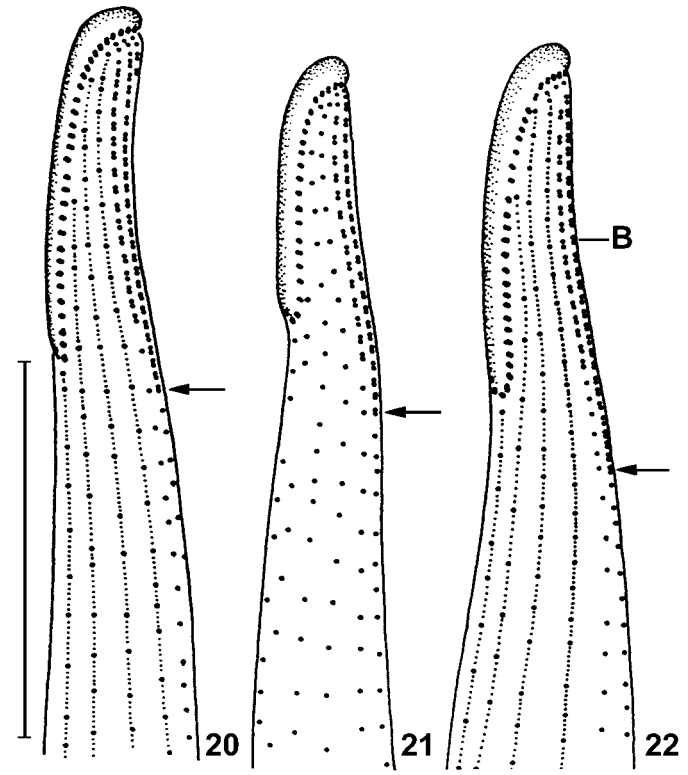

Figs 13-16. *Arcuospathidium pachyoplites*, right and left side view of oral body portion of two specimens after protargol impregnation. Dotted lines connect individual basal bodies of ciliary rows. These figures show: the rather long and very steep oral bulge; the dorsal brush dikinetids much more closely spaced in middle row 2 than in rows 1 and 3; that brush row 2 (arrows) is of about same length as the oral bulge; and, finally, the indistinct *Spathidium* pattern produced by the left side kineties, whose first basal body is very near to the circumoral kinety. B - dorsal brush, B2, 3 - dorsal brush rows, CK - circumoral kinety, MA - macronucleus, N - nematodesmata, OB - oral bulge. Scale bars 30 µm.
Figs 17-22. *Arcuospathidium vlassaki* from life (17-19; from Foissner 2000) and after protargol impregnation (20-22; new drawings from type population). **17** - left side view of a representative specimen (length 190 µm), showing that the oral bulge is much less conspicuous than in *A. pachyoplites*, where it is longer and studded with thick extrusomes (Fig. 1); **18** - frontal view showing extrusomes restricted to the left half of the oral bulge, while they are scattered throughout the bulge in *A. pachyoplites* (Fig. 4); **19** - extrusomes are 5 x 1 µm in size and attached by the broad end to the oral bulge; in *A. pachyoplites*, they are attached by the narrow end and considerably larger (6-8x1-1.7 µm), making the oral bulge very conspicuous (Figs 1, 5, 23, 25); **20-22** - the *Arcuospathidium* ciliary pattern is more distinct in *A. vlassaki* than in *A. pachyoplites* (Figs 14, 16) because the anterior end of the left side kineties is more distinctly directed dorsally (basal bodies of individual ciliary rows connected by dotted lines). Arrows mark end of dorsal brush row 2, which is distinctly longer than the oral bulge, a main difference to *A. pachyoplites*, where it is shorter or of same length as the oral bulge (Figs 14, 16). B - dorsal brush, B1-3 - dorsal brush rows, CK - circumoral kinety, E - extrusomes, MA - macronucleus, N - nematodesmata (oral basket rods), OB - oral bulge. Scale bar 30 µm (20-22).

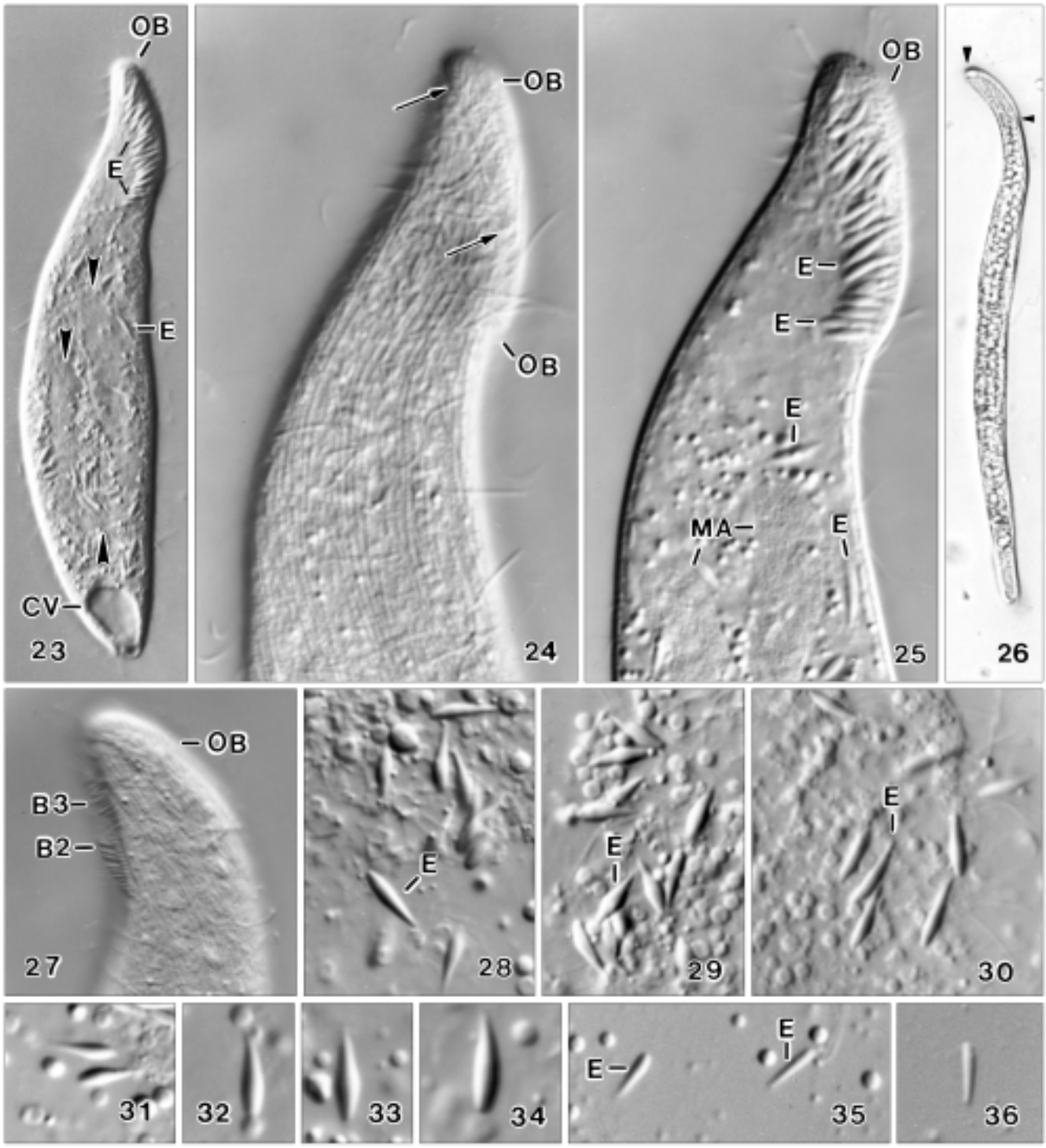

Figs 23-36. *Arcuospathidium pachyoplites* (23-25, 27-34) and *A. vlassaki* (26, 35,36; from Foissner 2000) from life. **23-25 -** overview and oral details of a slightly squashed and thus broadened specimen. *Arcuospathidium pachyoplites* is conspicuous due to the thick and numerous extrusomes contained in the oral bulge. Figure 24 is a surface view showing the closely spaced rows of cortical granules and the right margin of the oral bulge (arrows). Arrowheads in figure 23 mark the long, tortuous macronucleus; **26 -** *Arcuospathidium vlassaki* is usually more slender than *A. pachyoplites* and the oral bulge, marked by arrowheads, is less conspicuous because it contains fewer and smaller extrusomes (cp. figures 32-36); **27 -** right side view showing dorsal brush rows 2 and 3 with bristles up to 4 µm long; **28-31 -** oral bulge extrusomes are 6-8 x 1-1.7 µm in size and rather variable in shape, usually, however, they are lanceolate; **32-36 -** same scale comparison of extrusomes of *A. pachyoplites* (32-34) and *A. vlassaki* (35, 36). The extrusomes of *A. pachyoplites* are considerably larger (7 x 1.4 µm) than those of *A. vlassaki* (5 x 1 µm). B1, 2 - dorsal brush rows, CV - contractile vacuole, E - extrusomes, MA - macronucleus, OB - oral bulge.

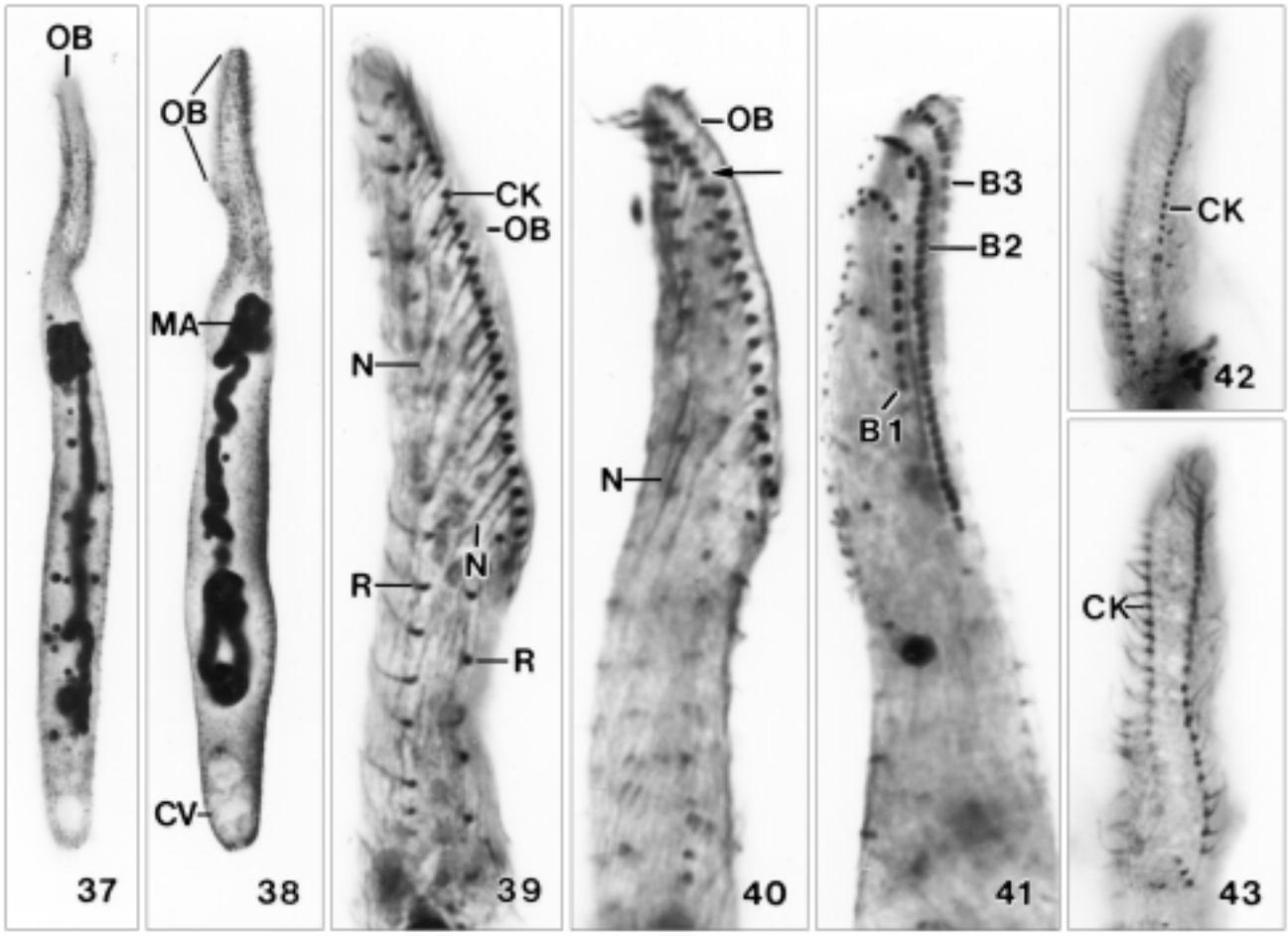

Figs 37-43. *Arcuospathidium pachyoplites* after protargol impregnation. **37, 38 -** ventral and left side overviews showing slender shape, steep oral bulge, and the long macronucleus with coiled ends; **39, 40 -** right side views of oral region showing the circumoral kinety composed of comparatively widely spaced dikinetids (arrow) associated with fine rods forming the oral basket; **41 -** left side view of oral body portion showing that dorsal brush dikinetids are much more closely spaced in row 2 than in rows 1 and 3. Note that dorsal brush row (2) is shorter than the oral bulge, a main difference to *A. vlassaki*, where it is longer (Figs 20-22); **42, 43 -** frontal views of circumoral kinety and oral bulge. The white dots within the circumoral kinety (oral bulge) are optical transverse sections of the large, unstained extrusomes. B1-3 - dorsal brush rows, CK - circumoral kinety, CV - contractile vacuole, MA - macronucleus, N - nematodesmata (oral basket rods), OB - oral bulge, R - ciliary rows.

Type material: 1 holotype slide and 2 paratype slides with protargol-impregnated specimens (Foissner's method) have been deposited in the Oberösterreichische Landesmuseum in Linz (LI). All specimens illustrated and some other well-impregnated cells are individually marked by a black ink circle on the cover glass. For comparison, we add a slide of protargol-impregnated *Arcuospathidium vlassaki* from type population, showing the cells illustrated in figures 20-22.

Description: this species does not fix well, as is often the case with saline material. Some specimens look rather distorted and/or inflated by large food inclusions and/or insufficient preservation. Furthermore, the slides contain some very small specimens (postdividers?) and cells with a distinctly shorter oral bulge, possibly belonging to another species. All these poorly preserved and unusual specimens, roughly 10% of the population, are excluded from the description and morphometry.

Size 120-230 x 15-40 µm *in vivo*, usually near 170 x 20 µm, as calculated from some *in vivo* measurements and the morphometric data (Table 1). Knife-shaped with an average length:width ratio of 9:1, but "handle" much longer than "blade", that is 4.7:1, flattened only in oral region; oral bulge bluntly pointed anteriorly and rather distinctly set off from narrowed neck, strongly oblique, that is, almost parallel with main body axis; posterior end

narrowly rounded, in preparations occasionally almost globular when the contractile vacuole is filled (Figs 1, 6, 7, 12, 37, 38). Macronucleus extending in posterior two thirds of body, basically a long, slightly tortuous rod with ends frequently coiled, spiralized and/or inflated; occasionally in two long pieces. Nucleoli small, globular and numerous, rarely reticulate (Figs 1, 6-8, 12, 23, 37, 38). Probably, 5-10 micronuclei not unequivocally distinguishable from extrusomes *in vivo* and protargol preparations; usually fusiform and about 3 x 1-1.5 µm in impregnated specimens (Figs 7, 8). Contractile vacuole in rear body end, several excretory pores in pole area; definitely no second contractile vacuole in anterior body half. Extrusomes accumulated in both sides of oral bulge and scattered in cytoplasm, attached to bulge cortex with pointed anterior end; basically lanceolate, but with several modifications within and between specimens, as shown in figure 5; 6-8 x 1-1.7 µm in size and compact, that is, rather long, thick, and highly refractive, making them very conspicuous at even low magnification (x100; Figs 23, 25) and in silver preparations, where they appear as strongly refractive inclusions (Figs 42, 43); mature (bulge) extrusomes never impregnate with the protargol method used, while a certain cytoplasmic developmental stage impregnates brownish, like the micronuclei (see above). Exploded extrusomes about 20 µm long and of typical toxicyst structure (Figs 1, 3, 5, 23, 25, 28-34, 42, 43). Cortex very flexible, contains about five rows of minute granules approximately 0.2 µm across between each two ciliary rows. Cytoplasm colourless, usually contains many lipid droplets 0.5-5 µm across; rarely specimens with a large food vacuole containing massive prey, likely a ciliate, were observed. Movement conspicuously slow and worm-like, but glides rather rapidly on microscope slide and between soil particles, showing great flexibility.

Cilia about 8 µm long *in vivo*, arranged in an average of 10 equidistant, straight, rather loosely ciliated rows abutting on circumoral kinety in acute angles more distinct at right than left side, where basal bodies are rather widely spaced, producing an intermediate *Arcuospathidium-Spathidium* pattern (Figs 13-16, 39-41, and Discussion). Dorsal brush not as stable as in many congeners, but often with small irregularities, such as minute breaks within rows, supernumerary dikinetids outside rows, or even some extra bristles forming a short fourth row; basically, however, three-rowed and inconspicuous because shorter than oral bulge, occupying only 17% of body length and bristles merely up to 4 µm long, decreasing to 2 µm at end of rows; all rows have one or few ordinary cilia anteriorly and continue as somatic kineties posteriorly; *in vivo*, bristles slightly inflated distally, and anterior bristles of dikinetids shorter than posterior. Brush rows 1 and 3 of similar length and with rather widely spaced dikinetids; row 2 distinctly longer than rows 1 and 3 and with dikinetids so narrowly spaced (~ 1 µm) that they are difficult to illustrate; row 3 with some minute, about 1 µm long, monokinetidal bristles forming short tail extending to second body third (Figs 1, 8-10, 12-16, 27, 39, 41; Table 1).

Oral bulge very conspicuous due to the large and highly refractive extrusomes contained and the strongly oblique orientation almost in parallel with main body axis (Figs 1, 6, 7, 12, 13, 15, 23-25, 38, 39, 41; Table 1); basically, however, of ordinary size and shape, that is, about twice as long as widest trunk region, moderately convex, and dorsally slightly higher than ventrally; oblong to narrowly cuneate and studded with extrusomes in frontal view (Fig. 4). Circumoral kinety of same shape as oral bulge, composed of comparatively widely spaced and frequently slightly irregularly arranged dikinetids, each associated with a cilium and a fine basket rod recognizable only in over-impregnated specimens (Figs 8, 12-16, 24, 39, 40, 42, 43).

Distribution and ecology: as yet found only at type location, that is, 10-20 m inshore the beach of Choroni (67°45'W 10°15'N), Henry Pittier National Park, north coast of Venezuela. The sample consisted of very sandy coastal soil up to 10 cm depth and the mouldy top leave litter from shrubs, Cactaceae, and grasses. The rewetted mixture had 10‰ salinity and pH 6.7. The species become abundant one week after rewetting the sample. Prey is obviously digested rapidly because only few specimens with food vacuoles containing prey remnants were found in the protargol slides.

Redescription of *Spathidium faurefremieti* nom. n. (Figs 44-59, 65-70; Table 2)

Nomenclature: Tucolesco (1962) named a new species *Spathidium faurei* in honour of the great French protozoologist Fauré-Fremiet (1883-1971). Unfortunately, this name is preoccupied by *Spathidium faurëi* Kahl, 1930a. Thus, a new name is required: *Spathidium faurefremieti* nom. n. Accordingly, in future, Tucolesco's species must be referenced as: *Spathidium faurefremieti* Foissner, 2003.

Material: from 3 sites, as described in the distribution and ecology section, but only the Kenyan population was fully investigated. The Brazilian specimens were also studied rather carefully, while the Australian popu-

lation was routinely identified *in vivo* by the main characteristics of the species, viz., the two contractile vacuoles, body and extrusome size and shape, and the nuclear pattern.

Voucher slides: 5 slides with protargol-impregnated specimens (Foissner's method) from Kenya have been deposited in the Oberösterreichische Landesmuseum in Linz (LI). All specimens illustrated and some other well-impregnated cells are individually marked by a black ink circle on the cover glass. The Brazilian specimens, which are only mediocre impregnated, are contained in the type slides of *Cultellothrix velhoi* Foissner, 2003a and *Cephalospatula brasiliensis* Foissner, 2003b.

Description of Kenyan population: size 170-330 x 13-22 µm *in vivo*, usually near 240 x 17 µm, as calculated from some *in vivo* measurements and the morphometric data (Table 2). Very slenderly spatulate or vase-shaped with an average length:width ratio of about 14:1, widest in or slightly underneath mid-body, rather distinctly narrowed subapically producing a slender neck bearing the slightly widened and flattened oral area; posterior end narrowly rounded, in preparations sometimes bulbous due to the contractile vacuole (Figs 44, 48; Table 2). Macronucleus extending in central body quarters, basically a long, irregularly nodulated rod with more or less tortuous, coiled ends; nucleoli small, globular, and numerous. On average 8.5 globular, spongious micronuclei near or attached to macronucleus (Figs 44, 48, 51, 69; Table 2). Invariably two contractile vacuoles without collecting canals: one, as usual, in rear end with scattered excretory pores in pole are; and a second slightly above mid-body with 2-7 serially arranged excretory pores attached to the kinety bearing the middle row of the dorsal brush (Figs 44, 48, 52, 70; Table 2). Extrusomes inconspicuous, accumulated in both sides of oral bulge and scattered in cytoplasm, where a certain, fusiform developmental stage impregnates with protargol; mature oral bulge extrusomes *in vivo* rod-shaped with rounded ends and slightly curved, about 6 µm long, do not impregnate with the protargol method used (Figs 44, 46, 52). Cortex very flexible, contains rows of inconspicuous granules less than 1 µm across. Cytoplasm colourless, contains few to many lipid globules, depending on state of nutrition, mainly in middle body third. Movement conspicuously slow and worm-like.

Cilia about 8 µm long *in vivo*, arranged in an average of 12 equidistant, straight, moderately densely ciliated rows abutting on circumoral kinety in typical *Spathidium* pattern (Foissner 1984), that is, in acute angles at right side and nearly at right angles at left with rows still attached to circumoral kinety fragments (Figs 44, 47-50, 65-67; Table 2). Dorsal brush of usual location and structure, inconspicuous because occupying only 20% of body length on average and bristles merely 3 µm long *in vivo*; all rows of similar length, an unusual feature; dikinetids narrowly spaced in rows 1 and 2, while widely spaced in row 3 which has, as usual, a monokinetidal bristle tail extending to second body third; specimens with a short, fourth row of bristles rarely occur (Figs 44, 49, 50, 52, 68; Table 2).

Oral bulge inconspicuous because only slightly longer than widest trunk region and ordinarily slanted (~ 45°); slightly convex and higher dorsally than ventrally; obovate and studded with extrusomes in frontal view (Figs 44, 45, 47-52, 65-68; Table 2). Circumoral kinety not obovate as oral bulge, but distinctly cuneate, composed of more or less perfectly aligned, dikinetidal kinetofragments frequently still attached to the somatic ciliary rows from which they were produced, especially at left side; dikinetids narrowly spaced, each associated with a cilium and a fine basket rod hardly recognizable *in vivo*; oral basket, however, fairly distinct in protargol-impregnated specimens (Figs 48-52, 65-68).

Observations on Brazilian and Australian specimens (Figs 53, 55-58; Table 2)

The Brazilian population matches the Kenyan specimens in many main features, for instance, the two contractile vacuoles and the dorsal brush, while the number of ciliary rows (17 *vs.* 11) and body width (27 µm *vs.* 15 µm) are conspicuously different (Table 2). Furthermore, the extrusomes are longer, viz. 9-12 µm and thus extend into the somatic cytoplasm, while the short (6 µm) extrusomes of the Kenyan specimens just fill the oral bulge; the macronucleus is more distinctly nodulated and thicker; body shape is cylindroidal rather than spatulate (Figs 56-58); and the oral bulge is elliptical, not obovate in frontal view (Fig. 55). These are rather distinct differences causing doubt on conspecificity (see Discussion).

The Australian specimens were identified *in vivo*, where they showed the same features as those from Kenya. Extrusomes, however, were 9-10 µm long and thus in between those of specimens from Kenya (6 µm) and Brazil (9-12 µm).

Distribution and ecology: Tucolesco (1962) discovered *S. faurefremieti* in subterranean cave water in Rumania. I found it, as yet, only in soils from Gondwanan areas, viz., Africa, South America, and Australia. These data indicate a cosmopolitan distribution of

Table 2. Morphometric data on *Spathidium faurefremieti* from Kenya (upper line) and Brazil (lower line).

Characteristics[a]	x	M	SD	SE	CV	Min	Max	n
Body, length	213.8	202.5	41.6	12.0	19.4	160.0	305.0	12
	255.9	240.5	43.4	14.5	16.9	186.0	330.0	9
Body, width	15.6	15.0	2.2	0.7	14.3	13.0	20.0	12
	28.3	27.0	8.6	2.9	30.2	21.0	47.0	9
Body length:width, ratio	13.9	12.9	2.9	0.8	20.6	10.4	20.3	12
	9.6	10.9	2.8	0.9	28.9	4.9	12.3	9
Oral bulge, length	22.7	22.0	2.0	0.6	9.2	19.0	25.0	12
	25.6	26.0	3.0	1.0	11.6	20.0	30.0	9
Body length:oral bulge length, ratio	9.6	9.5	1.1	0.3	11.8	8.0	12.2	12
	10.0	9.4	1.1	0.4	11.2	8.6	11.8	9
Circumoral kinety to end of brush row 1, distance	38.4	36.5	5.8	1.7	15.0	30.0	48.0	12
	39.2	40.0	8.9	3.0	22.7	22.0	52.0	9
Circumoral kinety to end of brush row 2, distance	43.3	40.0	8.5	2.5	19.6	30.0	58.0	12
	47.8	50.0	9.7	3.2	20.3	30.0	62.0	9
Circumoral kinety to end of brush row 3, distance	37.7	37.5	7.2	2.1	19.1	30.0	50.0	12
	35.6	36.0	9.2	3.1	25.8	20.0	47.0	9
Anterior body end to first excretory pore, distance	91.7	90.0	16.5	4.8	18.0	66.0	122.0	12
	91.3	90.0	14.2	4.7	15.6	60.0	110.0	9
Macronucleus figure, length	105.6	96.5	28.8	8.3	27.3	66.0	165.0	12
	115.0	105.0	26.0	8.7	22.6	82.0	150.0	9
Macronucleus, width in middle	3.6	4.0	-	-	-	3.0	4.0	12
	6.0	6.0	1.0	0.3	16.7	5.0	8.0	9
Micronuclei, largest diameter	3.1	3.0	-	-	-	3.0	3.5	12
	4.9	5.0	0.9	0.3	18.4	4.0	6.0	7
Micronuclei, number	8.5	8.5	1.0	0.3	11.8	7.0	10.0	12
	9.5	9.5	1.5	0.6	15.8	8.0	12.0	6
Somatic kineties, number (including brush)	11.7	11.0	0.9	0.3	7.6	11.0	13.0	12
	17.1	17.0	1.3	0.4	7.4	15.0	19.0	9
Ciliated kinetids in a lateral kinety, number	90.4	82.5	24.6	7.1	27.2	64.0	152.0	12
	62.1	63.0	7.2	2.7	11.6	50.0	70.0	9
Dorsal brush rows, number[b]	3.0	3.0	0	0	0	3.0	3.0	12
	3.0	3.0	0	0	0	3.0	3.0	9
Dikinetids in brush row 1, number	23.3	23.0	5.5	1.6	23.6	15.0	32.0	12
	24.0	25.0	3.6	1.2	15.0	15.0	27.0	9
Dikinetids in brush row 2, number	29.5	29.5	6.6	1.9	22.4	20.0	40.0	12
	34.8	34.0	4.7	1.6	13.6	25.0	42.0	9
Dikinetids in brush row 3, number	19.2	18.5	3.1	0.9	16.0	14.0	23.0	12
	23.1	23.0	3.8	1.3	16.4	17.0	27.0	9
Excretory pores of anterior contractile vacuole, number	3.3	3.0	1.5	0.4	45.7	2.0	7.0	12
	similar as above, but exact number difficult to count							

[a]Data based on mounted, protargol-impregnated, randomly selected specimens from non-flooded Petri dish cultures. [b]Only full rows counted. Measurements in µm. CV - coefficient of variation in %, M - median, Max - maximum, Min - minimum, n - number of individuals investigated, SD - standard deviation, SE - standard error of arithmetic mean, x - arithmetic mean.

S. faurefremieti, but this is not definite because conspecificity of all populations is doubtful (see Discussion).

In Kenya (Africa), *S. faurefremieti* occurred in a sample collected by Emmerich Petz (Upper Austria) in the surroundings of the Taita Hills Lodge in the Shimba Hills Nature Reserve (39°25'E 5°S), about 40 km south of the town of Mombassa. This sample was composed of red soil mixed with some grass and shrub litter. The Brazilian (South America) population occurred in a soil sample, kindly provided by Dr. L. F. Machado Velho, from the floodplain of the Paraná River near the town of Maringá (53°15'W 22°40'S). The dark, humic soil was mixed with much partially decomposed leaf litter and had pH 5.1 (in water). The Australian population of *S. faurefremieti* was found in soil from the Murray

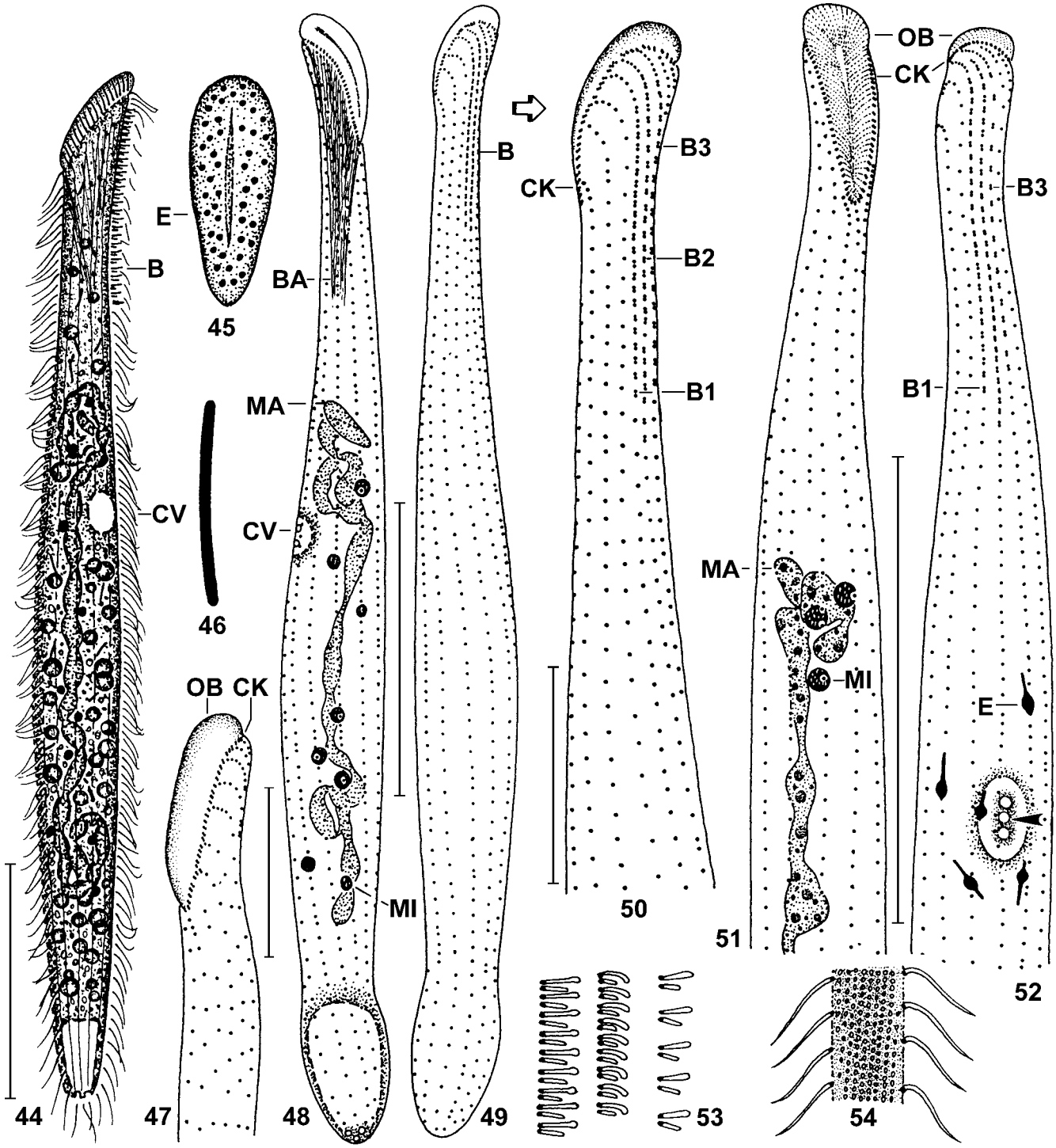

Figs 44-54. *Spathidium faurefremieti*, Kenyan (44-52, 54) and Brazilian (53) specimens from life (44-46, 53, 54) and after protargol impregnation (47-52). **44 -** left side view of a representative specimen, i.e., "constructed" from live observations and morphometric data shown in table 2. Note the slender shape and the second contractile vacuole above mid-body, a main feature of this species; **45 -** frontal view of oral bulge studded with extrusomes; **46 -** oral bulge extrusome, length 6 µm; **47 -** left side view of anterior body portion, showing circumoral kinety and somatic ciliary rows arranged in typical *Spathidium* pattern; **48-50 -** ciliary and contractile vacuole pattern and nuclear apparatus of main voucher specimen. Note the second contractile vacuole above mid-body and the dorsal brush rows, which terminate at almost same level, another unusual feature. The circumoral kinety and the ciliary rows are arranged in the typical *Spathidium* pattern (50); **51, 52 -** ventral and dorsal view of anterior body half of another specimen. Note the cuneate circumoral kinety, the widely spaced dikinetids of dorsal brush row 3, and the three excretory pores (arrowhead) of the anterior contractile vacuole; **53 -** middle portion of dorsal brush, longest bristles 5 µm; **54 -** surface view showing cortical granulation. B - dorsal brush, B1-3 - dorsal brush rows, BA - oral basket, CK - circumoral kinety, CV - contractile vacuoles, E - extrusomes, MA - macronucleus, MI - micronucleus, OB - oral bulge. Scale bars 20 µm (47, 50); 50 µm (44, 48, 49, 51, 52).

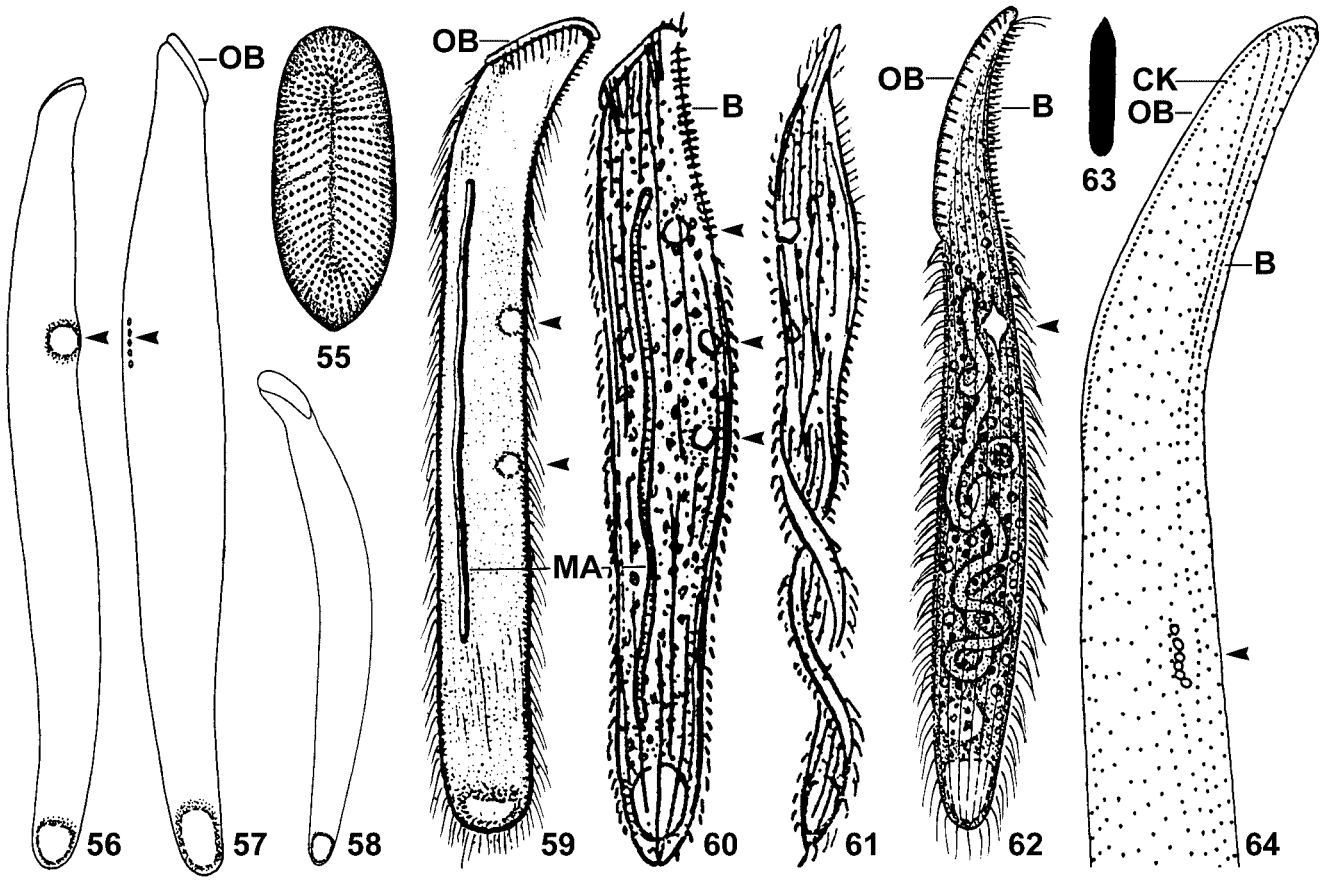

Figs 55-64. *Spathidium faurefremieti* (55-59) and related species, viz., *Spathidium vermiforme* (60, 61) and *Arcuospathidium bulli* (62-64) from life (55, 59-63) and after protargol impregnation (56-58, 64). Arrowheads mark the anterior contractile vacuole(s), a main feature of these species. **55 -** frontal view of oral bulge of a Brazilian specimen. The bulge contains distinct rows of cortical granules; **56-58 -** outline drawings of Brazilian specimens of *S. faurefremieti*, length 300 µm, 200 µm, 200 µm; **59 -** original figure of *S. faurefremieti*, length 400 µm (from Tucolesco 1962). Tucolesco did not mention the contractile vacuoles in the description, and thus it is unknown whether both or only one of the anterior contractile vacuoles has excretory pores; **60, 61 -** *Spathidium vermiforme* (from Penard 1922) is 200-400 µm long, strongly flattened, and has "une grande vésicule contractile postérieure, puis une autre en avant, dans laquelle viennent éclater des vacuoles plus petites"; **62-64 -** *Arcuospathidium bulli* (from Foissner 2000) is about 260 x 25 µm in size; has a long, steep oral bulge containing thick, 4 µm long extrusomes (63); and shows a typical *Arcuospathidium* ciliary pattern (64; somatic ciliary rows separated from circumoral kinety and directed dorsally), while *S. faurefremieti* has a *Spathidium* pattern (ciliary rows attached to circumoral kinety and curved ventrally to form ~ 90° angles with circumoral kinety; Figs 47, 50). B - dorsal brush, CK - circumoral kinety, MA - macronucleus, OB - oral bulge.

River floodplain near the town of Albury (37°S 147°E). The sample, kindly provided by Dipl.-Biol. Hubert Blatterer, was a mixture of leaf litter and light brown soil with pH 5.2 (in water).

The records from cave water (Tucolesco 1962) and two floodplain soils indicate that *S. faurefremieti* occurs in both soil and freshwater, while the slender shape suggests a preference for soil or muddy environments (Foissner 1987). Abundances were low at all sites, and Tucolesco (1962) possibly observed only a single specimen, as indicated by the range-less size value. None of the prepared cells contained definite food inclusions, indicating that prey is digested rapidly and/or dissolves during ingestion, as observed in several members of the group (Foissner, unpubl.).

DISCUSSION

Arcuospathidium pachyoplites

The boundaries between the spathidiid genera distinguished by Foissner (1984) and Foissner *et al*. (2002) are not very sharp, but greatly aid in distinguishing

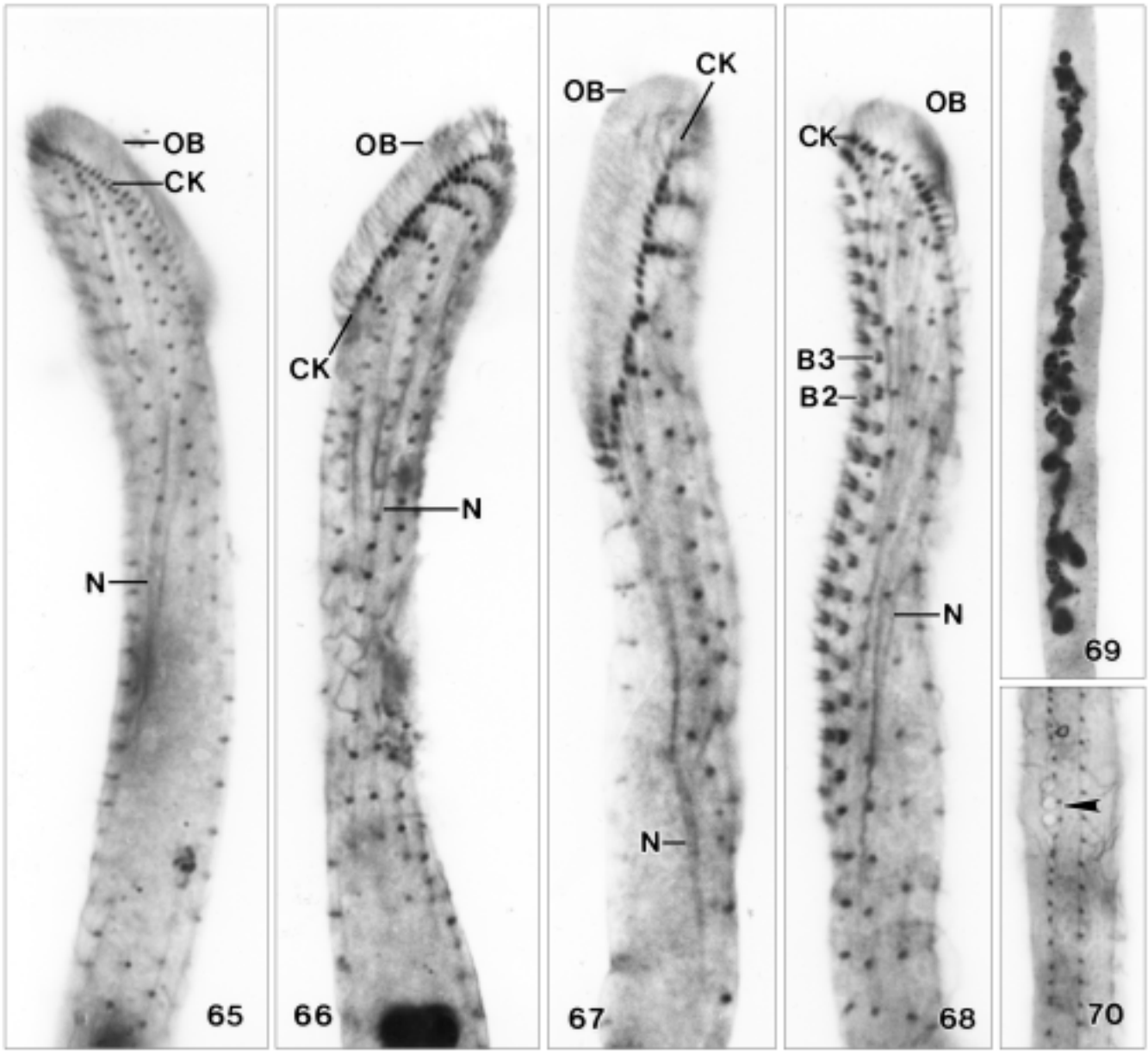

Figs 65-70. *Spathidium faurefremieti*, Kenyan specimens after protargol impregnation. **65, 66 -** ciliary pattern of right and left side in anterior body portion of same specimen. This species has a typical *Spathidium* ciliary pattern, that is, the somatic ciliary rows are attached to the circumoral kinety and curved dorsally at right side and ventrally at left, forming ~ 90° angles with the circumoral kinety; **67 -** left side view of another specimen showing the right angles formed by the circumoral kinety and the curved anterior end of the somatic ciliary rows; **68 -** dorsolateral view showing the widely spaced dikinetids of dorsal brush row 3; **69 -** nodulated and tortuous macronucleus; **70 -** the anterior contractile vacuole has three excretory pores (arrowhead). B2, 3 - dorsal brush rows, CK - circumoral kinety, N - nematodesmata, OB - oral bulge.

species groups within this highly diverse assemblage (for detailed discussion, see Foissner 1984 and Foissner *et al*. 2002). The present species, at first glance, appears as a typical *Arcuospathidium* because the anterior ends of the kineties seemingly are curved dorsally at both sides of the oral bulge, a diagnostic character for the genus. However, closer investigation shows that most left side kineties have a basal body very near to the circumoral dikinetids, giving the kineties a *Spathidium*-like pattern (Figs 14, 16). On the other hand, the knife-shaped body and the steep, oblong oral bulge argue for a classification in *Arcuospathidium*, as does a compari-

son with the supposed nearest relative, *A. vlassaki*, where the *Arcuospathidium* ciliary pattern is more distinct (Figs 20-22).

There are few species with a close resemblance to *A. pachyoplites*, viz., *A. vlassaki* Foissner, 2000; *A. etoschense* Foissner *et al*., 2002; and *Spathidium etoschense* Foissner *et al*., 2002. At first glance, *A. pachyoplites* is indistinguishable from *A. vlassaki* because all obvious features are rather similar (Figs 17-22). However, a more detailed comparison reveals differences significant at species level, most related to the extrusomes emphasizing the need of thorough *in vivo* data: lanceolate with narrow end attached to the oral bulge *vs.* oblanceolate attached with broad end (Figs 1, 5, 17, 19); scattered in entire oral bulge *vs.* forming a single row in left bulge half (Figs 4, 18); 7 x 1.4 µm and thus highly conspicuous *vs.* 5 x 1 µm and of ordinary appearance (Figs 32-36). Although there is some variation in these features, the differences are obvious and conspicuous. In this context, it should be mentioned that I found a second population of *A. vlassaki* in Saudi Arabia having the same extrusome characteristics as the type population from Namibia, especially the unusual broad end-attachment. The second main distinguishing feature concerns the relative lengths of the oral bulge and dorsal brush: in *A. pachyoplites* the longest brush row (2) is of same length or shorter than the oral bulge (Figs 8, 9, 12, 14, 16, 41), while in *A. vlassaki* the longest brush row (2) is of same length or longer than the oral bulge (Foissner 2000 and Figs 20-22); the average values are 34.4 µm and 27.2 µm *vs.* 21.8 µm and 25 µm. Further, minor differences in sum supporting separation of the South American from the African population: dikinetids very narrowly spaced (~ 1 µm) only in brush row 2 *vs.* rows 2 and 3; body width:oral bulge length ratio 0.56 *vs.* 0.75, that is, bulge relatively longer in *A. pachyoplites* than in *A. vlassaki*; *Arcuospathidium* ciliary pattern less distinct in the former than the latter, as proved by the reinvestigation of the African type population (Figs 20-22). Observations on other populations are needed to prove whether these minor differences are stable or within the range of natural variability of the taxa concerned.

Arcuospathidium pachyoplites differs from *A. etoschense* mainly by the macronucleus, which is tortuous in the former and nodular in the latter. Furthermore, *A. pachyoplites* is considerably stouter than *A. etoschense* (9.0:1 *vs.* 13.7:1), and its extrusomes are much longer and thicker (7 x 1.4 µm *vs.* 3-4 x < 1 µm). *Arcuospathidium pachyoplites* differs from *Spathidium etoschense* by the ciliary pattern, the much longer and tortuous macronucleus, and the thicker (1.4 µm *vs.* 1 µm), and thus highly conspicuous extrusomes.

Spathidium faurefremieti

This species poses the opportunity to discuss some basic problems, especially of recognizing the genus *Supraspathidium* and of species in general. I shall discuss these and other questions in a loose sequence showing my views and ways to solve them.

(1) The genus *Supraspathidium* and generic assignment of *Spathidium faurefremieti*: Foissner and Didier (1981) diagnosed *Supraspathidium* as follows: "Spathidiidae with several to many, serially arranged contractile vacuoles and the oral bulge indistinctly set off from body proper". They assigned to *Supraspathidium* all spathidiids with more than the ordinary posterior contractile vacuole and, unfortunately, fixed as a type species *Spathidium teres* Stokes, 1886, a poorly known species that awaits redescription. Nonetheless, three "typical" *Supraspathidium* species have been described meanwhile: *S. multistriatum* Foissner and Didier, 1981; *S. etoschense* Foissner *et al*., 2002; and *S. armatum* Foissner *et al*., 2002. All have a clear identity and are massive, densely ciliated organisms with one or two rows of contractile vacuoles, each comprising five or more individual vacuoles with several excretory pores. The ciliary pattern is *Epispathidium*-like, with ciliary rows and cilia within rows even more densely spaced, especially at the anterior end of the kineties, where a kinetofragment-like polymerization occurs. Clearly, such spathidiids represent a type of its own and can be classified in the genus *Supraspathidium*, for which I suggest the following refined diagnosis: Massive, densely ciliated Spathidiidae with *Epispathidium*-like ciliary pattern and many (> 5) contractile vacuoles, each having several excretory pores, in one or two rows.

Another group of spathidiids has the ordinary posterior contractile vacuole and a second one in the mid-body region. The general organization and the ciliary pattern of these bivacuolate species look like those of classical spathidiids, as shown by *Arcuospathidium bulli* Foissner, 2000 (Figs 62-64) and *Spathidium faurefremieti* redescribed here. Thus, generic separation would appear premature given the present state of knowledge, though the second contractile vacuole is a distinct feature. On the other hand, it is now obvious that an increased number of contractile vacuoles evolved independently in

several evolutionary lines of the Spathidiidae, viz., in *Spathidium*, *Arcuospathidium* and *Supraspathidium*. Each of these lines can be considered as a distinct evolutionary branch, requiring generic or subgeneric separation, especially when further such species are discovered differing also in other features, for instance, an *Arcuospathidium* with two contractile vacuoles (like *A. bulli*), but scattered macronuclear nodules (unlike *A. bulli*, which has a single, long strand).

(2) Conspecificity of the African and Brazilian population: Several main features, especially the two contractile vacuoles and the shape of the extrusomes agree well, while two other main characteristics do not even overlap, viz., the number of ciliary rows and body width (Table 2). While the latter might be considered as less important because both populations are still slender (body length:width ratio 13.9:1 and 9.6:1, respectively) and body width is known to depend on nutritional state, the former is an important difference because kinety number is rather stable within and between populations in many haptorids (Foissner 1984, Foissner *et al*. 2002). Furthermore, extrusome length also does not overlap (6 µm *vs.* 12 µm). This, however, is probably a minor difference because extrusome length is rather variable in general and the Australian specimens are intermediate (9-10 µm).

Basically, the differences argue to consider the Brazilian population as a distinct subspecies because two main morphometric features do not overlap, of which one is very important. Furthermore, geographic distance would support such a separation (Foissner *et al*. 2002). On the other hand, only one population each has been studied in detail so that the "true" variability of the species is insufficiently known. Furthermore, if such differences are rated too high at the present state of knowledge, it would hardly be possible to identify the populations with the European *S. faurefremieti*, whose description is much more incomplete and thus requires a broad species concept.

In this situation, the most pragmatic solution is to consider all populations as belonging to a single species, but to avoid neotypification, as suggested by Foissner (2002) and Foissner *et al*. (2002), because conspecificity is not beyond reasonable doubt and detailed data on the supposed European population (= *S. faurefremieti*) are lacking. However, if the detailed investigation of an European population shows similar differences as those found between the African and Brazilian populations (Table 2), all should obtain species or subspecies status. Ideally, such data should be supplemented by gene sequences.

(3) Identification: Identification largely depends on the species concept and the treatment of literature data. Our concept is thoroughly discussed in Foissner *et al*. (2002) and thus needs not to be explained here. Briefly, we apply a simple, population-based, morphological concept and identify populations with previously described species, even if data are poor, whenever it is feasible; specifically, at least the general appearance and one main feature must agree.

Tucolesco (1962) provided the following description of *Spathidium faurei* (now *S. faurefremieti*) and a single illustration, reproduced here as figure 59: "Taille 400 µ. Cellule de couleur jaunàtre, de forme allongée et très étroite, à bords parallèles. Pòle postérieur largement arrondi. Partie antérieur de la cellule fortement déviée. Troncanture antérieure presque droite, légèrement inclinée sur l'axe longitudinal. Noyau très long (un peu plus long que la moitié de la cellule) et très mince. Striation serrée. Cils fins, épais et courts. Trouvé dans les eaux souterraines de la grotte Pestera Ialomicioara, en août 1958".

Obviously, my populations agree with Tucolesco's species in several main features, suggesting conspecificity: size, slender shape; short, moderately oblique oral bulge; macronuclear and contractile vacuole pattern. Unfortunately, Tucolesco did not provide information on two other main features: extrusomes and the number of ciliary rows, which is possibly considerably higher than in my populations because Tucolesco's illustration appears to indicate a narrow striation pattern (Fig. 59). Further, details of the shape are different because my specimens are definitely not parallel-sided, especially those from Africa have a distinctly narrowed neck. Possibly, of even greater importance is the habitat difference, viz., soil *vs.* cave water. However, the Australian and the Brazilian populations are from floodplain soils, indicating that my species might occur also in freshwater.

In summary, uncertainties and differences are too pronounced to be entirely confident about conspecificity. Thus, neither the Kenyan nor Brazilian population can serve as a neotype given the present state of knowledge, as explained above.

(4) Comparison with related species: Unfortunately, Tucolesco (1962) did not compare *Spathidium faurefremieti* with any described species, especially *S. vermiforme* Penard, 1922. It is unclear whether he did not know of *S. vermiforme* or considered his

population as sufficiently different to classify it as a new species. In my opinion, *S. vermiforme* and *S. faurefremieti* agree in most main features, especially size, slender shape, and the nuclear and contractile vacuole pattern (Figs 59-61). However, there is an important difference in the habitat: Penard discovered *S. vermiforme* in a sapropelic environment, according to Kahl (1930b), while Tucolesco found *S. faurefremieti* in clean cave water. Sapropelic spathidiids are poorly known, but most are probably different from those living in ordinary freshwaters and soils (Kahl 1926, 1930b; Foissner 1998, and unpublished). Accordingly, synonymy of Penard's and Tucolesco's species is questionable given the present state of knowledge. This is emphasized by slight shape differences (Penard emphasized a dorsal convexity, while Tucolesco mentioned that his species is parallel-sided) and the remark of Penard that one of his populations has symbiotic algae, indicating that he might have mixed two species.

Both populations of *Spathidium faurefremieti* are very similar to *S. procerum* Kahl, 1930a, as redescribed by Foissner (1984), except of that the latter has only one ordinary, posterior contractile vacuole in over one hundred populations checked. At first glance, *Arcuospathidium bulli* Foissner, 2000 is also similar to *S. faurefremieti*, as already discussed by Foissner (2000), because it has two contractile vacuoles. However, the oral bulge is distinctly longer and much more oblique in *A. bulli*, and the ciliary patterns are conspicuously different (Figs 62-64). Thus, *Spathidium faurefremieti*, as redescribed here, is a very distinct species easily recognizable, even *in vivo*, by the long, slender body; the short oral bulge; the long macronucleus; and, especially, the two contractile vacuoles.

Acknowledgements. The technical assistance of Dr. B. Moser, Dr. E. Herzog and Mag. E. Strobl is gratefully acknowledged. Special thanks to Dr. Kuidong Xu and Mag. Yanli Lei for discussion. Financial support was provided by the Austrian Science Foundation (FWF project P-15017).

REFERENCES

Buitkamp U. (1977) Die Ciliatenfauna der Savanne von Lamto (Elfenbeinküste). *Acta Protozool.* **16:** 249-276

Dragesco J., Dragesco-Kernéis A. (1979) Cilies muscicoles nouveaux et peu connus. *Acta Protozool.* **18:** 401-416

Foissner W. (1984) Infraciliatur, Silberliniensystem und Biometrie einiger neuer und wenig bekannter terrestrischer, limnischer und mariner Ciliaten (Protozoa: Ciliophora) aus den Klassen Kinetofragminophora, Colpodea und Polyhymenophora. *Stapfia*, Linz **12:** 1-165

Foissner W. (1987) Soil protozoa: fundamental problems, ecological significance, adaptations in ciliates and testaceans, bioindicators, and guide to the literature. *Progr. Protistol.* **2:** 69-212

Foissner W. (1991) Basic light and scanning electron microscopic methods for taxonomic studies of ciliated protozoa. *Europ. J. Protistol.* **27:** 313-330

Foissner W. (1998) An updated compilation of world soil ciliates (Protozoa, Ciliophora), with ecological notes, new records, and descriptions of new species. *Europ. J. Protistol.* **34:** 195-235

Foissner W. (2000) Two new terricolous spathidiids (Protozoa, Ciliophora) from tropical Africa: *Arcuospathidium vlassaki* and *Arcuospathidium bulli*. *Biol. Fertil. Soils* **30**, 469-477

Foissner W. (2002) Neotypification of protists, especially ciliates (Protozoa, Ciliophora). *Bull. zool. Nom.* **59:** 165-169

Foissner W. (2003a) *Cultellothrix velhoi* gen. n., sp. n. a new spathidiid ciliate (Ciliophora: Haptorida) from Brazilian floodplain soil. *Acta Protozool.* **42:** 47-54

Foissner W. (2003b) The Myriokaryonidae fam. n., a new family of spathidiid ciliates (Ciliophora: Gymnostomatea). *Acta Protozool.* **42:** 113-143

Foissner W., Didier P. (1981) Morphologie und Infraciliatur einiger kinetofragminophorer und hypotricher Ciliaten aus den Fließgewässern von Besse-en-Chandesse (Frankreich). *Annls Stn biol. Besse* **15:** 254-275

Foissner W., Agatha S., Berger H. (2002) Soil ciliates (Protozoa, Ciliophora) from Namibia (Southwest Africa), with emphasis on two contrasting environments, the Etosha region and the Namib Desert. *Denisia* **5**: 1-1459

Kahl A. (1926) Neue und wenig bekannte Formen der holotrichen und heterotrichen Ciliaten. *Arch. Protistenk.* **55:** 197-438

Kahl A. (1930a) Neue und ergänzende Beobachtungen holotricher Infusorien. II. *Arch. Protistenk.* **70:** 313-416

Kahl A. (1930b) Urtiere oder Protozoa I: Wimpertiere oder Ciliata (Infusoria) 1. Allgemeiner Teil und Prostomata. *Tierwelt Dtl.* **18:** 1-180

Penard E. (1922) Études sur les Infusoires d'Eau Douce. Georg & Cie, Genève

Stokes A. C. (1886) Notices of new fresh-water infusoria. - V. *Am. mon. microsc. J.* **7:** 81-86

Tucolesco J. (1962) Protozoaires des eaux souterraines. I. 33 espèces nouvelles d'infusoires des eaux cavernicoles Roumaines. *Annls Spéléol.* **17:** 89-105

Recived on 25th June, 2002; revised version on 2nd February, 2003; accepted on 5th February, 2003

Acta Protozool. (2003) 42: 161 - 164

ACTA
PROTOZOOLOGICA

Short Communication

An Improved Silver Carbonate Impregnation for Marine Ciliated Protozoa

Hongwei Ma[1], Joong Ki Choi[1] and Weibo Song[2]

[1]Regional Research Center for Coastal Environments of Yellow Sea, CCEYS, Inha University, Incheon, Korea; [2]Laboratory of Protozoology, Ocean University of China, Qingdao, P. R. China

Summary. An improved silver carbonate impregnation method for marine ciliates is described. Compared to conventional methods, the new method of fixing and staining is easy to learn and yields easily reproducible results. Structures that are impregnated with silver carbonate such as nuclear apparatus, infraciliature as well as cortical and cytoplasmic microtubules and even contractile vacuole pore are stained evenly and with high contrast in all cells on the slides, therefore yielding perfect photographs. This method has the characteristic of simplicity, quickness and good reproducibility, so it is especially suitable for ecologists and ontogenetists. The slides with mounted cells can also be stored for months without loss in quality or staining capability.

Key words: marine ciliate, silver carbonate impregnation, staining method.

INTRODUCTION

In order to identify ciliates for taxonomic evaluation, silver impregnation techniques are indispensable. Even though there are many methods for ciliated protozoa (Klein 1926, Chatton and Lwoff 1930, Dragesco 1962, Deroux and Tuffrau 1965, Wilbert 1975, Fernandez-Galiano 1976, Montagnes and Lynn 1987, Foissner 1992), marine protozoologists and ecologists are still perplexed about the staining of the marine ciliated protozoa. Along with the development of marine ecological research, many ciliated protozoa are being more closely examined, so a simpler kind of and more user-friendly staining method for ciliates is necessary for marine ecologists and biologists. The method of silver carbonate impregnation described in this paper was improved so it is easy to learn and consistently yields easily reproducible results for marine ciliated protozoa.

Address for correspondence: Joong Ki Choi, Regional Research Center for Coastal Environments of Yellow Sea, CCEYS, Inha University, Incheon, Korea; Fax: 032-872-7734; E-mail: jkchoi@inha.ac.kr

DESCRIPTION OF THE METOD

Some of the ciliate species that were used in this work were either laboratory cultures or freshly collected and cultivated in Incheon, Korea or Qingdao, China. The ciliates were cultivated either in normal or in deep Petri dishes and kept at 20-25°C according to their special requirements, using either rice or organisms as food source. The following ciliate species were tested:

Chaenea teres, *Coleps hirtus*, *Dexiotricha granulose*, *Dysteria ovalis*, *Euplotes vanus*, *Fabrea salina*, *Glauconema trihymene*, *Halteria grandinella*, *Metanophrys sinensis*, *Paramecium caudatum*, *Paranophrys magna*, *Parauronema virginianum*, *Pelagostrobilidium simile*, *Pleuronema coronatum*, *Pseudocohnilembus hargisi*, *P. persalinus*, *Rimostrombidium orientale*, *Rimostrombidium venilie*, *Strombidinopsis elegans*, *Uronema marinum*.

Staining Procedure (reagents according to Fernandez-Galiano 1976)

(1) Place 2-3 drops of a rich ciliate culture or even a single specimen in an embryonic dish or in a concave slide.

(2) Add 2-3 drops of 10% formalin quickly to the embryonic dish if the organisms are freshwater species (final concentration is 5%), or add 2-3 drops of 10% (or even 50% depending on the kind of species) seawater formalin if the organisms are seawater species and fix for 1-3 min. Shake and try to concentrate the cells to the middle of the dish or concave slide.

(3) Carefully wash out the water with micropipette and add distilled water three times. Leave about two or three drops of water and organisms.

(4) Add 2 or 3 drops of formalin (10%) and refix for about 1 to 2 min (the final concentration is 5%).

(5) Add 2-3 drops of Fernadez-Galiana's fluid to the refixed ciliates, and mix one minute.

(6) Place the embryonic dish on a pre-heated (60°C) hot-plate for staining. Shake the dish in the process of heating. Immediately add 2-3 ml of 5% sodium thiosulfate solution as soon as the color turns golden brown. The process usually needs 5-7 min.

(7) Check the impregnation under microscope, take pictures with digital camera or draw figure if the impregnation is perfect.

(8) After stabilization with 5% sodium thiosulfate solution for about 8-15 min, wash the organisms very thoroughly in distilled water at least 3 times. For morphogenesis or genus identification, steps 1-8 are enough. For mounting slide, according to the following steps.

(9) Add a small drop of well impregnated ciliate to a clean slide and add an equal sized drop of albumen-glycerol, mix thoroughly but gently with a mounted needle and spread mixture in a moderately thin layer in the middle third of the slide and remove the redundant fluid with a thin micropipette.

(10) Allow to dry in the oven at 55-60°C for 10-30 min.

(11) Dehydrate in alcohol series (70-80-90-95-100-100%) for 5 min in each.

(12) Transfer the slide through 1:1 alcohol and xylene, then through xylene 2 times for 5 min in each.

(13) Mount the slide with Permount and cover with a coverslip. Ensure that no air is trapped under the coverslip and put the slide into the oven at 55-60°C for 24 h.

Remarks concerning the steps of the staining procedure

(1) This method is especially suitable for species with a firm pellicle. It is necessary to adjust the concentration of formalin and the solvent, if the organisms are freshwater species, use 10% distilled water formalin; seawater species, add 10% filtered seawater formalin. Some species cannot be fixed well with formalin and cells may even burst.

(2) Washing out the redundant liquid is also a most important step. Since the chemical component of the original liquid in which the organisms live are different, these chemicals can affect the staining result, so the original liquid should be washed out thoroughly with distilled water at least 3 times.

(3) The ratio of Fernandez-Galiano's fluid usually need not change, but the amount needed depends on many unpredictable factors, e.g., amount and concentration of fixative, kind of organisms. The trial and error method must be frequently used to obtain best results.

(4) The correct impregnation time depends on many factors that are difficult to control. The amount of pyridine and silver carbonate in the Fernandez-Galiano's fluid is especially important. Add another drop of pyridine and/or silver carbonate solution to the Fernandez-Galiano's fluid if impregnation is repeatedly too faint. Some species can be impregnated well before the fluid turn brown, while others even very faint after the fluid becomes dark brown, so try several times to get good results.

(5) Immediately add 2-3 ml 5% sodium thiosulfate solution as soon as the color turns golden brown. Because impregnation can develop well within 1-2 seconds, it is not advisable to check the impregnation results under the microscope. The quickly changing golden brown color is the best opportunity to stop the staining with the 5% sodium thiosulfate solution. Stabilization should occur in no less than 10 min, and only in this way can the mounting slide stay perfect in quality.

(6) Before preparing a permanent slide, the sodium thiosulfate solution must be washed out thoroughly with distilled water at least 3 times, or it will affect the staining quality.

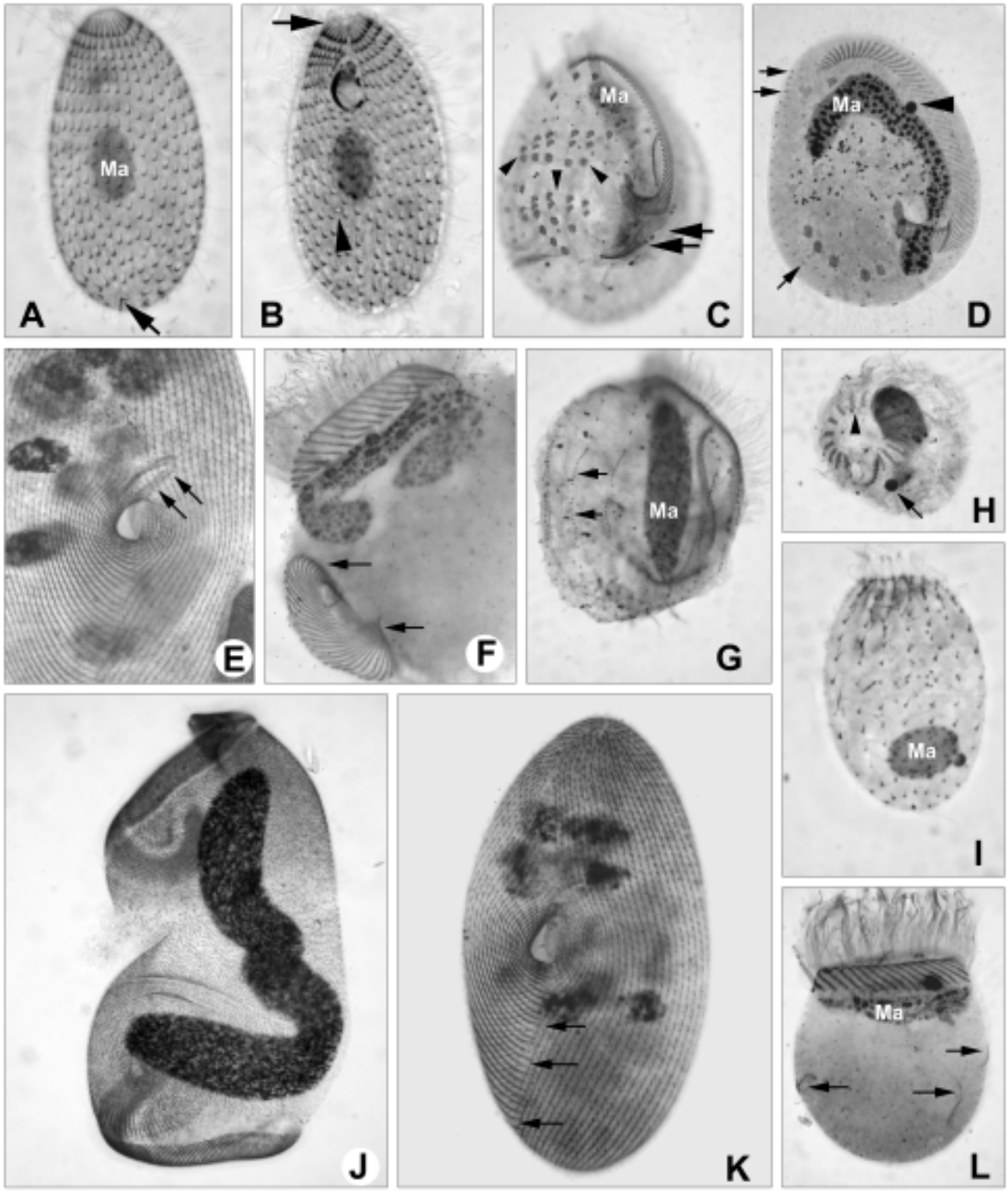

Figs 1A-L. Overview of slides stained by the silver carbonate impregnation method. **A, B** - *Dexiotricha granulose*, a scuticociliatid, arrow in **A** shows the caudal cilium complex, arrow in **B** indicates the cytoplasmic microtubules, arrowhead in **B** means the contractile vacuole pore; **C, D** and **G** - *Euplotes vanus*, a hypotrichid, arrows in **C** point to the new adoral membrane anlagen, arrowheads in **C** indicate the anlage of ventral cirri, arrows in **D** mean the dorsal kineties, arrowhead in **D** points to micronucleus, arrows in **G** display the dorsal kineties anlagen; **E, K** - *Paramecium caudatum*, a hymenostomatid, arrows in **E** indicates the buccal membranelles, arrows in **K** show the post suture; **F, L** - *Pelagostrobilidium simile*, an oligotrichid, arrows in **F** point to the new built buccal field, arrows in **L** show the kineties; **H** - *Halteria grandinella*, an oligotrichid, arrow shows the micronucleus, arrowhead indicates the external adoral membrane; **I** - *Coleps hirus*, a prostomatid; **J** - *Fabrea salina*, a heterotrichid. Ma - macronucleus.

(7) Pay extra attention to avoid foaming when adding the albumen-glycerol to the slide. The key is to use a very thin micropipette and suck a small amount of distilled water before removing the albumen glycerol. Only leaving the least possible amount of albumen glycerol behind results in good staining quality.

In the ciliates species we tested, the infraciliature, the nuclear apparatus, and part of the cortical and cytoplasmic fibrilla systems were stained excellently with the method (Figs 1A-J). Many of the published modifications of the protargol impregnation method, do not yield desired results. The main reason for this situation is that these modifications need more steps and much experience (Dieckmann 1995). Compared to the protargol impregnation, silver carbonate method can save much time, the whole staining procedure can finish within 20 min. The whole procedure is easy to grasp, even a newcomer can also stain slides well, so this method is welcome to ecologists.

Now, the digital camera is widely used to take photos under the microscope. The staining quality can be checked under a microscope directly, and when it is perfect, the photos can be taken right away. If not good, another staining procedure can start within a few minutes. Compared to mounting samples, taking photos with a digital camera has more advantages. Mounting the cells with albumen also has a decisive influence on the staining quality (Foissner 1991). A special advantage of the method is that it is very useful for ontogenetic specialists. A large amount of ciliate can be stained within a very limited time and the morphogenetic stages can be scouted under microscope with a wet slide directly. It is clearer and easier than mounting samples because the cells can be stressed heavily, and the color and structure of the organisms will not change within one or two hours.

Compared to Fernandez-Galiano's original method, a rinsing and post-fixing step was added in our method. This ensures the high staining quality and reproducibility, and also avoids the chemical interference of the solution. As for the seawater species, we do not use the centrifugal method as Fernandez-Galiano used, because in that way cells can easily burst and immingle with other sundries, and affect the mounting result. Compared to Foissner's (1992) modification, the content of Fernandez-Galiano's fluid is different, while two modifications can all produce perfect staining quality. We preferred embryonic dish or concave slide to slide because it is easy to rinse organisms and to avoid the loss of cells during washing, this also keeps a steady condition for staining.

The main problem of Fernandez-Galiano's is not fit for species of thin pellicle. So we fixed seawater sample with filtered seawater formalin and changed the salinity according to species. This is very useful, because most of species even that of thin pellicle can also get perfect staining quality with high concentration of Formalin. For some hypersalinitic species such as *Fabrea salina*, which grows better at the salinity of 90 psu, hypersalinitic seawater formalin can remedy the deficiency of distilled water formalin.

Acknowledgement. This work was supported by the Regional Research Center for Coastal Environments of Yellow Sea (KOSEF-RRC to Professor J. K. Choi) and The Natural Science Foundation of China (No. 40206021). We would like to thank Mr. H. P. Hong and M. H. Yoo, Department of Oceanography, Inha University, Korea, Mr. H. Ma and J. Gong, Laboratory of Protozoology, Ocean University of China, for collecting samples or culturing organisms, and Ms. Anne Radowick, Department of English Language and Literature, Inha University for improving the English draft.

REFERENCES

Chatton E., Lowoff A. (1930) Impregnation, par diffusion argentique, de I'infraciliature des cilies marins et d'eau douce, apres fixation cytologique et sans desiccation. *C. R. Seanc. Soc. Biol.* **104:** 834-836

Dieckmann K. (1995) An improved protargol impregnation for ciliates yielding reproducible results. *Europ. J. Protistol.* **31:** 372-382

Deroux G., Tuffrau M. (1965) *Aspidisca orthopogon* n. sp. Revision de certains mecanismes de la morphogenese a l'aide d'une modification de la technique au protargol. *Cah. Boil. Mar.* **6:** 293-310

Dragesco J. (1962) L'orientation actuelle de la systematique des cilies et la technique d'impregnation au proteinate d'argent. *Bull. Micr. Appl.* **11:** 49-58

Fernadez-Galiano D. (1976) Silver impregnation of ciliated protozoa: procedure yielding good results with the pyridinated silver carbonate method. *Trans. Am. Microsc. Soc.* **95:** 557-560

Foissner W. (1991) Basic light and scanning electron microscopic methods for taxonomic studies of ciliated protozoa. *Europ. J. Protistol.* **27:** 313-330

Foissner W. (1992) The silver carbonate methods. In: Protocols in protozoology (Eds. J. J. Lee and A. T. Soldo). Society of Protozoologists, Allen Press Inc. C7.1-7.3.

Klein B. M. (1926) Über eine neue Eigentümlichkeit der Pellicula von *Chilodon uncinatus* Ehrbg. *Zool. Anz.* **67:** 1-2

Montagnes D. J. S., Lynn D. H. (1987) A quantitative protargol stain (QPS) for ciliates: method description and test of its quantitative nature. *Mar. Microb. Food Webs* **2:** 83-93

Wilbert N. (1975) Eine verbesserte Technik der Protargolimpänation für Ciliaten. *Mikrokosmos* **64:** 171-179

Received on 16th December 2002; received version on 4th March, 2003; accepted on 6th March 2003

Acta Protozool. (2003) 42: 165 - 169

ACTA
PROTOZOOLOGICA

Short Communication

Extracellular Calcium Changes the Morphology of Induced Pinocytosis in *Amoeba proteus*

Wanda KŁOPOCKA, Anna WASIK and Lucyna GRĘBECKA

Department of Cell Biology, Nencki Institute of Experimental Biology, Warszawa, Poland

Summary. The morphology of pinocytosing *Amoeba proteus* induces by two monovalent cations: Na^+ and K^+ were examined at different calcium concentration. It was demonstrated that pinocytotic response of amoeba (number, size and shape of pinocytotic pseudopodia) was related to the amount of Ca^{2+} accumulated on the cell surface.

Key words: amoebae, $[Ca^{2+}]_e$, endocytosis.

INTRODUCTION

In *Amoeba proteus* a typical induced pinocytosis is manifested after external application of different agents: aminoacides, proteins, monovalent cations. This pinocytosis is a kind of fluid-phase endocytosis driven by cortical cytoskeleton and may be compared to macropinocytosis in *Dictyostelium discoideum* in which large fluid-filled vesicles are formed (Maniak 2002). During induced pinocytosis *A. proteus* attains a rosette form with specialized pinocytotic pseudopodia containing channel-like invaginations. The morphology of pinocytosing amoebae: number, shape, and size of pinocytotic pseudopodia and polarity of their distribution on the cell surface vary depending on the kind of inducer, as it was demonstrated for two monovalent cations: Na^+ and K^+ (Grębecka and Kłopocka 1986). Since Na^+ and K^+ can also exert variable effects on the pattern of Ca^{2+} shifting between the surface of amoeba and the medium during induction of pinocytosis (Kłopocka *et al.* 2000), it seems possible that there is a relationship between the type of pinocytotic reaction and the behaviour of calcium at the cell surface.

Address for correspondence: Wanda Kłopocka, Department of Cell Biology, Nencki Institute of Experimental Biology, ul. Pasteura 3, 02-093 Warszawa, Poland; E-mail: aniak@nencki.gov.pl

MATERIALS AND METHODS

Amoeba proteus was cultured in Pringsheim medium with standard concentration of Ca^{2+} (0.85 mM) and fed twice a week on *Tetrahymena pyriformis*. Before experiments cells were starved for 2 days. All experiments were carried out at room temperature.

The course of pinocytosis was compared in amoebae exposed to different concentrations of usually used pinocytotic inducers: KCl and NaCl, in the standard Pringsheim medium, and in Pringsheim solution with modified $[Ca^{2+}]$. Pinocytosis was induced by 30 mM KCl, 125 mM KCl and 125 mM NaCl in standard concentration of

Ca^{2+} (0.85 mM), by 125 mM KCl in $[Ca^{2+}]_e$ increased up to 4.85 mM, and by 30 mM KCl and 125 mM NaCl in the presence of 10 mM EGTA. Calcium concentration either was changed before application of the inducer or during pinocytosis.

Changes in the amount of cell-associated Ca^{2+} during pinocytotic induction were assessed by adding $^{45}Ca^{2+}$ (0.1 mCi/ml, Amersham Life Science, Little Chalfont, Buckinghamshire, England) according to the procedure described earlier (Kłopocka *et al.* 2000). Calcium shifts between the cell surface and the surrounding medium are shown as per cent increase or decrease of cell-associated radioactivity during the experiment. Pinocytosis was controlled 7, 12 and 17 min after application of the inducer.

Observations were carried out in the differential interference contrast (Pluta system, PZO Warsaw) and recorded on the tape with a Panasonic wv BL 600 camera and NV-8051 Panasonic time-lapse video recorder. Selected frames of various pinocytotic forms were stored in an IBM PC compatible computer memory. The morphology of pinocytosis is shown by scanning electron microscopy (SEM) of amoebae fixed and processed as it was previously described elsewhere (Grębecki *et al.* 2001).

RESULTS AND DISCUSSION

It was the purpose of present investigations to reveal whether there is a relationship between the decrease or increase of calcium amount on the cell surface and the pinocytotic response induced by two different monovalent cations: K^+ and Na^+.

Pinocytotic reaction of amoeba was graduated and characterised by a distinct polarity (the first pinocytotic structures appeared in the uroidal region, next ones at the former fronts) and by the development of numerous small pseudopodia with thin channels, after application of 125 mM NaCl (Fig. 1) or 30 mM KCl (Fig. 2) under standard medium conditions, and during pinocytosis induced by 125 mM KCl in the medium with $[Ca^{2+}]_e$ increased up to 4.85 mM (not shown). It means that this kind of pinocytosis occurred, when Ca^{2+} was binding to amoebae during stimulation, more or less similar as to the control cells (Fig. 5).

Stimulation by 125 mM K^+ applied in standard Pringsheim medium caused immediate cell contraction, the first pinocytotic pseudopodia were formed in any place of strongly deformed cells and, as a result, amoebae produced few large pseudopodia with very wide channels (Fig. 3). This was accompanied with a decrease of $[Ca^{2+}]_e$ associated to the surface of amoeba (Fig. 5). Similar coincidence between the alteration of the morphological features of pinocytosis and the displacement of calcium from the cell surface could be produced as well during pinocytosis induced by 125 mM NaCl and 30 mM KCl by Ca^{2+}_e chelating by EGTA (not shown).

On the contrary, addition of 4 mM $CaCl_2$ during pinocytosis induced by 125 mM K^+, that is increasing $[Ca^{2+}]_e$ from 0.85 mM up to 4.85 mM, caused immediate association of more calcium with the cell surface (Fig. 5) accompanied by changes in the morphology of pinocytosis. Within 30s after application of calcium, the pinocytosing cells with few and large pseudopodia (such as shown in Fig. 3) became rosettes with numerous, small pseudopodia with thin channels (Fig. 4).

In general, it may be concluded that changes in the concentration of extracellular calcium associated during pinocytosis with the cell membrane outer surface and/or with glycocalyx caused immediate alterations of size and number of existing pinocytotic structures.

One can suggest that the course of events during macropinocytosis in *Amoeba proteus* depends on the direction of extracellular calcium shifting between amoebae and the medium during cells stimulation. It was postulated that extracellular calcium plays an important role in controlling the physiological state of the plasma membrane in amoebae (Brandt and Freeman 1967, Brandt and Hendil 1972, Kukulis *et al.* 1986). Low concentration of Ca^{2+}_e in the presence of other cations can induce such cellular activities as endocytotic membrane internalisation (Marshall and Nachmias 1965, Hendil 1971, Braatz-Schade and Haberey 1975, Josefsson 1975, Stockem 1977), whereas high concentration of Ca^{2+}_e has a stabilising effect on the membrane (Gingell 1972). In our experiments neither 125 mM Na^+ nor 30 mM K^+ could not induce pinocytosis in *A. proteus* in $[Ca^{2+}]_e$ increased up to 4.85 mM.

The polarity of pinocytosis is probably related to stability of the cell membrane. When externally bound Ca^{2+} is substituted by the inducer, as it takes place in 125 mM K^+ in standard medium, the membrane potential immediately decreases around the whole cell (Braatz-Schade and Haberey 1975, Josefsson *et al.* 1975) and the first pinocytotic pseudopodia can develop in any place of the surface of amoeba. If calcium is not displaced from the cell surface by the inducing agent, it is in 125 mM Na^+ or 30 mM K^+ in the standard medium and 125 mM K^+ in the increased $[Ca^{2+}]_e$, the first channels are formed at the uroid where suitable conditions for a permanent pinocytosis exist (Wohlfarth-Bottermann and Stockem 1966), because of the strong membrane folding (Czarska and Grębecki 1966) and its low stability in this area (Batueva 1965a, b; Bingley

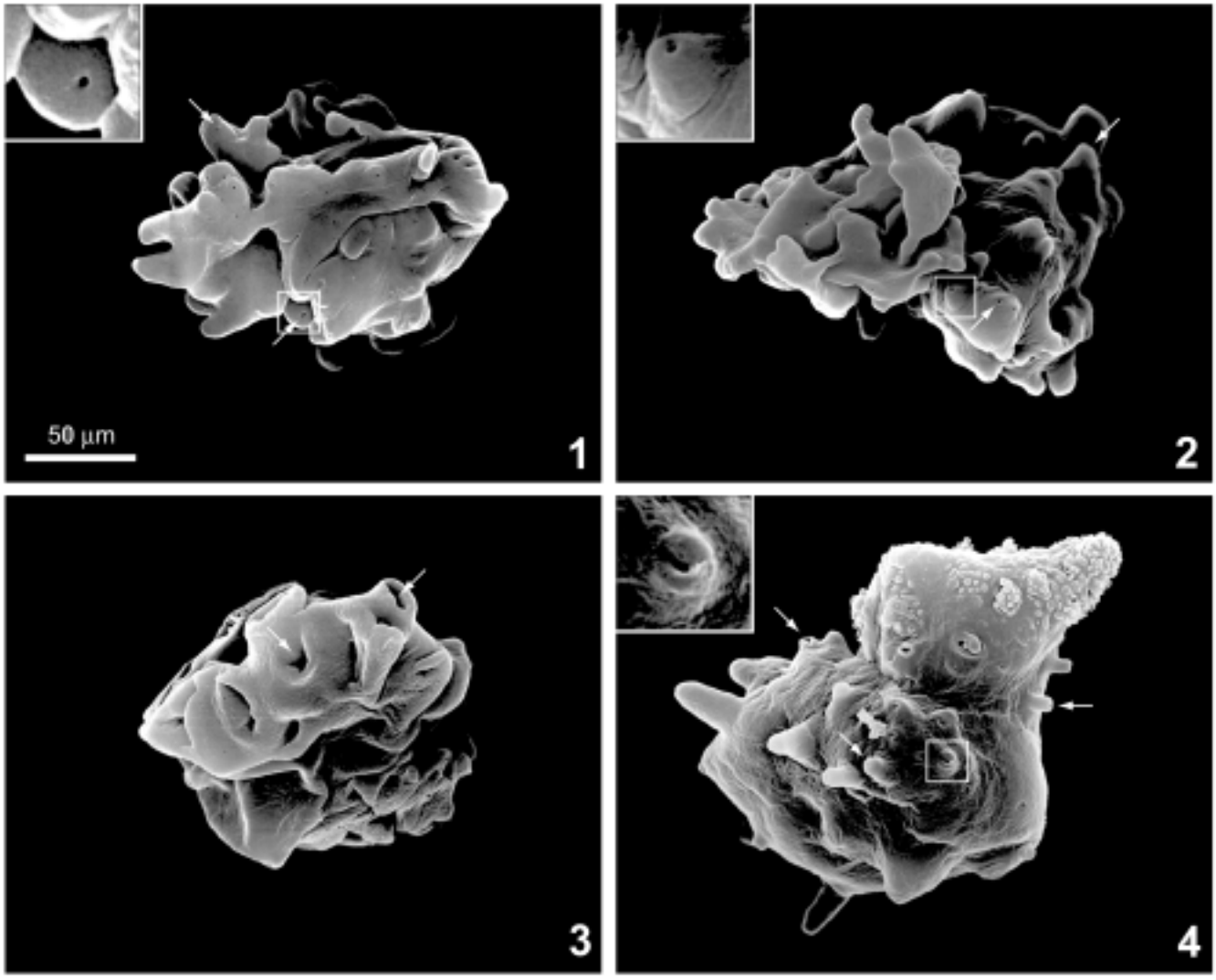

Figs 1-4. Morphology of *Amoeba proteus* pinocytosis shown in SEM. In all pictures arrowheads indicate pinocytotic structures. Scale bar on Fig. 1 applies to all figures. **1-** pinocytosis 7 min after induction by 125 mM NaCl introduced to the standard Pringsheim medium. **2 -** pinocytosis induced for 7 min by low (30 mM) concentration of KCl in the culture medium. **3 -** pinocytosis stimulated 7 min by high (125 mM) concentration of KCl in the culture medium. **4 -** pinocytosing amoeba initially stimulated 7 min by 125 mM KCl, and then followed by addition of 4 mM $CaCl_2$. Insets in Figs 1, 2, 4 are digitally enlarged 3.5 x.

1966). Next channels are formed at the front when it begins to contract (Grębecka and Kłopocka 1985, Grębecka 1988) and similar conditions as in uroid are established.

Calcium also controls cortical cytoskeleton functions that are responsible for cell shape changes and pseudopodia formation: reorganisation of cortical cytoskeleton in amoebae (Hellewel and Taylor 1979, Taylor and Fechheimer 1982, Bray 1992) and interactions of actin microfilaments with the plasma membrane (Taylor *et al.* 1980, Kawakatsu *et al.* 2000), and thus it may influence the course of pinocytosis. According to the view of Maeda and Kawamoto (1986) a low $[Ca^{2+}]$ activates pinocytosis in *Dictyostelium discoideum* because under such conditions the content of actin in the cell cortex and consequently the number of membrane-associated microfilaments are reduced, which may restrict the plasma membrane flexibility, necessary for pinocytotic structures formation. Our results seem to confirm this hypothesis and indicate that membrane flexibility in *A. proteus* may influence the number and size of pinocytotic structures.

According to Klein *et al.* (1988) the size of pinocytotic pseudopodia and the diameter of channels are

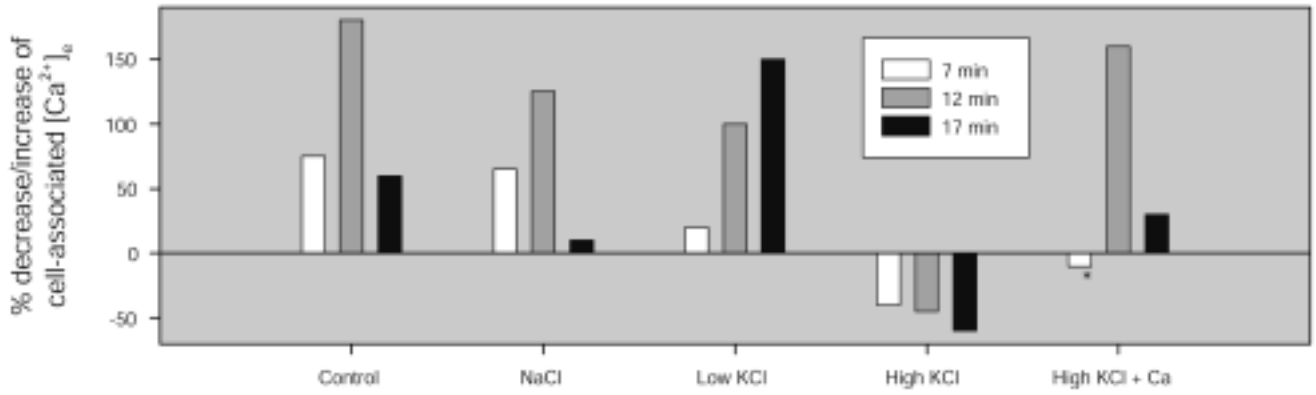

Fig. 5. Per cent changes in the increase or decrease of $[Ca^{2+}]_e$ associated with control cells, during pinocytosis induced by 125 mM NaCl, 30 mM KCl and 125 mM KCl under standard conditions in Pringsheim medium, and 125 mM KCl followed by application of 4 mM $CaCl_2$ (asterisk indicates the moment of calcium application).

regulated by the mode of membrane-microfilament interaction. Pinocytotic pseudopodia are developed due to the circular detachment of the microfilament layer from the plasma membrane with the exception of a central region of fast contact (Stockem *et al.* 1983, Grębecki 1991). The diameter of the channels depends on the extent of the areas of contact between the microfilament layer and the internal face of the plasma membrane (Klein *et al.* 1988). The size of pseudopodia is related to the area of detachment and probably the contraction degree. It seems possible that Ca^{2+}_e can control, *via* the membrane of amoeba, the rearrangement of actin cortical network and its attachment to the cell surface.

Conclusions:

1. The pinocytotic response of *Amoeba proteus* is related to the amount of Ca^{2+} accumulated on the cell surface during the induction of this phenomenon.

2. The direction of calcium shifting during the initiation of pinocytosis depends on the strength of inducer, its concentration, and the concentration of extracellular calcium.

Acknowledgement. Authors wish to express their sincere gratitude to Prof. A. Grębecki for his constructive suggestions for improvement and modification of the manuscript. Authors also thank to Dr. P. Pomorski for his help in preparation of figures.

REFERENCES

Batueva I. V. (1965a) The electrical parameter of *Amoeba proteus* I. Motionless amoebae. *Cytologya* **7:** 188-196

Batueva I. V. (1965b) The electrical parameters of *Amoeba proteus*. II. The motile amoebae. *Cytologya* **7:** 553-561

Bingley M. S. (1966) Membrane potentials in *Amoeba proteus*. *J. Exp. Biol*. **45:** 251-267

Braatz-Schade K., Haberey M. (1975) Bioelectrical potentials and motile activity in *Amoeba proteus*. *Cytobiologie* **11:** 87-94

Brandt P. W., Freeman A. R. (1967) Plasma membrane: Substructural changes correlated with electrical resistance and pinocytosis. *Science* **155:** 582-585

Brandt P., Hendil K. B. (1972) Plasma membrane permeability and pinocytosis in *Chaos chaos*. *C. R. Trav. Lab. Carlsberg* **38:** 423-443

Bray D. (1992) Integration of cell movement. In: Cell Movements (Ed. D. Bray) Garland Publishing, Inc. New York and London 309-375

Czarska L., Grębecki A. (1966) Membrane folding and plasma-membrane ratio in the movement and shape transformation in *Amoeba proteus*. *Acta Protozool*. **4:** 201-239

Gingell D. (1972) Cell membrane surface potential as a transducer. In: Membranes and Ion Transport **3:** 317-357

Grębecka L. (1988) Polarity of the motor functions in *Amoeba proteus* I. Locomotory behaviour. *Acta Protozool*. **27:** 83-96

Grębecka L., Kłopocka W. (1985) Relationship between the surface distribution of membrane reserves and the polarity of pinocytosis in *Amoeba proteus*. *Protistologica* **21:** 207-213

Grębecka L., Kłopocka W. (1986) Morphological differences of pinocytosis in *Amoeba proteus* related to the nature of pinocytotic inducer. *Protistologica* **22:** 265-270

Grębecki A. (1991) Participation of the contractile system in endocytosis demonstrated *in vivo* by video-enhancement in heat-pretreated amoebae. *Protoplasma* **160:** 144-158

Grębecki A., Grębecka L., Wasik A. (2001) Minipodia, the adhesive structures active in locomotion and endocytosis of amoebae. *Acta Protozool*. **40:** 235-247

Hellewell S. B., Taylor D. L. (1979) The contractile basis of ameboid movement VI. The solation-contraction coupling hypothesis. *J. Cell Biol.* **83:** 633-648

Hendil K. B. (1971) Ion exchange properties of the glycocalyx of the amoeba *Chaos chaos* and its relation to pinocytosis. *C. R. Trav. Lab. Carlsberg* **38:** 187-211

Josefsson J.-O. (1975) Studies on the mechanism of induction of pinocytosis in *Amoeba proteus*. *Acta Physiol. Scand*. **97 (Suppl. 423):** 1-65

Josefsson J.-O., Holmer N. G., Hansson S. E. (1975) Membrane potential and conductance during pinocytosis induced in *Amoeba proteus* with alkali metal ions. *Acta Physiol. Scand*. **94:** 278-288

Kawakatsu T., Kikuchi A., Shimmen T., Sonobe S. (2000) Interaction of actin filaments with the plasma membrane in *Amoeba proteus*: studies using a cell model and isolated plasma membrane. *Cell Struct. Funct*. **25:** 269-277

Klein H. P., Köster B., Stockem W. (1988) Pinocytosis and locomotion in amoebae. XVIII. Different morphodynamic forms of endocytosis and microfilament organization in *Amoeba proteus*. *Protoplasma* **2 (Suppl.):** 76-87

Kłopocka W., Balińska M., Kołodziejczyk J. (2000) Role of extracellular calcium in the induction of pinocytosis in *Amoeba proteus* by Na and K ions. *Acta Protozool*. **39:** 143-148

Kukulis J., Ackermann G., Stockem W. (1986) Pinocytosis and locomotion of amoebae. XIV. Demonstration of two different receptor sites on the cell surface of *Amoeba proteus*. *Protoplasma* **131:** 233-243

Maeda Y., Kawamoto T. (1986) Pinocytosis in *Dictyostelium discoideum* cells. A possible implications of cytoskeletal actin for pinocytotic activity. *Exp. Cell Res*. **164:** 516-526

Maniak M. (2002) Conserved features of endocytosis in *Dictyostelium*. *Int. Rev. Cytol*. **221:** 257-287

Marshall J. M., Nachmias V. T. (1965) Cell surface and pinocytosis. *J. Histochem. Cytochem*. **13:** 92-104

Stockem W. (1977) Endocytosis. In: Mammalian Cell Membranes, (Eds. G. A. Jamieson and D. M. Robinson). Butterworths, London, **5:** 151-195

Stockem W., Naib-Majani W., Wohlfarth-Bottermann K. E. (1983) Pinocytosis and locomotion in amoebae. XIX. Immunocytochemical demonstration of actin and myosin in *Amoeba proteus*. *Eur. J. Cell Biol*. **29:** 171-178

Taylor D. L., Fechheimer M. (1982) Cytoplasmic structure and contractility: the solation-contraction coupling hypothesis. *Phil. Trans. R. Soc. Lond. B* **299:** 185-197

Taylor D. L., Blinks J. R., Reynolds G. (1980) Contractile basis of ameboid movement VIII. Aequorin luminescence during ameboid movement, endocytosis, and capping. *J. Cell Biol*. **86:** 599-607

Wohlfarth-Bottermann K. E., Stockem W. (1966) Pinocytose und Bewegung von Amöben II. Permanente und Induzierte Pinocytose bei *Amoeba proteus*. *Z. Zellforsch*. **73:** 444-474

Received on 28th March, 2003; accepted on 31st March, 2003

INSTRUCTIONS FOR AUTHORS

Acta Protozoologica publishes original papers, short communications, as well as longer review articles on comprehensive and updated basic, experimental, and theoretical contributions to the broad aspects of protistology and cell biology of lower Eukaryota including: behavior, biochemistry and molecular biology, development, ecology, genetics, parasitology, physiology, photobiology, systematics and phylogeny, and ultrastructure. Contributions should be written in English. Submission of a manuscript to ***Acta Protozoologica*** implies that the contents are original and have not been published previously, and are not under consideration or accepted for publication elsewhere. There are no page charges except colour illustration. Names and addresses of suggested reviewers will be appreciated. In case of any question please do not hesitate to contact Editor.

Mrs Małgorzata Woronowicz-Rymaszewska
Managing Editor of ACTA PROTOZOOLOGICA
Nencki Institute of Experimental Biology,
ul. Pasteura 3
02-093 Warszawa, Poland
Fax: (4822) 822 53 42
E-mail: jurek@ameba.nencki.gov.pl

Extensive information on ACTA PROTOZOOLOGICA is now available *via* internet. The address is: **http://www.nencki.gov.pl/ap.htm**

Organization of Manuscripts

Submissions

Please enclose three copies of the text, one set of original of line drawings (without lettering!) and three sets of copies with lettering, four sets of photographs (one without lettering). In case of photographs arranged in the form of plate, please submit one set of original photographs unmounted and without lettering, and three sets of plates with lettering.

The ACTA PROTOZOOLOGICA prefers to use the author's word-processor disks (format IBM or IBM compatible, and MacIntosh 6 or 7 system on 3.5" 1.44 MB disk only) of the manuscripts instead of rekeying articles. If available, please send a copy of the disk with your manuscript. Preferable programs are Word or WordPerfect for Windows. Disks will be returned with galley proof of accepted article at the same time. Please observe the following instructions:

1. Label the disk with your name: the word processor/computer used, e.g. IBM; the printer used, e.g. Laserwriter; the name of the program, e.g. Word for Windows.
2. Send the manuscript as a single file; do not split it into smaller files.
3. Give the file a name which is no longer than 8 characters.
4. If necessary, use only italic, bold, underline, subscript and superscript. Multiple font, style or ruler changes, or graphics inserted the text, reduce the usefulness of the disc.
5. Do not right-justify and use of hyphen at the end of line.
6. Avoid the use of footnotes.
7. Distinguish the numerals 0 and 1 from the letters O and l.

Text (three copies)

The text must be typewritten, double-spaced, with numbered pages. The manuscript should be organized into Summary, Key words, Abbreviations used, Introduction, Materials and Methods, Results, Discussion, Acknowledgements, References, Tables and Figure Legends. The Title Page should include the full title of the article, first name(s) in full and surname(s) of author(s), the address(es) where the work was carried out, page heading of up to 40 characters. The present address for correspondence, Fax, and E-mail should also be given.

Each table must be on a separate page. Figure legends must be in a single series at the end of the manuscript. References must be listed alphabetically, abbreviated according to the World List of Scientific Periodicals, 4th ed. (1963). Nomenclature of genera and species names must agree with the International Code of Zoological Nomenclature, third edition, London (1985) or International Code of Botanical Nomenclature, adopted by XIV International Botanical Congress, Berlin, 1987. SI units are preferred.

Examples for bibliographic arrangement of references:

Journals:

Häder D-P., Reinecke E. (1991) Phototactic and polarotactic responses of the photosynthetic flagellate, *Euglena gracilis*. *Acta Protozool.* **30:** 13-18

Books:

Wichterman R. (1986) The Biology of *Paramecium*. 2 ed. Plenum Press, New York

Articles from books:

Allen R. D. (1988) Cytology. In: *Paramecium*, (Ed. H.-D. Görtz). Springer-Verlag, Berlin, Heidelberg, 4-40

Zeuthen E., Rasmussen L. (1972) Synchronized cell division in protozoa. In: Research in Protozoology, (Ed. T. T. Chen). Pergamon Press, Oxford, **4:** 9-145

Illustrations

All line drawings and photographs should be labelled, with the first author's name written on the back. The figures should be numbered in the text as Arabic numerals (e.g. Fig. 1). Illustrations must fit within either one column (86 x 231 mm) or the full width and length of the page (177 x 231 mm). Figures and legends should fit on the same page. Lettering will be inserted by the printers and should be indicated on a tracing-paper overlay or a duplicate copy.

Line drawings (three copies + one copy without lettering)

Line drawings should preferably be drawn about twice in size, suitable for reproduction in the form of well-defined line drawings and should have a white background. Avoid fine stippling or shading. Computer printouts of laser printer quality may be accepted, however *.TIF, *.PSD, *.CDR graphic formats **(Grayscale and Color - 600 dpi, Art line - 1200 dpi)** on CD are preferred.

Photographs (three copies + one copy without lettering)

Photographs at final size should be sharp, with a glossy finish, bromide prints. Photographs grouped as plates (in size not exceeding 177 x 231 mm including legend) must be trimmed at right angles accurately mounted and with edges touching and mounted on firm board. The engraver will then cut a fine line of separation between figures. Magnification should be indicated. Colour illustration (charged) on positive media (slides 60 x 45 mm, 60 x 60 mm, transparency or photographs) is preferred.

Proof sheets and offprints

Authors will receive one set of page proofs for correction and are asked to return these to the Editor within 48-hours. Fifty reprints will be furnished free of charge. Orders for additional reprints have to be submitted with the proofs.

Indexed in Biosis, Current Contents (Agriculture, Biology and Environmental Sciences), Elsevier BIOBASE/Current Awareness in Biological Sciences, Protozoological Abstracts, Science Citation Index, Chemical Abstracts Service, Librex-Agen, Polish Scientific Journals Contents - Agric. & Biol. Sci. Data base are available in INTERNET under URL (Uniform Resource Locator) address: http://psjc.icm.edu.pl any WWW browser; Abstracts and Whole Articles Free in http://www.nencki.gov.pl/ap.htm; in graphical operating systems: MS Windows, Mac OS, X Windows - mosaic and Netscape programs and OS/2 - Web Explorer program; in text operating systems: DOS, UNIX, VM - Lynx and WWW programs.

ACTA
PROTOZOOLOGICA

ORIGINAL ARTICLES

SHORT COMMUNICATIONS

2003 MAY

VOLUME 42 NUMBER 2